# Development of a Predictive Bayesian Data-Derived Multimodal Gaussian Model of Sunken Oil Mass Location and Transport

**Final Report**
**Submitted to**

**The Coastal Response Research Center**

**Submitted by**

**James D. Englehardt, Ph.D., P.E.**
**M. Angélica Echavarría Gregory, M.S.**
**Pedro M. Avellaneda, Ph.D.**

**Department of Civil, Architectural and Environmental Engineering**
**University of Miami**
**1251 Memorial Drive**
**McArthur Engineering Building, Suite 321**
**Coral Gables, Florida, 33124-0630**

**Project Period: August 15, 2008 to August 14, 2010**

**Submission Date: September 13, 2010**

This project was funded by a grant from NOAA/UNH Coastal Response Research Center. NOAA Grant Number(s): NA04NOS4190063. Project Number: 08-088

# Abstract

The problem addressed in this project is the need for cost-effective tracking of sunken oil following a spill, to target cleanup activities and to support cleanup termination decisions. Sunken oil is difficult to locate because remote sensing techniques cannot as yet provide views of sunken oil over large areas. Moreover, the oil may re-suspend and sink with changes in salinity, sediment load, and temperature, making fate and transport models difficult to deploy and calibrate when even the presence of sunken oil is difficult to assess. For these reasons, together with the expense of field data collection, there is a need for a statistical data-limited technique integrating field data collection with statistical fate and transport modeling.

Predictive Bayesian modeling techniques have been developed and demonstrated for exploiting limited information for decision support in many other applications. These techniques implemented in a Lagrangian modeling framework represent such an integrated approach to modeling based on real-time field data. The objectives of this project were to (1) compile and summarize data on the occurrence of sunken oil, directed by the project advisory team and National Oceanographic and Atmospheric Administration (NOAA) Emergency Response Division liaison; (2) develop a multi-modal predictive Bayesian Gaussian model to project in time relative unconditional probabilities of finding sunken oil at locations across a relatively flat bay bottom, based on limited available spatial field data on sunken oil concentrations; and (3) verify the model versus sunken oil data, as possible, and simulated datasets. Methods included (1) development of conceptual model and data base by literature review, including team kickoff meeting to identify data sources and define model capability, (2) development of an open-source computer model with graphical user interface capable of accepting limited available field data on oil concentrations in time and space, including development of combinatorial methods of oil patch identification and superimposed image methods to account for curved shoreline boundaries, and (3) model optimization and confirmation versus available real and/or simulated field data, and dissemination by website, presentation, publication, and media release.

The model was developed and initially confirmed versus real and simulated data, presented at the Clean Gulf 2009 conference, described in the media including *USA Today* online, and offered to the State of Florida for use in the current Gulf of Mexico oil spill cleanup effort. The model represents a new approach to pollutant tracking by inference from limited field data alone, and the mapping of unconditional relative probabilities of finding pollutant mass in space and time with rigorous accounting of uncertainty. The model was developed in the open-source Python language, for potential interface with new response, cleanup, and damage assessment models under development by NOAA as appropriate. Several extensions and refinements are recommended, including the addition of capability for accepting available information on bathymetry and bottom currents as Bayesian *prior* information, and extension to tracking of suspended oil. It is expected that the model will be implemented by NOAA Emergency Response Division for support of emergency response and recovery efforts, as an aid for rapid and cost-effective location and tracking of sunken oil during response and recovery efforts and to support cleanup termination decisions.

**Keywords:** sunken oil, Bayesian, Gaussian, model, emergency response, recovery

# Acknowledgements

The Coastal Response Research Center (CRRC) at University of New Hampshire and the National Oceanographic and Atmospheric Administration (NOAA) are gratefully acknowledged for support and funding of this project (NOAA Grant Number NA04NOS4190063). In particular, Christopher Barker is thanked for his collaboration and contributions to the development of the model. Stephen Lehmann and CJ Beegle-Krause are thanked for their substantive and timely provision of information in terms of oil spill emergency response capabilities and needs. Nancy Kinner and Amy Merten are thanked for their guidance and project management. Ruochen Li and Aarthi Narayanan are thanked for their contributions to model development as members of the supporting research team.

# Table of Contents

## List of Figures and Tables

# 1.0 Introduction

The ultimate impact of an oil spill stems from several factors, including its size, geographical location, political and practical context of the response, as well as the occurrence of suspended or sunken oil. Sunken oil can occur following a spill of heavy oil, or of lighter oil that entrains sediment. The term sunken oil is used in this report to refer to oil on the bottom, though some of the discussion and approach may also apply to oil suspended in the water column. As noted by the Coastal Response Research Center (CRRC, 2007), "In the past few years, spills of non-floating oil and oils that become submerged as a function of sediment entrainment have presented significant response challenges and have resulted in enormous dollar-per-barrel recovery costs. Currently, the ability to forecast submerged oil movement, estimate water column concentrations of large droplets, and efficiently recover sunken masses in an operationally expedient way is quite limited. Additionally, as this category of oil is difficult to locate, track, and retrieve, managers have difficulty maintaining public confidence with regard to response termination." Problems in locating and tracking sunken oil are further exacerbated by the expense of developing and deploying new remote sensing techniques, and because some oils may re-suspend and sink with changes in salinity, sediment load, and temperature.

Many models have been used to simulate the drift and fate of oil slicks in one, two, or three dimensions using Eulerian or Lagrangian modeling techniques (Ojo *et al*, 2007; Spaulding *et al*, 1994; Spaulding *et al*, 1997; Beegle-Krause, 2001; Yapa, 1994; Sugioka *et al*, 1999). The spill-trajectory model developed and used most recently by the National Oceanic and Atmospheric Administration (NOAA) is the General NOAA Oil Modeling Environment (GNOME), developed by the Hazardous Materials Response Division (HAZMAT) Office of Response and Restoration. GNOME includes statistical capability in the form of Best Guess and Minimum Regret solutions (Galt, 1998). However, existing models are not developed for the detection and mapping of sunken oil. Other possible approaches to locating and tracking sunken oil include electro-acoustic detection, mechanical detection, and inspection by divers, as summarized in the Technical Guidelines on Sunken Oil Assessment and Removal Techniques (NOAA, 2006). However, integrated models for short and long-term sunken oil tracking with on-scene calibration capability during emergency response have been identified as research needs (CRRC, 2007).

The occurrence of sunken oil is difficult to predict in time and space before, during, and after cleanup, using either contaminant transport models or field data, for two reasons. First, hydrodynamic or particle tracking models may be difficult to deploy and calibrate for tracking of sunken oil, due to the site-specific and potentially transient nature of sunken oil occurrence and location under changing field conditions, and limitations in the available information on advective/dispersive forces acting on sunken oil. Second, the collection of field data on sunken oil locations is intrinsically expensive. Modeling techniques that accept near-real time field data as input and account quantitatively for both uncertainty and variability are not well-developed, and have not been available to support response, cleanup, and damage assessment decisions.

The use of Bayesian modeling techniques to incorporate non-numerical types of information in probabilistic assessments has exploded in recent years due to the development of new computational approaches (e.g. Markov Chain Monte Carlo). The approach allows integration of available numerical data together with any less-quantitative information, with rigorous accounting for uncertainty in accordance with the laws of probability. Therefore, it represents an approach to exploiting available field data on sunken oil locations together with estimated ranges of values for coefficients of advection and dispersion. The Bayesian approach involves inclusion of non-numeric information to develop *posterior* probability distributions for the uncertain parameters of probability distributions for uncertain quantities of interest.

Predictive Bayesian methods involve the development of unconditional probability distributions for the quantity of interest, by integrating over all possible values of the uncertain parameters (expressed by the posterior). The approach has been used in oil spill prevention and preparedness planning (Obie and Englehardt 1996; Douligeris *et al*., 1998) and for other applications including hurricane, environmental, health, and safety risk analysis (Aitchison and Dunsmore, 1975; Englehardt, 2004, 1995; Bloetscher *et al*., 2005; Englehardt and Swartout, 2004; Englehardt *et al.*, 2003; Anex and Englehardt, 2001; Englehardt and Peng, 1996). For example, a predictive Bayesian compound Poisson model was developed to forecast changes in oil spill volumes onshore in the Gulf of Mexico in response to proposed changes in oil transportation and response equipment and policies, given geographically-defined historical oil spill data, shipping routes and volumes, and hydrodynamic modeling results (Obie and Englehardt, 1996; Douligeris *et al*., 1998). However, the approach has not been brought to bear on the problem of locating sunken oil.

This project addresses current limitations in techniques for locating sunken oil on relatively flat bay bottoms. The intended audience is oil spill emergency response professionals, and those involved in oil spill recovery and remediation. Beneficiaries of the research are expected to include the National Oceanographic and Atmospheric Administration, oil spill responsible parties, and the oil spill response and recovery communities.

## 2.0 Objectives

Given the site-specific nature of the occurrence of sunken oil and the need to project its location in time, a statistical data-limited technique representing a cross between a statistical static sampling plan and a contaminant transport model was proposed for development in this project. In discussions with the project advisory group, it was determined that information on bottom "currents" and their potential forcing of the movement of sunken oil was too limited to be a primary source of input information for the model. Rather, the capability to exploit limited field data collected following a spill was desired. It was also agreed that the model should be developed as a stand-alone, open-source, executable application with graphical user interface (GUI), for possible incorporation in future oil spill response software.

To meet current needs in terms of locating sunken oil during emergency response operations, the objective of the project was to develop a stand-alone, open-source, executable model with GUI, with capability for:

1. Assessing sunken oil locations based on limited available field data collected shortly after a spill event,
2. Projecting oil location in time based on subsequent limited field data together with shoreline boundaries and the values or estimated ranges of values of the coefficients of advection and diffusion, and
3. Providing updated projections based on additional field data as they become available.

Specifically, a predictive Bayesian multimodal Gaussian model of sunken oil locations across a relatively flat-bottomed bay was proposed, to accept possibly irregularly-sampled field data at times shortly after each spill event when sunken oil has appeared on the bottom. The calibrated model also was to have capability for accepting input in the form of ranges of parameter values based either on hydrodynamic data or professional judgment, to over-ride default ranges assigned in the research. In that way, limited field data can be integrated with certain other types of information to assess and project the location of dispersing sunken oil masses both before and after cleanup begins, for spill response and decision-making, cleanup, and damage assessment. Finally, it was agreed that the model should be capable of being enhanced in the future to accept bathymetric information as input.

Based on discussions with project advisers, the scope of the project was limited to:

- Sunken oil;
- Relatively flat bay bottoms, dredged bays, reef flats and lagoons or pools protected by offshore rocks; bays with steeply sloped bottoms would require capability for the use of bathymetric data as prior information, a possible future enhancement;
- Resolution down to the scale of the tidal excursion (oil locations effectively averaged across this excursion);
- Discrete accidental oil releases (as opposed to natural, progressive oil seepage);
- Relatively uncomplicated concave and convex shoreline geometries; modeling in straits, inland water bodies, harbors, islet areas, and like geographies are not addressed due to computational limitations and the sometimes transient nature of small-scale features.

This report describes the development of the Sunken Oil Simulation (SOSim) model, to be used for identifying sunken oil hotspots, tracking sunken oil following a spill, targeting cleanup activities, and supporting cleanup termination decisions. The final product of the project is a computer executable stand-alone software package created and tested under Microsoft Windows 32 bit operative system, programmed in the Python language and embedded in its own GUI. Included in this report is a user's manual for the open-source product (Appendix A). Because the model was developed using only open source software and GPL derivatives, its use is governed under the GPL (General Public License) license terms (see license terms included in the source code, Appendix A). This tool will allow the response coordinator to choose and customize response options, including actions at the source, at sea, near the shore, and onshore, plan operations at predetermined times and locations based on projected sunken oil locations, and plan the overall cleanup and recovery phase to mitigate impacts.

First, current information reported in the literature and relevant to the transport of sunken oil is reviewed and, based on that information; a conceptual model for development of the software is presented. Then, the mathematical and computational aspects of the model are developed. Finally the results of model verification versus real and synthetic data on sunken oil location are presented, with conclusions regarding application of the model as a predictive, decision-making tool.

## 3.0 Methods

The project was organized according to three essential tasks, as follows:

1. Development of an understanding of the factors relevant to the modeling of sunken oil fate and transport, particularly as related to the bathymetric characteristics of bays for which a Gaussian modeling approach would be applicable,
2. Development of a computational approach that would allow a highly parameterized predictive Bayesian multimodal Gaussian model of sunken oil location to be executed on a desktop or workstation computer,
3. Verification of the model versus real and synthetic sunken oil location filed data.

### 3.1 Task 1 Methods

The objective of Task 1 was to compile and summarize data on the occurrence and transport of sunken oil as reported for previous spills, and to synthesize input knowledge from the Research Team to develop a conceptual approach for the model. Thus, the team gathered information from the literature and oil spill response professionals including the project advisory team to (a) evaluate possible methodologies and approaches, (b) understand the processes of hydrodynamic fate and the transport governing the behavior of sunken oil mass as a basis for development of the conceptual model and specification of default values and/or ranges of values of model parameters, and (c) determine appropriate the geographical scale and resolution for the model. Simultaneously, regular meetings with the project advisory team were held to discuss and develop a conceptual model for development of the mathematical and software models.

### 3.2 Task 2 Methods

The objective of Task 2 was to develop a multi-modal predictive Bayesian Gaussian statistical model of sunken oil locations across a bay that would accept spatial field data on sunken oil mass following a spill, to project assessments of sunken oil locations in time. Input data for the algorithms were to include field data collected after oil has begun to sink at and around a spill site, dates of spill occurrence and sampling campaign(s), and shoreline conditions if applicable for the desired modeling zone. Algorithms were to infer Bayesian posterior probability distributions for uncertain model parameters describing the dispersion and movement of sunken oil patches in time.

The multimodal aspect of the Gaussian model was needed to accommodate oil accumulating in multiple areas of the bay as a result of localized sediment entrainment, localized bathymetric catchment areas, and other effects. This capability was provided by superimposing multiple 2-D Gaussian *patches* in the model. Each patch was assigned a weighting parameter, representing the fraction of the total sunken oil contained in that patch, with all fractions summing to an arbitrary constant value of unity representing the unknown total sunken oil mass. Because the total mass of sunken oil was not expected to be known, the output of the model is referred to as *relative* oil mass. Thus, the traditional requirement for normalizing the area under the Gaussian distributions to a value of unity was not necessary and was relaxed. Because of the lack of a need to normalize individual Gaussian distributions, there was no need to normalize the likelihood functions used to develop the Bayesian posterior distributions, as will be described in Section 4 (Results). Therefore, Markov chain Monte Carlo (MCMC) computation was not required. Because of the computational demands of MCMC methods, the likelihood that the approach would not be successful for such a highly-parameterized model, and the relatively unskewed and regular nature of the parameter distributions to be integrated, it was decided to use a straightforward Riemann sum to obtain the final predictive result. Modeling techniques and advances developed during the course of the research are described in Section 4 (Results).

## 3.3 Task 3 Methods

The objective of Task 3 was to verify the model versus available real sunken oil data, as possible, and versus simulated submerged oil data, and disseminate software and results to the national and international oil spill community via an actively maintained website. The need for synthetic data for verification was identified, due to the limited nature of available sunken oil data recorded after a spill. Thus, the model was first verified versus data interpreted from a graphical presentation of spatially-defined qualitative data on oil spill concentrations on the bottom of the Gulf of Mexico following the DBL 152 spill (Barker, 2009). In addition, synthetic oil spill data hypothetically collected in two successive sampling campaigns for a double patch of sunken oil in a nearshore area were generated statistically, and used to verify aspects of model functionality including superposition, boundary effects, and multiple sampling times.

### 3.3.1 Use of Available Qualitative Sunken Oil Concentration Data

Data available for use in this project was obtained from NOAA for the DBL 152 spill, which occurred on 11 November 2005 in the Gulf of Mexico. The data were available only in the graphical form shown in Figure 3.1. Data were collected by dragging absorbent mop-like samplers, termed *pom-poms*, along the bottom, and recording the geographical trace of the pom-pom and the visually-estimated amount of oil collected as ≤ 1%, 5-10%, 11-50%, 51-100%. This figure was interpreted by assigning each recorded relative concentration in percent to the midpoint of the drag trace shown in the figure. Coordinates of the spill location, also shown, and sampling points were approximated based on the figure. The date of this sampling campaign was taken as 25 November 2005, as indicated in the figure. No further information was available to the project team, and therefore this information was taken as an example test case for the use of limited information in a spill scenario.

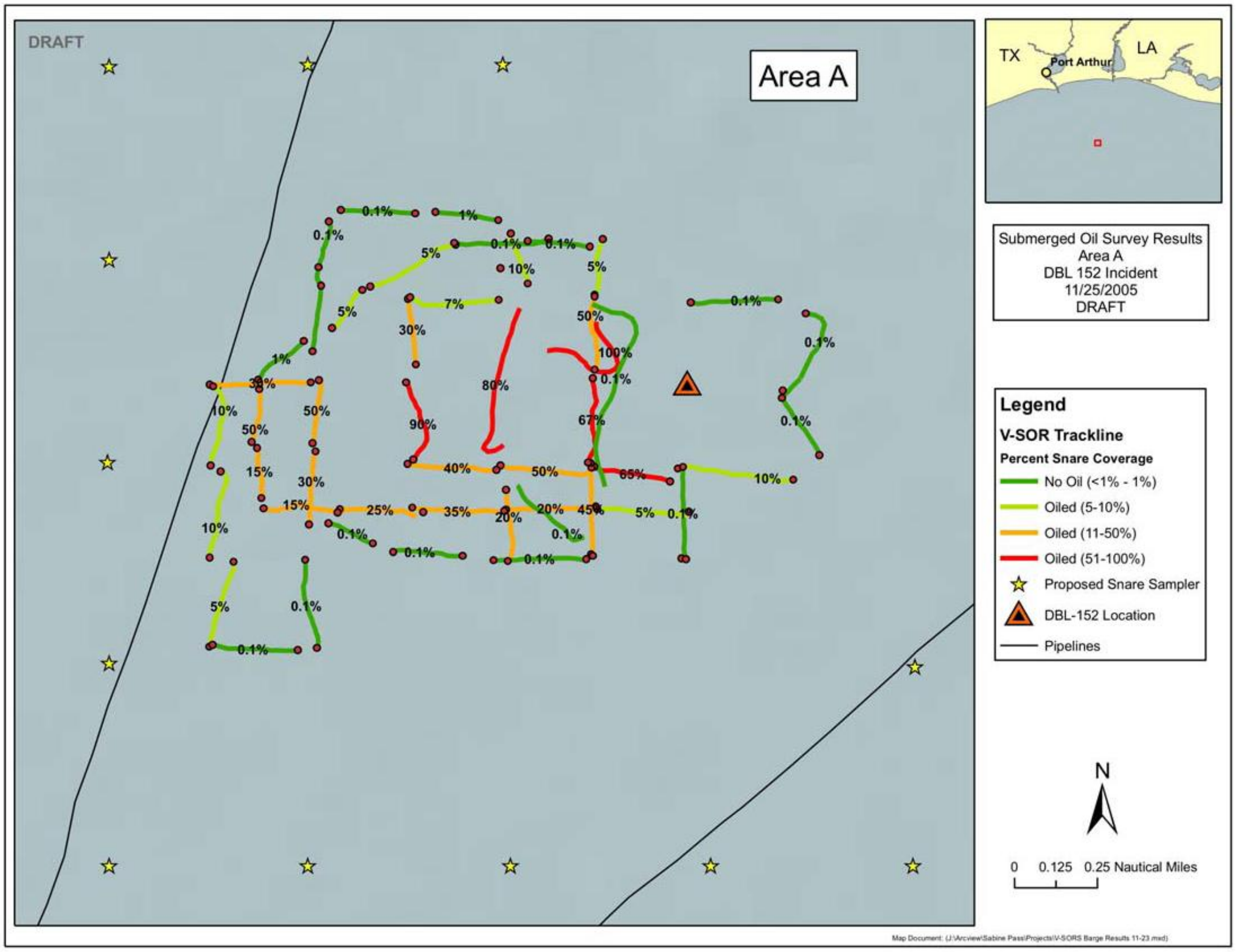

Figure 3.1. Aerial plot presenting the results of a sampling campaign following the 2005 DBL 152 spill near Port Arthur, TX.

### 3.3.2 Development of Synthetic Spatially-Defined Sunken Oil Concentration Data

To verify additional functionality of the model including superposition, boundary effects, and multiple sampling times, synthetic data was generated. This was done by assuming a roughly bi-modal Gaussian distribution of oil on the bottom, that is, oil in patches (that might in turn have internal patchy character). However, real oil spill data will not be neatly Gaussian in shape and will come from a distribution of experimental error. Therefore, the bi-modal, bivariate Gaussian distribution was used as the assumed mean oil concentration on the bottom, with relative concentration then sampled from a distribution of variability around that mean, exponential in form. The exponential distribution is the most likely distribution of sampling error around a fixed mean, given that concentrations cannot be negative, by the Principle of Maximum Entropy (Jaynes, 1957), as will be described more fully in Section 4 (Results) in reference to model development. Thus, the concentration, $C_i$, at each assumed sampling point in space and time was sampled from an exponential error distribution with scale parameter $\lambda$, and mean $1/\lambda$ equal to a superimposed bivariate Gaussian distribution as follows:

- Mean concentration at the *i*-th of 90 (in space) x 2 (in time) samples was found by superposition of two assumed Gaussian patches of sunken oil, as $\overline{C_i} = \sum_{j=1}^{2} \gamma_j \mathcal{N}_j$ , in which $\mathcal{N}_j = \mathrm{f}_j (\mathbf{X}, t \mid \boldsymbol{\mu}_j, \boldsymbol{\sigma}_j, \rho_j)$ is the *j*-th assumed patch of sunken oil and $\gamma_j$ is the relative mass of oil contained in that patch. The oil was assumed to occur in a nearshore environment;
- To account for real experimental and natural variability, measured sample concentrations, $C_i$ , were then sampled from an exponential distribution with parameter $\lambda = 1/\overline{C_i}$.

# 4.0 Results

## 4.1 Task 1 Results

### 4.1.1 Literature Review

The expression “oil spill” refers to a violent spillage of hydrocarbons concentrated in a specific area, surpassing the natural assimilation capacities of the surrounding environment. Sinking is the physical mechanism by which oil masses that are denser than the receiving water are transported to the bottom. The oil itself may be denser than seawater, or it may sink by chemical or physical means: chemically, the soluble fractions separate from denser fractions, leaving the latter with the capability of sinking; physically, oil may have incorporated enough sand to become denser than the water and therefore sink.

Vast quantities of crude oil and refined products are transported over long distances, incurring constant and substantial risks of accidents. In particular, roughly one half of the oil consumed worldwide is transported by sea, in ~9,130 oil tankers counted worldwide (ITOPF, 2009). High vessel densities in maritime routes and loading/offloading ports, longer journeys, and intricate aspects of geographical location all increase the risk of oil spills due to collision, negligence, grounding, or defects in a vessel’s structure. Insurance statistics indicate that most oil tanker accidents resulting in marine oil spills result from human error, including “… badly handled maneuvers, neglect maintenance, insufficient checking of systems, lack of communication between crew members, fatigue, or an inadequate response to a minor incident …” (Cedre, 2007). From a more practical point of view, examination of the circumstances surrounding accidents (ITOPF, 2004) indicates a high percentage of spills due to groundings and collisions. Figure 4.1 shows statistics on the reasons of oil spill occurrences.

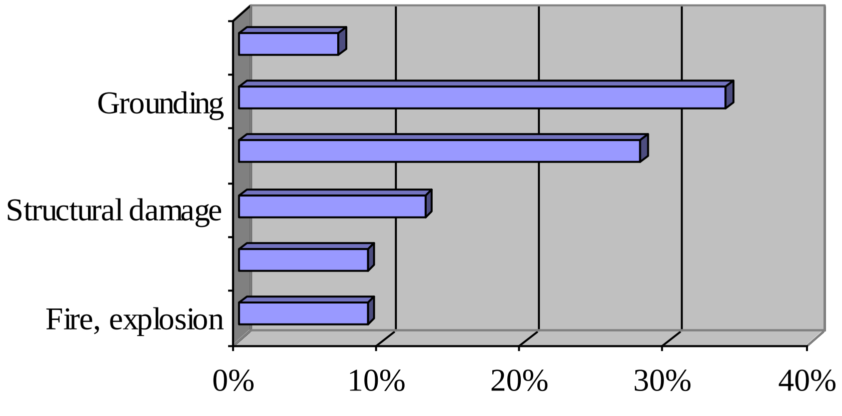

Figure 4.1. Principal causes of oil spills in the world, Source: ITOPF, 2009.

The nature of oil transported by sea varies from the lightest oil (highly volatile hydrocarbon or gasoline) that floats on the sea water and evaporates to the atmosphere, to heavy fuel oils, of which perhaps only 10% will evaporate (ITOPF, 2009) with much of the remainder sinking to the bottom. Processes that affect sinkable oil mass following a spill include evaporation, water and oil mixing and sedimentation. Figure 4.2 shows case-based examples of the approximated fractions of spilled oil mass that undergo evaporation and all other processes in seawater.

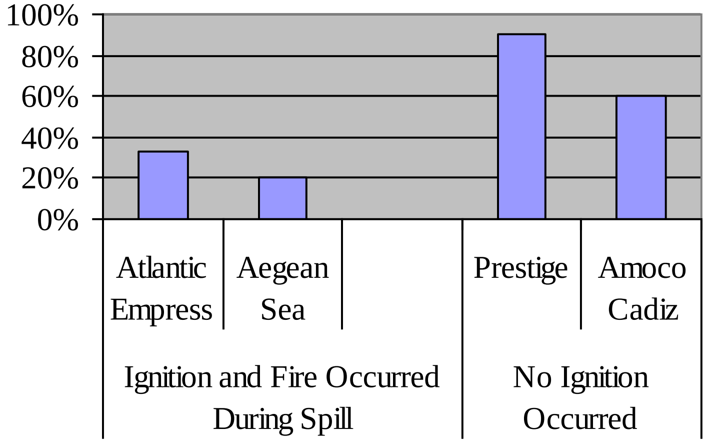

Figure 4.2 . Case-based fractions of oil spilt that undergo processes in the seawater and the atmosphere. Source: Cedre, 2009.

In general, crude oils and certain heavy refined products and sludge deposits have the potential to sink, with sinking of oil generally becoming important from 1-8 days following a spill (Coastal Response Research Center, 2007). Sunken oil then accumulates on the bottom in reported thicknesses of about 2.5 inches, regardless of the size of the oil patches (Beegle-Krause *et al.*, 2006). Sedimentation of thick and heavy oil occurs rapidly, and involves the majority of the oil minus a small percentage (< 10%) that evaporates and a portion that remains in bubbles in the water column for a short time. Evaporation and mixing with water diminish the sinkable fraction, while sediment entrainment increases sedimentation. Incorporation of water into the oil mass due to mixing may prevent sinking for periods of hours to days following the spill. For spills of light oil, sedimentation generally occurs over a long period of time and involves < 5% of the oil mass (Cedre, 2007).

Sinking of heavy oils (API gravities less than ~7.0) due to gravity is more likely in quiescent seawater where currents are under 0.1 knot (Research Planning Inc., 2001) because higher currents typically keep oil droplets suspended in the water column longer. According to NOAA event comparison charts, oils denser than local water have not been observed to impact the shoreline unless the source of the oil was within the surf zone or the oil moved into relatively denser water and thus became buoyant (Beegle-Krause *et al*., 2006). From Protocols for NRDA Surveys (Research Planning Inc., 2001), "... sunken oil can be buried by silt in harbors or sand in offshore areas within days to weeks. Once buried, it can remain for years, only to be exposed by storms or dredging operations." If near shore, sunken oil and tar can wash up on beaches following storms for years following a spill. Gravity will induce flow of the oil in the offshore direction, towards deeper water (Beegle-Krause *et al*., 2006).

As reported in Protocols for NRDA Surveys (Research Planning Inc., 2001), heavy oil can temporarily accumulate in low-flow zones. In rivers, accumulation may occur in backwaters, sloughs, inactive scour pits, and in the lee of point bars, wing dams, and other man-made obstructions. In estuaries, potential accumulation areas include man-made depressions (e.g., dredged channels, marinas and boat slips, prop scour pits, turning basins), natural scour pits active during periods of high flow, and abandoned channel meanders. Along the outer coast, accumulation may occur in troughs between offshore bars, lagoons or pools protected by offshore rocks or coral, reef flats protected by reef crests, and in the lee of any obstruction of currents along the coast (e.g., rocks, jetties, and breakwaters).

Oils lighter than the receiving water may sink by (a) adhering to sand-sized particles during mixing in the surf zone; (b) stranding on shore, picking up sand, then being eroded from the beach by waves and deposited in the near-shore zone; and (c) adhering to the substrate during low water, then not re-floating when water levels rise. The latter mechanism is more likely in rivers and streams where water levels may fluctuate. In general, sunken oil that is intrinsically lighter than surrounding water (i.e., that sank by mixing with sand) can re-float if the oil separates from the sand or bottom substrate. Such separation may occur upon warming, due to the reduction in viscosity.

Sedimentation is of significant concern even if the oil has a light density, if a spill occurs in a nearshore environment where the oil can mix with sand or sediment causing it to sink, as happened in the Braer, Erika and Prestige incidents (ITOPF, 2009). In such cases the sunken oil is extremely difficult to detect and recover. In general, once on the bottom, most hydrocarbons easily enter gaps and flow by gravity so deep that it may be impossible to find by inspection.

Sunken oil mats tend to remain stationary in the absence of storms; local bottom currents typically do not have enough energy to move the mat. Release and resuspension of parts of submerged oil mats by long period gravity wave energy occurs most often along the near-shore shelf where water is shallower and wave energy extends closer to the bottom depth (Dean and Dalrymple, 1991). As a result of this increasing tendency to remain stationary following deposition in deeper water, the mats tend migrate in the offshore direction over time (Beegle-Krause *et al.*, 2006). If the mat is broken up into particles during mixing, it does not tend to re-coalesce. There is a significant difference in the oil content of oil masses that sink by gravity and those that sink by entrainment and sedimentation. The former may contain only a few percent sediment, whereas oil-contaminated sediments accumulated on the seafloor generally contains less than 1% oil (Research Planning Inc., 2001).

Hydrocarbons that are not removed from certain ocean bottoms can seriously damage populations living within the sediment substrate. Sunken oil weathers slowly; therefore toxic components can persist and be a source of exposure during re-floatation or benthic transport. A spill of heavy fuel oil is likely to cause much more damage than a crude oil spill of a corresponding size. The duration of spillage also plays an important role. A sudden violent release will concentrate the effects on a smaller area as compared with a long, slow leak.

Several properties affect the classification of oil as heavy or light, and consequently can modify the propensity of the oil to sink as explained above. These combined properties, including density, viscosity, pour point, solubility, chemical composition and potential for emulsification, along with associated short-term behavior in the environment and impacts to natural resources (Research Planning Inc., 1994), allowed for the classification of oil into six broad categories. In general, Type 1 oils are very light, including gasoline and very volatile hydrocarbons. Type 2 are moderately volatile and soluble, including jet fuels, diesel fuel, number 2 fuel oil, and light crude oils. Type 3 oils include most crude oils, known by their persistence and diminished propensity to evaporate (about one third of the total mass evaporates within 24 hours). Type 4 oils may have little propensity to evaporate or dissolve, and high likelihood of sinking. Type 5 oils have essentially no evaporation potential, weather very slowly, and sink immediately, including heavy industrial fuel oils. Type 6 oils include heavy animal or plant oils. This classification of oils is tightly related to API gravity, a measurement of the relative density of petroleum liquids developed by the American Petroleum Institute and adopted by the oil industry worldwide. Type 1 oils may have API gravities around 31 °API, whereas a Type 4 oil can have an API gravity of less than about 10 °API, in which case the oil will typically sink in water.

### Transport and Accumulation

The following points concerning characteristics of the initial fate and transport of sunken oil have been excerpted, adapted, interpreted, and/or condensed from the references cited:

- After events of high bottom energy, sunken oil can be resuspended and sometimes mixed until it is broken up into small globules. These smaller globules of heavy oil are not expected to coalesce into a larger slick at some later time (Beegle-Krause *et al.*, 2006), but rather to weather and degrade over long periods. At depth, the so-called "convergence zones" found in the surface are not found, and a mechanism for bringing the globules together no longer exists in the bottom (Beegle-Krause *et al.*, 2006);
- Long-term transport of heavy oil is seldom compared to long-term sediment transport on continental shelves. Events with sufficient energy are more likely to be caused by long-period waves than by the local bottom currents (Beegle-Krause *et al.*, 2006); and
- Sediment is typically transported greater distances along the shelf than across the shelf (Beegle-Krause *et al.*, 2006). This observation could represent prior information for the development of Bayesian prior probability distributions for coefficients of advection and dispersion in directions perpendicular and parallel to shore.

### Mechanisms of Resuspension of Sunken Oil

When a high-density oil spill occurs, a large portion of the oil will sink to the bottom to form large discrete mats in many areas and smaller globules in others (Beegle-Krause *et al.*, 2006). Here, the term "globule" is equivalent to "tarball", also used in the literature. Observational data in NOAA data bases suggest that oil remains in areas of heavier concentration until high-energy storms redistribute the oil. The following are excerpted or adapted from Beegle-Krause *et al.* (2006), except as noted:

- Literature suggests that average current conditions will not be sufficient to move the oil in a continuous manner (Beegle-Krause *et al.*, 2006; Boehm *et al.*, 1981). Rather, “The oil will remain stationary on the bottom until an event occurs with enough energy to stir it up into the water column;”

- “Tarmats occur when floating oil moves into the surf zone, collects sediment, and sinks;”
- “With enough energy, tarmats in the bottom generally break up into smaller pieces of oil that spread out into a large area. Otherwise, the tarmats remain stationary and intact;”
- “Outside the inner shelf, where coastal current jets form, long-period waves will be the only source of turbulent energy at the bottom other than large storms strong enough to mix the entire water column;”
- “The oil will behave similarly to local sediments in terms of episodes of burial and re-exposure and mobilization into the water column;”
- The energy required to move the oil varies with depth and site and is unknown. A break-up energy level has been estimated as 6 $m^2$/Hz (Beegle-Krause, *et al.*, 2006).

### 4.1.2 Conceptual Model

The literature review developed in this task was used together with discussions with the project advisory team (Christopher Barker, NOAA Office of Response and Restoration, Emergency Response Division and Assessment & Restoration Division, Technical Liaison; Nancy Kinner, Co-Director, Coastal Response Research Center, University of New Hampshire; Amy Merten, Co-Director, Coastal Response and Research Center, NOAA) to develop the conceptual model targeting end user needs. The initial concept was a predictive Bayesian superimposed 2-D Gaussian model incorporating computer algorithms to allow estimation of the highly parameterized model given limited numerical data and possibly additional information on the surroundings after the oil has begun to sink. As a result of Task 1, it was decided to develop a stand-alone, open-source model with graphical user interface. The model was to be capable of accepting limited available field data on oil spill concentrations, whether quantitative or qualitative in nature, sampled randomly in space, from multiple sampling campaigns, and to include default ranges for coefficients of advection and dispersion in two horizontal directions. Additional model input would include the time and location of the spill and of all oil concentration data.

## 4.2 Task 2 Results

Predictive Bayesian distributions are distributions of unconditional (on knowledge of the parameter vector) probability. The predictive distribution is obtained by multiplying the sampling distribution (e.g., the multinormal), by a Bayesian posterior distribution describing numerical and other knowledge of the parameter vector, and integrating the product over the uncertain parameter space according to the Theorem of Total Probability. The result is a distribution that evolves in shape, becoming progressively narrower as the level of available information increases, converging on the underlying distribution of variability. Figure 4.3 shows this evolution in a general, one-dimensional case.

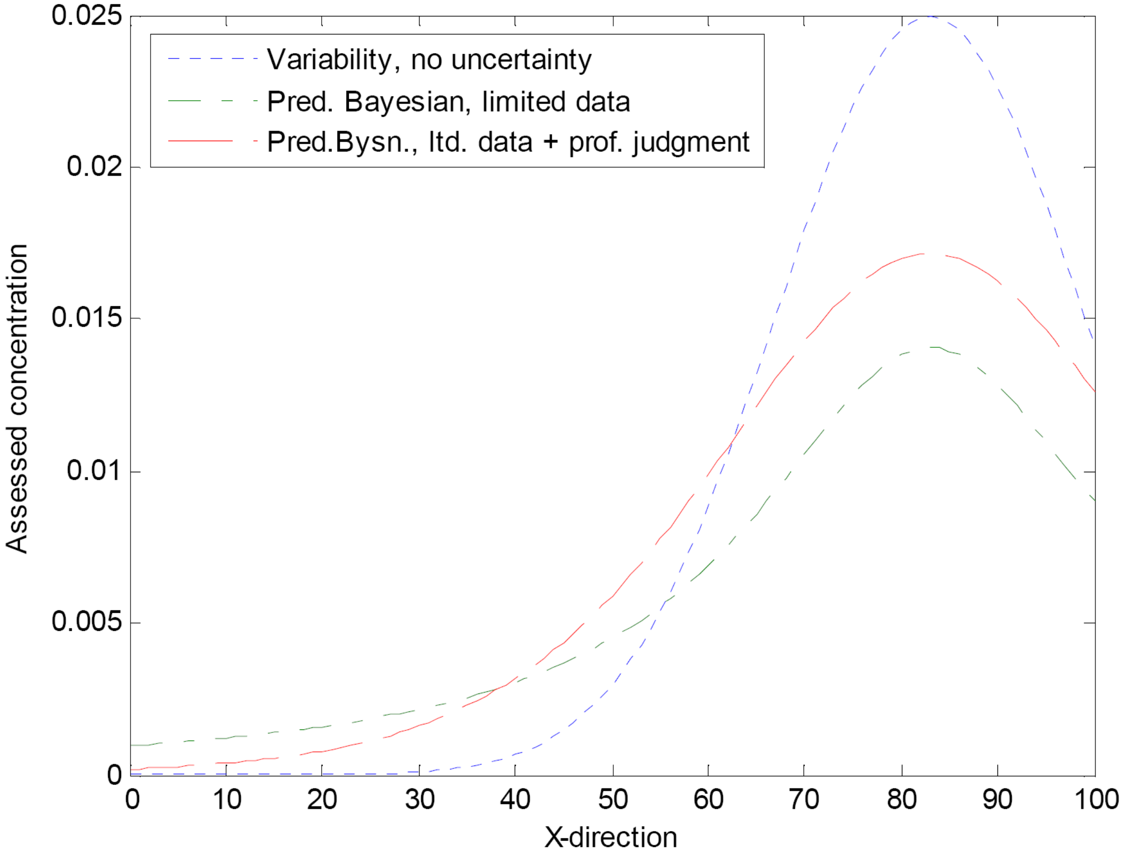

Figure 4.3. Distribution of physical variability assuming perfect information, or no uncertainty, and predictive Bayesian distributions based on limited data, and limited data with professional judgment, showing the decrease in information entropy with increased information availability.

The general predictive Bayesian analytical model that represents the unconditional probability of a particle of oil at $\mathbf{X} = (\mathbf{x}, \mathbf{y})$ is the following expression, in which the integration is over an uncertain parameter space:

$$\mathrm{f}(x, y, t) = \int \left( \sum_{j=1}^{J} \gamma_j \, \mathrm{f}_j (x, y, t \mid \mu_{x,j}, \mu_{y,j}, \sigma_{x,j}, \sigma_{y,j}, \rho_j) \right) \mathrm{L}(\mathbf{C}_\mathrm{i} \mid \boldsymbol{\mu}, \boldsymbol{\sigma}, \boldsymbol{\rho}, \boldsymbol{\gamma}) \, \partial\boldsymbol{\mu} \, \partial\boldsymbol{\sigma} \, \partial\boldsymbol{\rho} \, \partial\boldsymbol{\gamma} \qquad (4.1)$$

in which $\mathrm{f}_j(\mathbf{X}, t \mid \boldsymbol{\mu}_j, \boldsymbol{\sigma}_j, \rho_j)$ is the *j*-th Gaussian patch given knowledge of the range of parameters mean $\boldsymbol{\mu}_j = (\boldsymbol{\mu}_x \boldsymbol{\mu}_y)_j$, standard deviation $\boldsymbol{\sigma}_j = (\boldsymbol{\sigma}_x \boldsymbol{\sigma}_y)_j$, correlation coefficient $\rho_j$, and sunken oil fraction $\gamma_j$, with $\sum \gamma_j = 1$ to maintain conservation of mass; $\boldsymbol{\mu}_j = \mathbf{v}_j t$; $\mathbf{v}_j$ is the average velocity vector (**L**/T) of the *j*-th Gaussian patch; $t$ is time (T); $\sigma_j^2 = 2Dt$ is the standard deviation or measure of the effective "breadth" of the patch at time $t$; $D$ is the horizontal average sunken oil dispersion coefficient (L$^2$/T); and $L(\mathbf{C_i} \mid \boldsymbol{\mu}, \boldsymbol{\sigma}, \boldsymbol{\rho}, \boldsymbol{\gamma})$ is the likelihood function of the observed concentration data, $\mathbf{C_i}$, at the irregular sampling locations and times, in which $\mathbf{C_i}$ represents the vector of relative concentration data, ($C_1, C_{2,\ldots,} C_{i,} \ldots C_I$), at locations ($x_i$, $y_i$) and times, $t_i$. The parameter space is described as follows:

$$\boldsymbol{\mu} = \{(\mu_x, \mu_y)_1, \ldots, (\mu_x, \mu_y)_J\}$$

$$\boldsymbol{\sigma} = \{(\sigma_x, \sigma_y)_1, \ldots, (\sigma_x, \sigma_y)_J\}$$

$$\rho = \{\rho_1, \ldots, \rho_J\}$$

$$\gamma = \{\gamma_1, \ldots, \gamma_J\} \qquad (4.2)$$

Note that one of the patches has no $\gamma$ parameter since $\gamma_4 = 1 - (\gamma_1 + \gamma_2 + \gamma_3)$).

In essence, field data are sampled from a distribution of sampling variability around a mean concentration. This mean is modeled by the value of the multimodal 2-D Gaussian distribution at that point in space. The distribution of sampling variability was assumed to be exponential in form, because the maximum Shannon entropy distribution around a fixed mean over a non-negative range is exponential (Shannon, 1948). This form is proposed as the most likely distribution of concentrations that might be observed at a point on a bay bottom, by the Principle of Maximum Entropy (Jaynes, 1957). That is, entropy is the average log of the inverse height of the density and so, assuming normalization, is a measure of distribution "breadth." Therefore, maximizing entropy means maximizing the range of feasible outcomes and, all-the-more-so, the number of ways to satisfy the constraints. The ME distribution is then realized because it can be obtained in overwhelmingly many more ways. For example, the Gaussian diffusion equation itself results if the entropy of a distribution of diffused mass is maximized subject to independent constraints in terms of the mean (or advective velocity, controlled by pressure gradient) and the variance (or coefficient of diffusion, controlled by e.g. viscosity, temperature). Likewise, entropy can be the starting point in deriving many physical laws, if the governing constraints are known (Kapur 1989; Jaynes 1957).

Assuming an exponential distribution of oil concentration sampling variability around the mean, modeled by the multimodal Gaussian distribution, the likelihood function in Equation 4.1 can be written in terms of the relative concentration as follows:

$$\mathrm{L}(\mathbf{C_i} \mid \boldsymbol{\mu}, \boldsymbol{\sigma}, \boldsymbol{\rho}, \boldsymbol{\gamma}) = \prod_{i=1}^{I} \lambda \exp(-\lambda \mathbf{C_i}) \qquad (4.3)$$

in which $1/\lambda = \sum_{j=1}^{J} \gamma_j \, \mathrm{f}_j(x_i, y_i, t_i \,|\, \boldsymbol{\mu}_j, \boldsymbol{\sigma}_j, \rho_j)$. That is, it is assumed that the concentration sampled at a point in space and time comes from an exponential distribution of sampling error with mean $1/\lambda$.

The conceptual model, though Bayesian in character to address uncertainty and speed of computation, was developed primarily to accept field (sampling) data. Due to its structure, the capability for accepting prior information such as derived from bathymetry or professional judgment regarding model parameter values can be added as appropriate. Particular terms in the model are described in more detail in the following sections.

### 4.2.1 Assumed or specified parameter domains

It was determined in discussions with project advisors to design the model with capability for operation without specific information on average water velocity vectors and diffusion coefficients found on the bay bottom. Accordingly, default ranges of values were assigned for each of these parameters. The model uses these ranges as the ranges of integration for Equation 4.1. Default ranges are wide, as shown in Table 4.1, having been assigned based on literature values and initial confirmation runs, together with a margin of uncertainty. It is expected that default ranges can be refined further in the future. In addition, the SOSim model is equipped with an *Options* menu that can be used to change and set up the built-in default parameter ranges shown in Table 4.1.

| Parameter | Symbol | Units | Minimum | Maximum |
|---|---|---|---|---|
| Velocity in the east-to-west direction | $v_x$ | $km/d$ | -3.0 | 3.0 |
| Velocity in the north-to-south direction | $v_y$ | $km/d$ | -3.0 | 3.0 |
| Coefficient of diffusion in the east-to-west direction | $D_x$ | $km^2/d$ | 0.01 | 1.1 |
| Coefficient of diffusion in the north-to-south direction | $D_y$ | $km^2/d$ | 0.01 | 1.1 |
| Coefficient of correlation between directions | $\rho$ | [-] | -0.999 | 0.999 |
| Mass conservation weighting parameter | $\gamma$ | [-] | 0 | 1 |

Table 4.1. Default parameter ranges included in SOSim, which can be edited by the user.

### 4.2.2 Conditional bivariate Gaussian distribution

Mass concentration in a fluid subject to advection and dispersion in any media can be shown, for example by maximizing the Shannon entropy of a distribution of (oil) particles subject to a mean location and variance, to have a Gaussian concentration profile subject to bounds with real mean and real positive variance domains (Shannon, 1948). Conditional on knowledge of the parameter vector, a bivariate Gaussian is adopted as the conditional sampling distribution for the two-dimensional Bayesian model of sunken oil locations on a relatively flat bay bottom. Therefore, we have that:

$$f_j(\mathbf{X},t\,|\,\boldsymbol{\mu}_j,\boldsymbol{\sigma}_j,\rho_j)=\mathcal{N}(\mathbf{X},t\,|\,\theta_j)=\frac{1}{2\pi\sigma_{x,j}\sigma_{y,j}\sqrt{1-\rho_j^{\,2}}}\exp\left[\frac{-Bm_j}{2(1-\rho_j^{\,2})}\right] \tag{4.4}$$

in which $Bm=\frac{(x_m-x_0-\mu_x)^2}{\sigma_x^2}-\frac{2\rho(x_m-x_0-\mu_x)(y_m-y_0-\mu_y)}{\sigma_x\sigma_y}+\frac{(y_m-y_0-\mu_y)^2}{\sigma_y^2}$

and $\boldsymbol{\mu}_j$ and $\boldsymbol{\sigma}_j$ represent the two dimensional means and covariance matrices, respectively, for each patch. In Equation 4.4, $x_m, y_m$ are the coordinates of a point to be modeled, and $\theta_j$ represents the set of parameters $\boldsymbol{\mu}_j,\boldsymbol{\sigma}_j$ and $\rho$ as described in the conceptual model.

### 4.2.3 Bayesian posterior distribution

Bayesian methods involve first assigning a joint (that is, multivariate, to address all uncertain parameters) *prior* probability distribution to the uncertain parameters of a sampling distribution such as the Gaussian. This distribution is assigned based on non-numerical forms of information, such as bathymetry that might affect sunken oil locations. In the model developed, no prior information was assumed, such that the probability prior to data collection of finding oil on the bottom was constant spatially (for relatively flat ocean bottoms, dredged bays, reef flats and lagoons or pools protected by offshore rocks). Therefore, based on the Principle of Maximum entropy, the prior distribution was taken to be a uniform distribution over the uncertain parameter space. This can be done by setting the prior equal to unity as an arbitrary constant, so that it drops out of the equation, because normalization if required is obtained in a subsequent mathematical step.

A Bayesian *posterior* distribution is obtained as a refinement (narrowing) of the prior distribution using Bayes Law:

$$f(\theta\,|\,x_1,x_2,...,x_I)=\frac{L(x_1,x_2,...,x_I\,|\,\theta)\,\xi(\theta)}{\mathrm{g}(x_1,x_2,...,x_I)}, \tag{4.5}$$

in which $L(x_1,x_2,...,x_I\,|\,\theta)$ is the likelihood function, $\varepsilon(\theta)$ is the prior, and $\mathrm{g}(x_1,x_2,...,x_I)$ is the probability that the data was observed, a normalizing constant with respect to $\theta$. As mentioned previously, the total mass of sunken oil is generally unknown, and as a result the final predictive distribution need not be normalized, as a distribution of relative, not absolute, concentrations. Therefore, the normalizing constant, $\mathrm{g}(x_1,x_2,...,x_I)$, is also not needed, and the (un-normalized) posterior for the model becomes $f(\theta\,|\,x_1,x_2,...,x_I)\;\alpha\;L(x_1,x_2,...,x_I\,|\,\theta)\xi(\theta)=L(x_1,x_2,...,x_I\,|\,\theta)$.

### 4.2.4 Multimodality and Superposition

The model was developed as a multimodal Gaussian, to account for example for the presence of multiple patches of oil collecting on the bottom, or for oil concentrating more highly in deep bathymetric features at any or all times. The predictive model is able to infer from the data whether or not the sunken oil is distributed in single or multiple patches, and to track and predict this multimodal behavior in time. As a consequence, the assessed concentration profile can be, or become, either multimodal or unimodal in time. Results depend upon the data, as well as on boundary conditions, desired prediction times, and the resolution selected by the user.

The total mass of sunken oil is not typically known as a function of time, considering ongoing sinking and re-suspension processes. Therefore, computations of the model arbitrarily assume a constant mass of sunken oil with time, producing maps of relative sunken oil in space which identify areas with the most oil. As such, relative masses cannot be compared across time. Therefore, in an emergency response scenario, the occurrence of increases or decreases in the total mass of sunken oil over time would need to be assessed from the field data, for example, by inspection. With this basic assumption, the model can infer the relative mass of oil contained in each patch from the field data. This relative mass is represented by the parameter $\gamma_j$, representing the fraction of total sunken oil that belongs to the *j*-th patch, which can be considered the mass weighting parameter among patches. Summation of the $\gamma_j$ to a constant value over time was therefore one important test of internal model consistency used for verifying the model as it was developed.

An expansion of the Bayesian Bivariate Gaussian analytical expression for multiple modes shows how superposition is mathematically attained in the model:

$$f(\mathbf{X},t\,|\,\theta)_{overall} = \sum \gamma_j \mathcal{N}(\mathbf{X},t\,|\,\theta_j), \qquad \sum \gamma_j = 1 \tag{4.6}$$

That is, the overall conditional Gaussian sampling distribution is composed of the sum of any possible combinations of a weighting parameter, the fraction $\gamma_j$, among patches and a bivariate normal distribution $\mathcal{N}_j$ with parameters $\mu_{x\,j}, \mu_{y\,j}$, $\sigma_{x\,j}, \sigma_{y\,j}$ and $\rho_j$, that represents a single mode or oil patch $j$, such that the sum of the weighting parameters is equal to one. To maintain this sum equal to unity over multi-dimensional integration operations with some computational efficiency, an algorithm based on combinatorial mathematics was developed, as described in the section Algorithm and Code Development.

### 4.2.5 Projecting the oil mass in time

The concentration profile in a (one dimensional) media following the instantaneous introduction of a mass, *M*, can be found either starting with the Fick's Law-based advection-diffusion equation and applying the inverse Fourier transform (Chin, 2006), or solving the random walk model for a particle (of oil) (Einstein, 1925). The result takes the form of a Gaussian distribution with variance growing in time:

$$c(x,t) = \frac{M}{A\sqrt{4D_x t}} \exp\left( -\frac{(x_0 - vt)^2}{4D_x t} \right), \tag{4.7}$$

in which $D_x$ is the uncertain diffusion coefficient of a Gaussian path in one dimension [L$^2$/T], $vt$ is the distance the mass $M$ has traveled from the initial point $x$, $v$ is the uncertain mean velocity vector of the Gaussian patch [L/T], and $A$ is the transverse area of mass introduction. In the model developed, the mass per unit area, *M/A*, of sunken oil is taken as an arbitrary constant.

Comparing the fundamental solution of the diffusion equation (Equation 4.7) to the equation of a Gaussian distribution (Equation 4.4 in one dimension), it is seen that $\mu = vt$ and $\sigma = \sqrt{2Dt}$. Furthermore, by the time an oil mass reaches the bottom of the sea from the initial aerial spill location ($x_0, y_0$), it will already be characterized by an initial velocity and an initial diffusion coefficient, which results in:

$$\boldsymbol{\mu} = \mathbf{v}_0 + \mathbf{v}t \qquad \text{and} \qquad \boldsymbol{\sigma} = \boldsymbol{\sigma}_0 + \sqrt{2\mathbf{D}t} \tag{4.8}$$

Equations 4.8 contribute uncertain parameters to the likelihood function which vary with sampling time, and to the Gaussian model which vary as a function of user-defined times of oil mass prediction.

### 4.2.6 Taking Into Account the Potential for Sinking and the Short-Term Weathering

The SOSim model infers oil location as a function of time by comparing the initial point of accumulation with data on its distribution at a later point in time. If only one sampling campaign is available, the initial point of accumulation is critical to these predictions in time. While many times the spill location and time are known, and may represent the initial point of accumulation for floating oil, the initial time and point of accumulation are not as well known for sunken oil, depending on oil density, sediment entrainment, and other factors. In fact, while oil may take a week or more to start a weathering process that may result in sinking, Type 4, 5 and 6 oils start a process of sinking by gravity immediately after abrupt release or during a continuous spill event (each oil type at its own pace).

For the SOSim model, the initial spill time is indicative of the major release at the actual coordinates of the accident at the surface, but the approximated time at which oil starts to collect at the bottom is really what defines the framework of the model with respect to time. The difference between the spill time and the time at which oil starts to collect at the bottom is considered a "retardation factor", included in the model as a function of the oil type as identified by the user. Oil is identified as one of the accepted Types 1 through 6 described in the literature review, accounting for multiple properties of oils related to the potential for sinking by gravity and for weathering by evaporation and/or dissolution. Accordingly, all times that modify the likelihood of finding sunken oil at a given location are adjusted by the *retardation factor*, *RF*, as $t = t - RF$ , in which *RF* reflects an assessed, generalized delay associated with the particular oil type before starting to collect at the bottom. It is assumed that no sampling campaigns will be useful if performed before the assessed retardation gap.

### 4.2.7 Incorporating Multiple Sampling Times

In order to better account for changes in sunken oil movement due to e.g. tidal action, storm events, and sediment entrainment, the model was built with capability for accepting data from multiple sampling campaigns (sampling campaigns performed at different times and different areas). Input of data subsequent to the initial sampling campaign increases the number of product terms in the likelihood function, increasing the information content and increasing information concerning oil movement, in particular.

The likelihood function of the observed data, $\mathbf{C_i}$, at each i-th irregular sampling location and times with respect to the uncertain parameter space is:

$$\mathrm{L}(\mathbf{C_i} \mid \boldsymbol{\mu}, \boldsymbol{\sigma}, \boldsymbol{\rho}, \boldsymbol{\gamma}) = \prod_{i=1}^{I} \lambda \exp(-\lambda \mathbf{C_i}) \tag{4.3}$$

in which $\mathbf{C_i}$ represents the vector ( $C_1, C_2, ..., C_i, ...C_I$ ) of measured concentrations at different location-times. The SOSim GUI allows up to ten different sampling campaigns or times, with an unrestricted number of sampling locations at each time.

### 4.2.8 Development of Boundary Capabilities by the Method of Images

The method of images (or method of image charges in electrostatics, or reflection theory in physics) was used in the SOSim model as a numerical approach to calculate the reflection of sunken oil from shorelines in nearshore spill scenarios. The physical reality of the ocean boundaries (the shoreline) is approximated to an ideal condition in which a "relatively-flat ocean bottom" is truncated by a theoretically vertical barrier that is assumed to retain the sunken oil without compromising the oil's mass conservation and the Fickian nature of the transport process; that is, it is assumed that phenomena that might occur close to a shoreline environment such as oil adsorption onto the barrier's material or flow into the porous medium do not occur. Figure 4.4 replicates the physical approximation in one dimension. The method is used as a numerical approach to calculate the effect of the vicinity of coastlines in oil spill scenarios.

The scheme used in this research also involves the assumption of uniqueness of the current modeling conditions, maintaining conservation of mass, while redistributing it consistent with each source and at each time within the nearby boundaries imposed by the  geometry of the coastal zone, approximated and projected to the bottom (see Figure 4.4). A novel implementation using a polyline approximation of shoreline geometry was developed and implemented in SOSim, as described in this section.

Consider an example in which an oil patch is denominated ‘the source’. The source occurs at a certain point $(x_0, y_0) = (x, 0)$ on the bottom of a bay and has a concentration distribution $c(x, y)$. This point lies at some distance $x$ from the shoreline which, by definition, has a concentration gradient of zero. As the patch approaches the shore, oil at the leading edge begins landfall. It is then assumed that this oil mass is reflected back into the water, producing an accumulation in the nearshore environment by the principle of superposition. In one dimension the reflection is easily computed as a sum of the inflowing mass and the reflected mass. However, in two dimensions when the shoreline is not straight, reflections are not perpendicular with respect to only one line and calculations become cumbersome. Therefore, (relative) mass accumulation is computed in SOSim by setting up imaginary conditions to replicate the curve of the boundary. The method of images momentarily replaces the boundary by an “image source” or a “reflection”, equal in concentration distribution but located at opposite coordinates $(-x, 0)$ across the boundary. This new situation is equivalent to the original layout because superposition of the source and its reflection concentration distributions will simulate the zero concentration gradient at the boundary and will account for spreading and contention of oil. The result is then the summation of concentration distributions on the source side, and all results imagined to occur beyond the boundary can be ignored. Figure 4.4 depicts the concept.

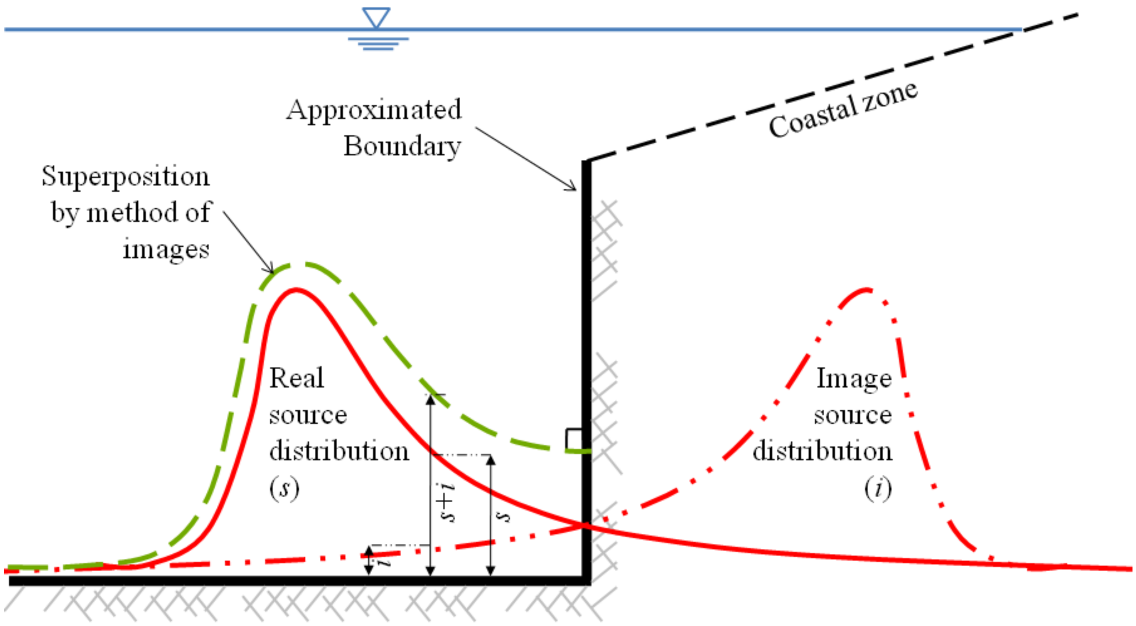
Approximated Boundary
Coastal zone
Superposition by method of images
Real source distribution (*s*)
Image source distribution (*i*)
s+i
s
i

Figure 4.4. Graphical depiction of the physical idealization of the boundary conditions to apply the Method of Images in the SOSim model.

In the single boundary case described above, no other boundary has effect on any of the sources, and thus reflection stops at once and the case is considered of zero order. When multiple boundaries coexist, reflections are not perpendicular with respect to only one line but instead it is assumed that they are perpendicular with respect to each segment of a boundary interpreted as a series of connected lines, where every single source is reflected with respect to each of the line segments. In the application of the method of images in groundwater hydraulics to modeling flow near aquifer boundaries, the source is reflected with respect to each horizontal or vertical aquifer boundary, and each subsequent reflection is in turn affected by the boundary that did not reflect it before (Bear, 1979 and Todd, 2005).  This approach to considering perpendicular or parallel boundaries (that are not necessarily contiguous) was adapted and implemented for the case of non-orthogonal contiguous line segments representing geographical boundaries to sunken oil movement. That is, the requirement for perpendicular or parallel boundaries was relaxed using a new method developed to address the change in correlation between the x and y directions. The multi-reflection process creates a series of mass imbalances that must be balanced back with further reflections. As a result, computation must be iterated to attain both mass conservation and zero-concentration gradient values at the shoreline.

To approximate shorelines with polylines, the user is shown a map of the spill area, and instructed to click on the map to define up to 10 vertices. These vertices are connected by straight lines to approximate the shoreline contour. The algorithm allows the addition of as many superimposed terms as needed to the conditional Gaussian bivariate distribution. However, computational demands increase nonlinearly with the number of vertices, due to the nature of the numerical integrations across the multi-dimensional parameter space and the combinatorial numerical approach. Therefore, the program incorporates a limit of ten vertices.

This approach, like many numerical methods, requires a stopping rule to define the limit of iteration needed to obtain an acceptable solution. In this research, it was found that the sum of second and lower order reflections provided sufficient detail to obtain an observable mass balance in the water body. Thus third and higher order reflections are neglected, greatly reducing computational demands (currently model runs require several hours on desktop computers). Also, because the Gaussian tail is mathematically infinite, reflection is calculated beginning when a patch center reaches a distance of $2\sigma$ from the shoreline, and ending when the tails of the outgoing source and the incoming image have already "crossed" (refer to Figure 4.4) and no longer sum to a value higher than the concentration at the mean $\pm 2\sigma$. To prevent calculation of sunken oil projections at times beyond the estimated time of landfall, when the patches would appear to "bounce" off of the shoreline, a warning message is issued by SOSim when the requested prediction time is estimated *a priori* to be beyond the time of landfall. Such prediction times are beyond the reasonable capability of SOSim to assess relative concentrations.

### 4.2.9 Integration to obtain the predictive relative concentration profile

Several different integration techniques were considered for the multivariate integration expressed in Equation 4.1. The first was an analytical solution, which is available for the predictive Bayesian multinormal distribution (Aitchison and Dunsmore, 1975). However, no solution is available for the multimodal analog, that would allow the inference of varying numbers and weights of multiple patches of oil. Second, the use of Markov chain Monte Carlo (MCMC) simulation was considered, to generate vectors of random variates sampled from the Bayesian posteriors over which averages could be computed at each point in space and time. MCMC is the most popular approach to computation of Bayesian posteriors. However, the approach was not considered likely to estimate posteriors successfully, due to the high dimensionality of the model, without the development of new computational approaches. In addition, the principal advantage of the approach is the ability to compute the normalizing constant for the likelihood function, not needed in the SOSim model. Moreover, the distributions applicable to the uncertain parameters of a Gaussian distribution are not highly skewed, and are therefore relatively easy to integrate as a discretized sum. Therefore it was concluded that the most efficient approach would be a direct Riemann sum approximation. The approach involves approximating the volume under a surface (or area under a curve) as a sum of small differential volumes, partitioned over the domain of the parameter space. Figure 4.5 shows the basic principle of the Riemann sum integration.

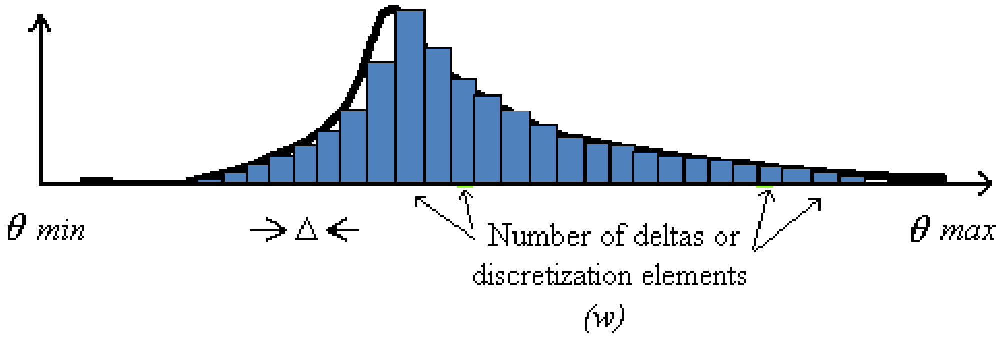

Figure 4.5. Sketch of a Riemann sum concept with forward approximation to the function (the value on the curve corresponds to the first discretization value of each element).

The Riemann sum requires one initial input: the approximate domain of the uncertain parameters. As mentioned, default values for this range are included in the model based on literature information and statistical principles, and handled as explained in the section Algorithm and Code Development. The Riemann sum integration, though simple in concept, consumes considerable computational resources in the SOSim model because of model dimensionality and the programming structure required in the Python programming language used. Algorithms are explained under Algorithm and Code Development, including how the resolution of the integration (the number of discretizations of each parameter range) are related nonlinearly to the number of oil patches and to the precision of prediction.

### 4.2.10 Geographical Versus Modeling Units

Sampling campaigns should be recorded and accepted by the model in World Geodesic System (WGS) units (degrees, minutes and seconds expressed in decimal degrees in the GUI prompts). Interaction of the user with the canvas of the graphic user interface also results in operations in WGS units, because none of the embedded maps are projected to a flat surface. Equations 4.4 to 3.8, on the other hand, all require distances in planar units (SI or metric system). Therefore, conversions using the Universal Transverse Mercator (UTM) projection are used to translate WGS input into distances in km that can be used in the diffusion, advection, and statistical equations, and to convert gridded model output back to WGS format for graphical presentation in map format. The process, other than involving the creation of global Python functions for the conversions, engages certain computational algorithms to guarantee that (a) precision is not lost in the double conversion process (error is on the order of 1e-9), and (b) operations over points located at overlapping borders of UTM zones are correctly converted without affecting precision and guaranteeing that user inquiries concerning the locations of sunken oil are accurately displayed on the map canvas of the GUI application.

### 4.2.11 Algorithm and Code Development

This section describes algorithm and code development, including the programming environment chosen, algorithms developed for implementation, and graphical user interface development.

#### 4.2.11.1 Python: The Programming Language:

The Python programming language was chosen for development of the SOSim model in discussions with NOAA based on the following criteria:

- The programming software is non-proprietary and open source,
- The programming environment supports relatively rapid prototyping and testing,
- The language is robust in terms of functioning in various operating environments with minimal damage, alteration or loss of functionality, and
- The source code is viewable at all times.

Python is a general-purpose, high-level programming language first released by Guido Van Rossum in 1991 in The Netherlands. Python is flexible, applicable to many programming domains and available on many platforms. The language has an open, community-based development model managed by the non-profit Python Software Foundation. Python's design philosophy emphasizes programmer productivity and code readability (core syntax and semantics are minimalistic, employing white spaces and easy commands). Python supports multiple programming paradigms (primarily object oriented) and features a fully dynamic type system and automatic memory management, similar to Perl, Ruby, Scheme, and Tcl.

The Python programming language has an open, general public license (GPL) that allows source code modification, addition of original code as "imported" packages, and publication of derived work (as GPL). Packages that are created around the world are available to the Python community. Python has also been used as an extension language for many existing systems, including GIS, Web programming, numerical tools, and the R statistical package.

The SOSim model, although using and relying for much of its functionality on several existing Python packages and modules, consists of three principal Python modules developed by the research team: the graphical user interface (GUI) module, the operating and processing interface (OPI) module, and the core module. The GUI module (ui_SOSim.py in the electronic deliverable) automatically lays out and retains characteristics of widgets, labels, canvases and templates in the graphical user interface, retains raw user input, and imports Windows palettes and display. The OPI module (SOSimOPI.py in the electronic deliverable) is the executable file. It imports and links all other modules, captures input information entered by the user in the GUI module, and operates interrelated buttons and activities of the GUI; it filters, organizes, and processes the input; passes ready-to-use variables and attributes to the core code; accepts modeling results back from the core module; processes the results; and sends display signals to the canvas layout of the GUI module to allow it to depict relative sunken oil concentrations on a map for further user interaction. It also controls modal behavior of the main windows, pop outs, menus and toolbars. The core module (SOSimCore.py in the electronic deliverable) uses variables and attributes passed by the OPI module to compute the predictive Bayesian relative concentrations, saves output files, and passes results back to the OPI module for display by the GUI or for further use. The GUI has the capability to communicate with the core module through the OPI module during a model run, after a predictive result has been presented, to allow the user to request the modeling of contiguous or other areas as needed.

### 4.2.11.2 Software Development

The SOSim software is in essence a PyQGIS - PyQt application. PyQGIS are the Python bindings of the Quantum Geographic Information System (QGIS) software, consisting of three modules written in Python. QGIS is an official project of the Open Source Geospatial Foundation (OSGeo), distributed under the GNU General Public License. The main components of QGIS are the GDAL library and the GRASS geographic information system, both written in Python. QGIS is multi-platform and supports numerous vector, raster, and database formats and functionalities. The use of the PyQGIS bindings allowed the research team to use all the functionalities of QGIS through scripting in Python, to build an original interactive GIS computer application. The PyQGIS end product is an interactive map canvas that is embedded in PyQt as a widget.

PyQt are the Python bindings of the Qt project, a C++ toolkit for cross-platform application development owned by Nokia. Like some versions of the Nokia's Qt, PyQt is open source, free software developed by the British firm Riverbank Computing and distributed under a variety of licenses including GNU General Public License (GPL) and commercial license. PyQt is implemented as a Python extension module, in such a way that it can be incorporated into a customized Python installation and used from the Python console or any editor. Computer applications developed in PyQt have the capability to support Linux, Unix, Mac OS X and Microsoft Windows. Version 1.0.2 of PyQGIS under OSGeo4W Kore distribution and version 4.4.3 of PyQt were used to develop the SOSim model. GUI programming aids were adapted from Summerfield (2007) and online developer communities (QGIS Organization, 2009; Qt Development Frameworks, 2009).

The SOSim computer application falls in the category of software derived from Python, PyQt and PyQGIS.  As such, the Python Software Foundation requires that the application developed be open source and have a GPL license (PSF, 2001). The terms for distribution, expansion and derivation of new tools from the current version 1.0 of SOSim are included in the executable and source code distribution as required by law.

#### 4.2.11.3 Bayesian Computational Methods

Bayesian computations are distributed throughout three Python classes located in the core module of SOSim. Each class, by definition of object-oriented programming, contains methods. The term *methods* refers to functions that perform unique activities to define and to provide different actions to its class, to be used by an extra parameter which is the object that it is to run on, and which belongs within the same class.

The first class, called *Preliminars*, involves calculating and passing initial setup, global constants and global variables to the other two classes, named *LF* and *Model*, whenever needed. Initial setup includes, for each of the four patches: an assumed integration domain for the coefficient of diffusion, $\mathbf{D}$, and velocity, $\mathbf{v}$, vectors; the domain of the correlation coefficient, $\rho$, from -0.999 – 0.999; and the domain of and restrictions on the weighting parameter, $\gamma$. Global constants include the number of discretization elements, *w*, of the domain of the parameters (the same number for all parameters) and the magnitude of the partial differential elements, $\partial\mathbf{D}, \partial\mathbf{v}, \partial\rho$ and $\partial\gamma$, based on *w*. Global variables are directly related to the programming structure of the Bayesian algorithm, and are produced within the *Preliminars* class using the *doAll( )* method. Note that in order to facilitate reference to the parameters in this report, parameters have been divided in two types: the Gaussian parameters and weighting parameters. The first group includes $\boldsymbol{\mu}_j, \boldsymbol{\sigma}_j$ and $\rho_j$, a total of 5 parameters per patch and 20 overall for four possible patches. In the second group there are the weighting parameters $\gamma_j$, one per patch. The weighting parameters each have the same domain, {0, 1}, but a shared and conditional codomain, $\sum_{j=1}^{J} \gamma_j = 1$, so that one of the four weighting parameters is not variable but is fixed by the values of the remaining three.

The *doAll( )* method starts by finding all possible quadruplets of the weighting parameter, $\gamma$, of each patch; that is, by placing all quadruplets of weighting parameters $\gamma_1, \gamma_2, \gamma_3$ and $\gamma_4$ that sum to one in a global variable *GammaPossible* of type Python list. This operation is performed accounting for the order of the patches. Thus, further combinatorial operations involving only the possible values of weighting parameters will have the same sorting and can therefore be related. Other important global variables defined in the *doAll( )* method are: the number of valid weighting parameter combinations that sum to one (*valid*); the total number of positions (*sze*) that would result in a hypothetical array of 5 dimensions (one per Gaussian parameter in a single patch) in which each dimension is discretized equally (using the discretization constant *w*); and the number of possible sums of bivariate Gaussian combinations times weighting parameter values among patches (*newsze*), that would honor the conservation of mass restriction on the weighting parameters.

The second class of the core module of SOSim is named *LF*, standing for Likelihood Function. This class executes all operations needed to compute Equation 4.3:

$$\mathrm{L}(\mathbf{C_i} \mid \boldsymbol{\mu}, \boldsymbol{\sigma}, \boldsymbol{\rho}, \boldsymbol{\gamma}) = \prod\nolimits_{i=1}^{I} \lambda \exp(-\lambda \mathbf{C_i}) \tag{4.3}$$

in which $1/\lambda = \sum_{j=1}^{J} \gamma_j \, \mathrm{f}_j(x_i, y_i, t_i \mid \boldsymbol{\mu}_j, \boldsymbol{\sigma}_j, \rho_j)$ and $\mathrm{f}_j(x_i, y_i, t_i \mid \boldsymbol{\mu}_j, \boldsymbol{\sigma}_j, \rho_j)$ is the bivariate Gaussian probability function modified by a variable number of Gaussian terms representing superimposed reflected images in the case that a sampling campaign occurs in the nearshore environment. Expanding the function for open-ocean conditions,

$$\mathrm{f}_j(\mathbf{X}_i, t_s \mid \boldsymbol{\mu}_j, \boldsymbol{\sigma}_j, \rho_j) = \mathcal{N}(\mathbf{X}_i, t_s \mid \theta_j) = \frac{1}{2\pi\sigma_{x,j}\sigma_{y,j}\sqrt{1-\rho_j^{\,2}}} \exp\left[\frac{-B_{i\,j}}{2(1-\rho_j^{\,2})}\right] \tag{4.4}$$

in which $B_i = \dfrac{(x_i - x_0 - \mu_x)^2}{\sigma_x^2} - \dfrac{2\rho(x_i - x_0 - \mu_x)(y_i - y_0 - \mu_y)}{\sigma_x \sigma_y} + \dfrac{(y_i - y_0 - \mu_y)^2}{\sigma_y^2}$.

The initialization arguments of the *LF* class include input from the *Preliminars* class (parameters settings and variables) and input from the GUI through the OPI module (processed spill coordinates, $x_i, y_i$, and sampling campaigns, $s$, in terms of processed longitudes, latitudes, concentrations, and sampling times, $t_s$). Equation 4.3 is solved using the *LF* class' method *calculateLV.* The first step in solving this equation is to find $\lambda$ at each sampled point $i$, by finding, for each sampling point, the inverse of the sum of the bivariate Gaussian distributions of all patches, maintaining complete and balanced sunken oil mass within their collective volume.

In order to evaluate the complete parameter space at each sampling point, the concept of a hypothetical array of 5 dimensions, one for each Gaussian parameter within a single patch, was adopted, in which each dimension takes *u* = *w*+1 discretized values representing the endpoints of the *w* discretizations of the parameter range. Now, proceeding conceptually to fill all positions within the array with the corresponding result of the bivariate Gaussian distribution $\mathrm{f}_j(x_i, y_i, t_s \mid \boldsymbol{\mu}_j, \boldsymbol{\sigma}_j, \rho_j)$, it can be seen that the values of $\mathrm{f}_j(x_i, y_i, t_s \mid \boldsymbol{\mu}_j, \boldsymbol{\sigma}_j, \rho_j)$ at time $t_i$ change from one sampling point, ($x_i$, $y_i$), to another. In the *calculateLV* method code, since a matrix analysis of this dimensionality is not possible in Python, a set of nested loops finds and annotates to disk the $\mathrm{f}_j(x_i, y_i, t_s \mid \boldsymbol{\mu}_j, \boldsymbol{\sigma}_j, \rho_j)$ value for each and all *positions* within the hypothetical array, that is for each sampling point at every sampling time. Thus, each annotation of $\mathrm{f}_j(x_i, y_i, t_s \mid \boldsymbol{\mu}_j, \boldsymbol{\sigma}_j, \rho_j)$ becomes an element of a Python list object, which is stored on disk to reduce memory footprint.

To this point, the description has been of an array corresponding to the first patch. However, it can be seen that because the possible domain of the Gaussian parameters is the same for all four patches, the array described (stored in a Python list object) is the same, such that it contains the same values, for all patches. Once the value of $\mathrm{f}_j(x_i, y_i, t_s \mid \boldsymbol{\mu}_j, \boldsymbol{\sigma}_j, \rho_j)$ at all positions is recorded, the superposition of patches is computed using the four identical 5-D conjectural arrays (actually, Python list objects, hypothetical structures with all values positioned in a list on file). Referring to the set of values of $\mathrm{f}_j(x_i, y_i, t_s \mid \boldsymbol{\mu}_j, \boldsymbol{\sigma}_j, \rho_j)$ at each position, for the *j*-th patch, as $\mathcal{N}_j$, superposition consists mathematically of summing $\gamma_1\mathcal{N}_1 + \gamma_2\mathcal{N}_2 + \gamma_3\mathcal{N}_3 + \gamma_4\mathcal{N}_4$, in all possible ways (to use the entire domain of the weighting parameters $\gamma_j$) such that weighting parameters sum to unity, $\sum_{j=1}^{4}\gamma_j = 1$. Because the 5-D hypothetical array is the same for every patch, $\mathcal{N}_{k,j} = \mathcal{N}_{k,1} = \mathcal{N}_{k,2} = \mathcal{N}_{k,3} = \mathcal{N}_{k,4}$, in which the subscript $k$, $1 \le k \le K = u^5$, is a position index indicating a sampling point and time and a point in the uncertain parameter space.

Figure 4.6 illustrates the computation of superposition using all possible combinations of $\mathcal{N}_{k,j}$ values, for $\gamma_j$. As shown, the X-axis contains weighting parameters, $\gamma_j$, discretized in steps of 0.1. The Y-axis represents the patches, *j* = 1 - 4. The Z-axis represents the values $\mathcal{N}_{k,j}$. The line traced in the Y-Z plane joins one parameter vector-sample (position), $k$, of a patch with another one, representing just one of the possible combinations of $\mathcal{N}_{k,j}$. The line traced in the X-Y plane represents one possible combination of values of $\gamma_j$. The superposition combination in this figure would be the product of the $\mathcal{N}_{k,j}$ values indicated by a star for the first patch, plus the product of the $\mathcal{N}_{k,j}$ values indicated by a star for the second patch, and so on for the remaining two patches. Exploration of all the possible combinations and the summations is performed in the code using the *GammaPossible* variable array and the *validList( )* generator.

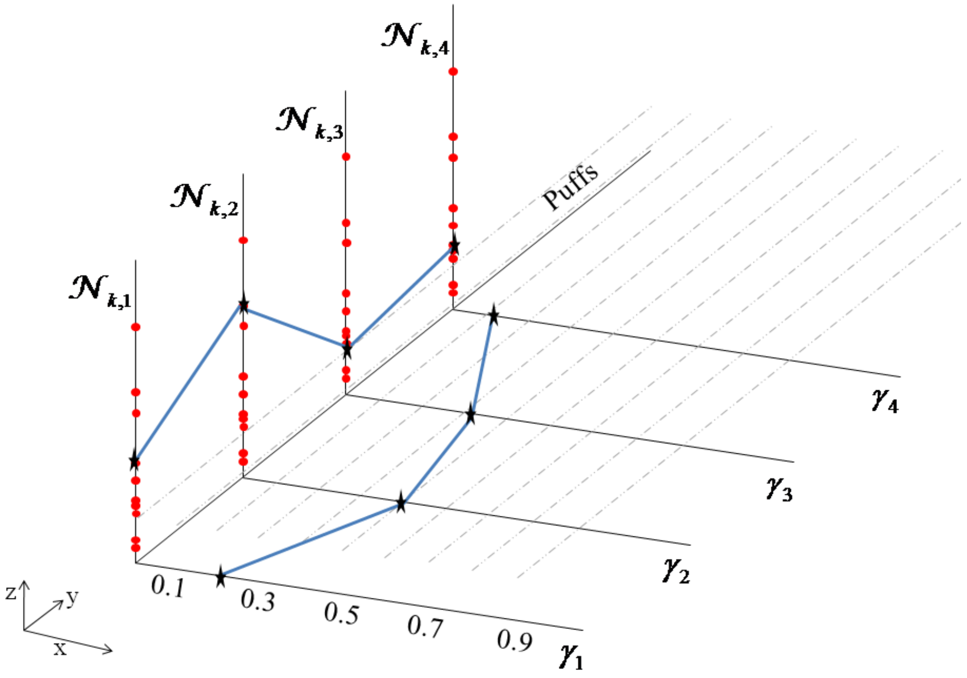

Figure 4.6. Representation of the superposition concept in three dimensions.

*GammaPossible* is one of the variables produced by the *Preliminars* class under the *doAll( )* method. In its initialized form, *GammaPossible* is an empty list. One sub-list is added at a time when four counters traveling through four zero-to-one $\gamma$ domains encounter four fractions that sum to one, e.g.: a sub list [0.2, 0.4, 0.3, 0.1] is added to the *GammaPossible* list for the example shown in Figure 4.6. All possible combinations that comply with $\sum_{j=1}^{4}\gamma_j = 1$ are appended to *GammaPossible* in this fashion. Components to assemble the superposition list, representing $1/\lambda$ in Equation 4.3, are completed with the *GammaPossible* list, but require an organized one-by-one generation that is attained in the next step.

A generator is a Python structure comparable to a function: the generator, instead of returning a final, condensed variable, has the capability of 'yielding' one individual result of a loop calculation at a time, at the point requested by the developer, until the series is exhausted. Generators are resource-efficient and add versatility to the code while reducing memory footprint and, in most cases, run time. The generator *validList( )* yields individual superposition values as long as the iterating loop has not been exhausted. The computational methodology for the generator includes looping over the Y-Z plane of Figure 4.6 (*sumComb* argument in the code) to find possible combinations of $\mathcal{N}_{k,j}$, and coupling them with each of the *GammaPossible* sublists that are equivalent to all possible combinations in the X-Y plane of the same figure. Individual superposition yielding for each weighting parameter combination *z* in *GammaPossible* is called later in the process of building $\lambda$. The total number of elements yielded by the *validList( )* generator is $Z\left(u^{5}\right)$, in which $Z$ is the number of ways of combining the four weighting parameters $\gamma_j$ such that $\sum_{j=1}^{4}\gamma_j = 1$, and the exponent five accounts for the number of Gaussian parameters per patch. The *validList( )* generator is staged, meaning that it has the capability to divide the total number of elements yielded into different $Z$ groups of $u^5$ yieldings each, depending on the particular combination $z$ being analyzed.

Continuing in the *calculateLV* method of the *LF* class, the components needed to compute Equation 4.3 are now available. A local variable *supValue* is set equal to each superposition result using a *validList( )* generator object, to compute likelihood values for each $z$, according to Equation 4.3. The precision limits in Python are set at approximately $10^{-300}$ and $10^{300}$, and so variables holding superposition results of such orders of magnitude must be avoided to prevent numerical error. If *supValue* > 1e-300, then a likelihood value $LVComb_{k,z,i}$ is calculated as

$$LVComb_{k,\ z,i} = \frac{1}{supValue_{k,z,i}}\exp\left[-\frac{1.0}{supValue_{k,z,i}}C_i\right]$$ for every $i$-th sampling point, *z*-th combination, and *k*-th possible element within. If $LVComb_{k,z,i}$ is different from zero, this *k*<sup>th</sup> term is included as a term in the sum for the likelihood function of the currently analyzed combination, $z$, and if $LVComb_{k,z,i}$ is equal to zero, it is discarded. The summation

$\sum_{i=1}^{I}\ln\left(LVComb_{k,z,i}\right)$ for each $z$ is performed across sampling points, $i$, not across the $k$ elements of the array according to the definition of a likelihood function. This process leaves a sum for each $z$, which is still a 1-D array with $k$ positions. Note that $\sum_{i=1}^{I}\ln\left(LVComb_{k,z,i}\right)=\prod_{i=1}^{I}LVComb_{k,z,i}$ .

To compute this sum in code, the variable *Likelihood* is of type 2-D array, with $Z$ positions in the first dimension and $k$ positions per $z$ element. The *Likelihood* variable can also be understood as one *K*-element, 1-D array per each possible weighing parameter combination $z$. While the loop for a point $i$ is being performed, each value in the $k$ position is added to the natural log of the $LVComb_{k,z}$ value that is being produced for the current sampling point. This procedure is repeated until all sampling points in all campaigns are exhausted. As a result, the likelihood function remains a 2-D array with $K$ elements per each $z$ combination, each position inheriting the combinatorial nature of its immediate predecessor, $LVComb$ . The last set of instructions performed by the *calculateLV* method occurs outside of the looping structure because the information from all the sampling points and times is already contained in the *Likelihood* local variable. The maximum among the $z$ -dimensions of the 2-D array is computed and the selected maximum (a 1-D array with $K$ elements that belong to the most likely combination, $z$ , of weighting parameters, $\gamma_j$ ), becomes the natural log of the final likelihood function. The preceding maximum likelihood calculation allows for the knowledge of the most likely values of the weighting parameters that have been selected to be employed in successive computations. Then for every position, $k$, in *Likelihood*, the numerical value is transformed back to the linear domain as $Likelihood_k = \exp(Likelihood_k)$. The *Likelihood* array is then the likelihood function. The *LF* class accomplishes these tasks and frees memory by writing the *Likelihood* array to disk for further use.

The third Python class of the core module of the software developed to perform the Bayesian calculations is the *Model* class. The main objective of the *Model* class is to complete the computation of Equation 4.1, by computing the conditional bivariate Gaussian distribution, multiplying this result by the likelihood function, and integrating over the parameter space. The latter is found in the code of the method *calculateCG( )*. However, the *Model* class includes many other Python methods that share responsibilities with the SOSimOPI.py module, such as assigning boundary conditions to the Gaussian equations, managing coordinate systems (WGS v. UTM), and managing model spatial resolution, units and mapping.

The *calculateCG( )* method uses a programming approach similar to that described for computing the bivariate Gaussian distribution values and superposition for the likelihood function. The principal difference is that the conditional distribution is computed at the nodes, $\mathbf{X}_m$, of a regular grid defined for the region of the spill, and user-specified times, $t$, of prediction, instead of at the locations, ($x_i$, $y_i$), and times, $t_s$, of field sample collection. The arguments passed to the *calculateCG( )* method include grid coordinates, prediction times and a Boolean variable indicating the presence of land within the modeling area.

Consider again the hypothetical 5-D array (one dimension for each parameter of a single Gaussian patch), in which each dimension has *u* discretized values. Again, the parameter space is evaluated over the bivariate Gaussian function, written for this case as $\mathrm{f}_j\left(\mathbf{x}_m, t \mid \boldsymbol{\mu}_j, \boldsymbol{\sigma}_j, \rho_j\right)$. The function is evaluated using the same nested programming structure as described for the likelihood function, with each position written to a Python list object stored on disk. Again, because the same parameter domain is used for all four patches, the new Python list object is identical for all patches. After the value of $\mathrm{f}_j\left(\mathbf{x}_m, t \mid \boldsymbol{\mu}_j, \boldsymbol{\sigma}_j, \rho_j\right)$, modified or not by the boundary conditions, is written to the list for all positions, superposition is performed as before, with the difference that the most likely combination of weighting parameters has already been selected by the likelihood function using the data. That is, letting $\mathrm{f}_j\left(\mathbf{x}_m, t \mid \boldsymbol{\mu}_j, \boldsymbol{\sigma}_j, \rho_j\right) = \mathcal{CN}_j$, the sum $\gamma_1\mathcal{CN}_1 + \gamma_2\mathcal{CN}_2 + \gamma_3\mathcal{CN}_3 + \gamma_4\mathcal{CN}_4$ is computed subject to $\sum_{j=1}^{4}\gamma_j = 1$, which has been already accomplished. The procedure depicted in Figure 4.6 is used to find the 1-D array of superimposed values, $CG_{k,m}$, each value representing a possible parameter vector, for each node, $\left(x_m, y_m\right)$, of the user-defined modeling grid. The number of possible elements is now the total number of elements yielded by the *validList( )* generator when it uses the $\mathcal{CN}_j$ values as one of its arguments and the most likely weighting parameter combination, $z$, as another argument (instead of the complete *GammaPossible* list of possible combinations).

The $CG_{k,m}$ arrays are used directly in the integration, according to Equation 4.1, of the product of the conditional Gaussian sampling distribution by the Bayesian posterior distribution, the latter of which is equivalent to the likelihood function. The likelihood function, $LF_k$, consists of a single array of $K$ elements, one element for each possible parameter vector. The conditional Gaussian distribution, on the other hand, consists of one $K$-element array, $CG_{k,m}$, for each point, $\mathbf{X}_m$. The conditional Gaussian array at each point, $\mathbf{X}_m$, is multiplied on a one-to-one element basis with the likelihood function, as $LF_k \times CG_{k,m}$. The resulting $K$-element array is multiplied by the product of the Gaussian parameters' differentials and summed at each point, $\mathbf{X}_m$, as $SOM_m = \left[\sum_{k=1}^{K} LF_k \times CG_{k,m}\right] \times delta$, in which $SOM_m$ stands for the relative probability of finding sunken oil mass at $\mathbf{X}_m$, $K$ is the total number of elements $Z\left(u^5\right)$, and $delta$ is the product of the Gaussian parameters' differentials. Subsequently, the method *mapping( )* of the class *Model* rearranges results to perform plotting, and creates the corresponding input for the mapping methods of the OPI and GUI modules.

#### 4.2.11.4 Graphical User Interface (GUI)

The graphical user interface (GUI) maps the output predictive relative concentrations geographically, presenting to the user the inferred location of sunken oil as a function of time, while controlling, with user input, the modeling area and shoreline boundaries used in the computations.

A preview of the GUI is shown in the Users Manual in Appendix A. The GUI contains three basic layouts other than the main toolbars and menus: (1) the pre-run layout or input section, where the user is prompted for input information concerning the spill, sampling campaign(s) and time(s), land boundary, desired modeling area, and prediction times, (2) the canvas layout, where results are displayed in interactive, georeferenced maps, and (3) the post-run layout or output section, which contains tools that allow the user to display the results at different times of prediction, run the model for contiguous areas, save results, print images, and perform other formatting tasks.

The GUI is the point of connection between the user and the OPI module, this last performing all required processing of raw input from users and providing the core module with the appropriate information. Among the most important tasks of the GUI, controlled through the OPI module, are:

- Collection of basic information on the spill in terms of the time of occurrence and coordinates (longitude and latitude) of the most significant loss;
- Display of the location of the spill on the map canvas within a 2-degree radius around the spill to allow selection of the desired modeling area;
- Assignment of the resolution and scale (rectangular) of the results based on default values or a user-defined number of modeling nodes in each direction: north-south and west-east, within the desired or default modeling area;
- Setting of customized dates and times at which sunken oil mass prediction is desired,
- Acceptance of output from the core module and geo-referenced by the OPI module, for display of it on the local map; presentation of relative probabilities of finding sunken oil, (0-1), on a relative, color-coded scale, with hotspots in red (1) fading to blue (0). Although probabilities of sunken oil decrease in time, the hue is re-rendered in every time calculation, such that the areas with the highest probability of finding sunken oil are shown in red at each modeled time, independently of relative probabilities shown for other times of prediction; and
- Display of post-run results at different prediction times and for contiguous modeling areas.

Detailed information on the operation of each of the features just described can be found in the Users Manual (Appendix A).

#### 4.2.11.5 Operating and Processing Interface (OPI) Module: Internal Processing of Input

Detailed mathematical algorithms were created and implemented in the OPI module of SOSim to convert user input into programmable structures, compile graphical interactions, operate interrelated buttons, actions, signals and toolbars of the GUI, and process information needed for the predictive Bayesian calculations. These algorithms are extensive and include:

- Unit conversions;
- Interrelated and single operation of signals, actions, dialog boxes, menus and toolbars;
- Maintenance of scale and units across statistical calculations; plotting and interactive tools and devices;
- Operation of the interactive tool to assign boundary conditions, translation into mathematical expressions, and solving for geometry of boundary conditions;
- Differentiation of types of oil and calculation of the slick’s sinking retardation;
- Storage and processing of input data from single or multiple sampling campaigns;
- Processing, storage, and passage to the core module of user input;
- Processing of results from the core module into maps and processing of optional post-run operations, which include management of prediction times and performance of partial recalculations to view results for contiguous modeling areas. Useful documentation functions including saving the results as images and printing are also included in the software under the OPI module.
- Uploading, saving, and using different files and images on disk (I/O) including calibration files; management of variable and default values, structures and map registry, relative time and locations management; and post-run functionality.

### 4.2.12 Model Operation

The details of SOSim operation are described in the Users Manual (Appendix A). Characteristics of operation and interpretation of results include:

1. If sunken oil mass is predicted to extend beyond the selected graphical domain for the prediction times requested, maps may be developed from partial re-runs for contiguous areas;
2. Resolution of prediction within any desired area of a plot can be enhanced by running the model for a “zoomed-in” area, following each model run; and
3. Color hues are not constant from figure to figure, but show relative probabilities from high to low at each time. This also implies that a result generated by zooming into another plot will show independent hotspots, not constant in color with respect to the parent figure.

## 4.3 Task 3 Results: Model Verification

The SOSim model was verified using one real and one synthetic data set, as described in this section. First, the model was verified versus the available data on the DBL-152 spill in the Gulf of Mexico, a major spill involving sunken oil. The event occurred 11 November 2005. Oil was observed to collect in a single, roughly Gaussian-shaped patch about 28 nautical miles from shore near Port Arthur, TX. In such cases when the spill is not expected to impact the shoreline, as determined by the user, shoreline boundary conditions are not taken into account by the model, saving considerable computational time. To then verify model functionality in terms of boundaries, superposition, and multiple sampling campaigns, the model was verified versus synthetic data on sunken oil collecting nearshore, initially in two overlapping patches and then dispersing along divergent paths. In the second scenario, two sampling campaigns are assumed. Shoreline boundaries are accounted for based on a polyline approximation of the shoreline entered interactively by the user using the GUI. The international system (SI) of units (km, days) is used in model calculations, whereas geographical user input is in terms of coordinates expressed and shown on non-projected maps in the World Geodesic System (WGS).

### 4.3.1 Verification Scenario 1: DBL 152 Spill

Table 4.2 indicates required and optional input and default and optional output for this verification case:

| Input | Output |
|---|---|
| Required input:<br>• Spill coordinates and time: 29.205° N, 093.4683° W (United States Coast Guard, 2005), on November 11, 2005 (General Counsel for Natural Resources/NOAA Office of Response and Restoration, 2009).) at zero hours (midnight, assumed as the initial hour of most significant loss)<br>• Subjective relative concentration data (Figure 4.7 obtained from Figure 3.1) and sampling time from Figure 3.1: November 25, 2005, 14 days after the spill<br>• Desired prediction dates and times: 12 hours after sampling, 17.5 days after the spill, and 19.5 days after the spill<br>Optional input:<br>• User-defined modeling area: approximately 0.2° around the spill, total about 0.4° longitude x 0.4° latitude<br>• Interactive spatial scale and resolution: 40 grid nodes in each direction | Default output:<br>• Maps of relative concentration (unconditional probability) at desired times (Figure 4.9, 4.10 and 4.11)<br>Optional (post-processing) output:<br>• None for this scenario |

Table 4.2. Input and output for Scenario 1

The sampling campaign provided by NOAA (Barker, 2009) shown in Figure 3.1 was interpreted as follows. The relative oil concentration, in percent, recorded for each sample taken was assigned to the midpoint of its graphically-depicted sampling path, through which the pompom sampler was apparently dragged prior to observing the amount of oil collected. Thus the following distribution of subjective concentrations was obtained as input for SOSim:

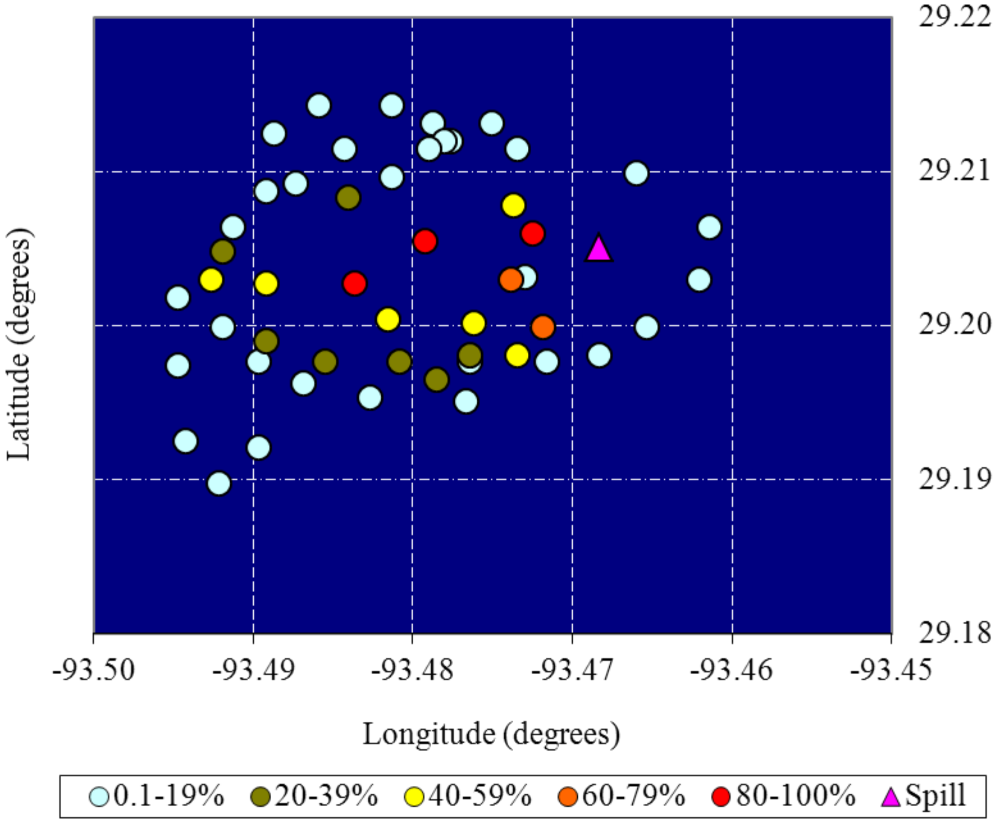

Figure 4.7. Recorded relative sunken oil concentrations evaluated subjectively, interpreted from Figure 3.1. The spill occurred at 29.205° N, 093.4683° W as shown in Figure 4.8.

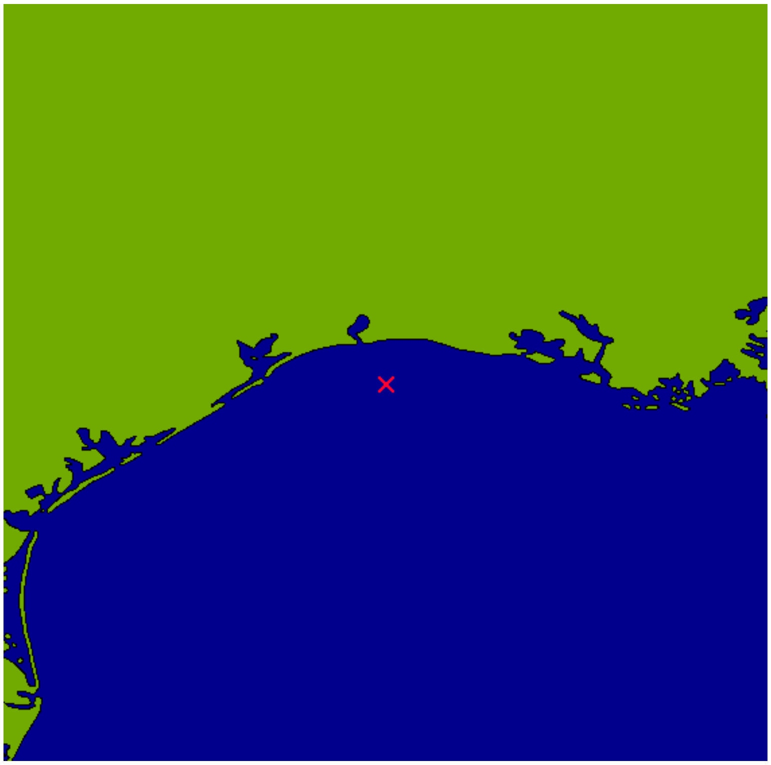

Figure 4.8. General location of the DBL 152 spill, Scenario 1

The apparent date of data collection shown in Figure 3.1 (November 25, 14 days after the spill) was assumed, the approximate time of most significant loss was assumed as 12:00 AM (midnight), and it was presumed that the sampling procedure was performed during a single campaign (at once). Note that the sampling points in Figure 4.7 are scattered randomly throughout the sampling area as was found expedient during the response effort. Therefore, SOSim was built with capability for accepting data at random points in space, as opposed to data sampled according to a lattice (regular) sampling plan.

All input data were entered following prompts of the graphic user interface, as described in the Users Manual (Appendix A). The map of assessed relative unconditional probabilities of finding sunken oil at 12:00 PM (noon)  on November 25, 2005; 12:00 PM on November 28, 2005; and 12:00 PM  on November 30th, 2005, is shown, corresponding respectively to times of 14.5, 17.5, and 19.5 days after the spill. Figure 4.9, 4.10 and 4.11 show the predicted probability of finding sunken oil at such times.

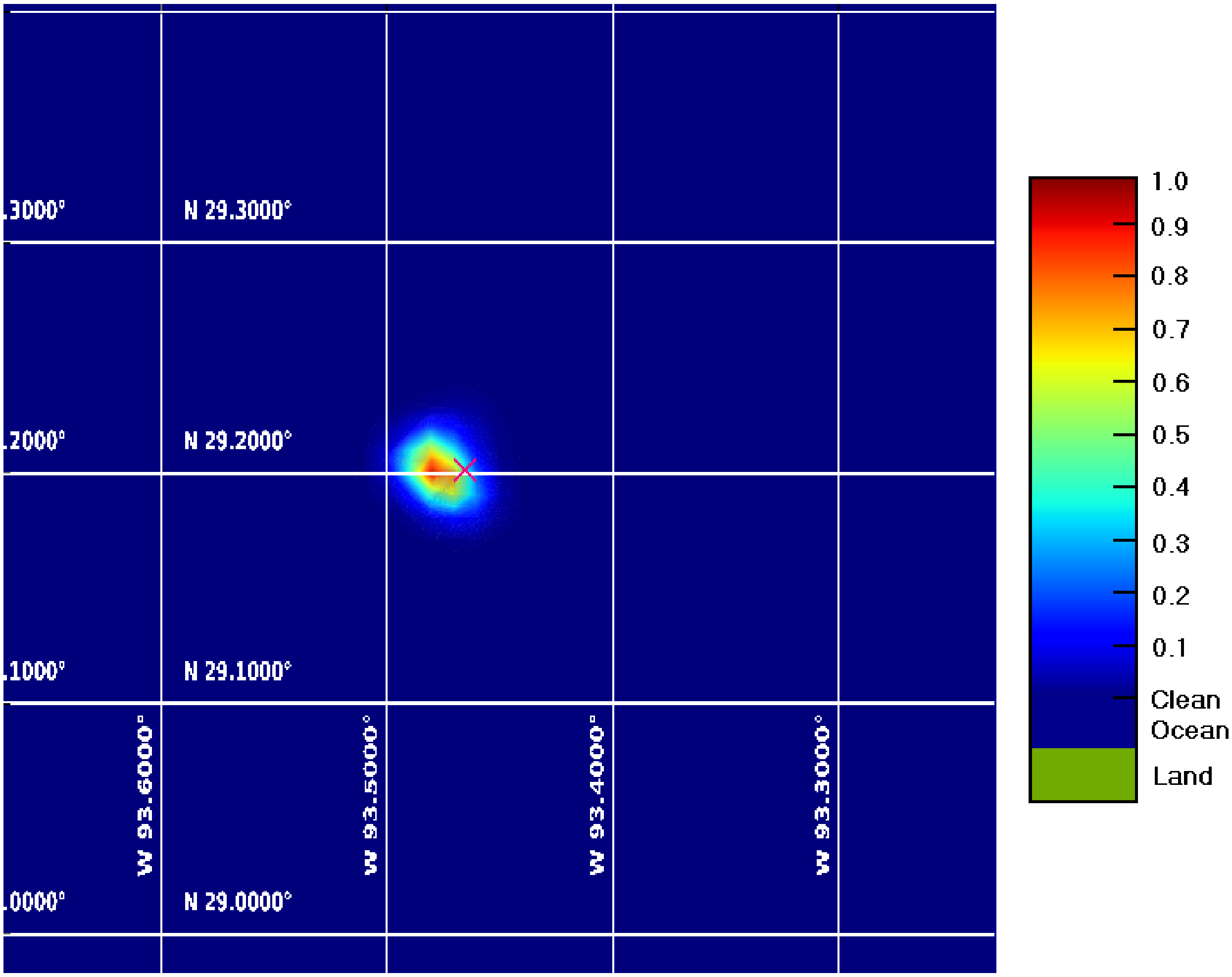

Figure 4.9. Relative probability of finding sunken oil 12 hours after the spill.

Figure 4.9 shows relative probabilities a short time after the first sampling campaign. Given that the location and shape shown in the figure resemble the given data, it is deduced that the model has the capability of interpreting the sampling campaign very precisely. The GUI prevents the user from requesting prediction times prior to the most recent sampling event. If the user needs a prediction between sampling campaigns, only the sampling campaign(s) conducted prior to the requested prediction time should be entered and on file.

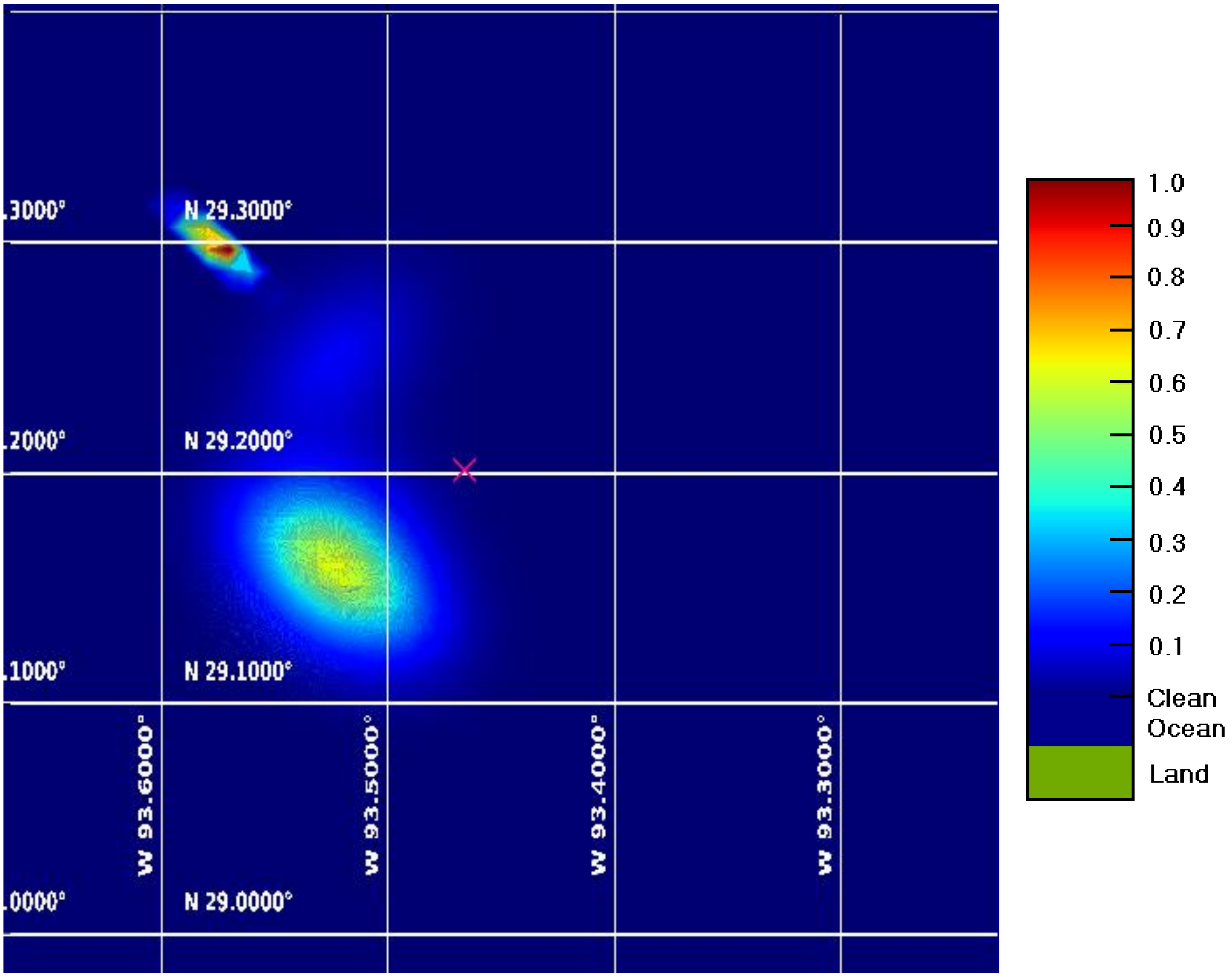

Figure 4.10  Relative probability of finding sunken oil 17.5 days after the spill.

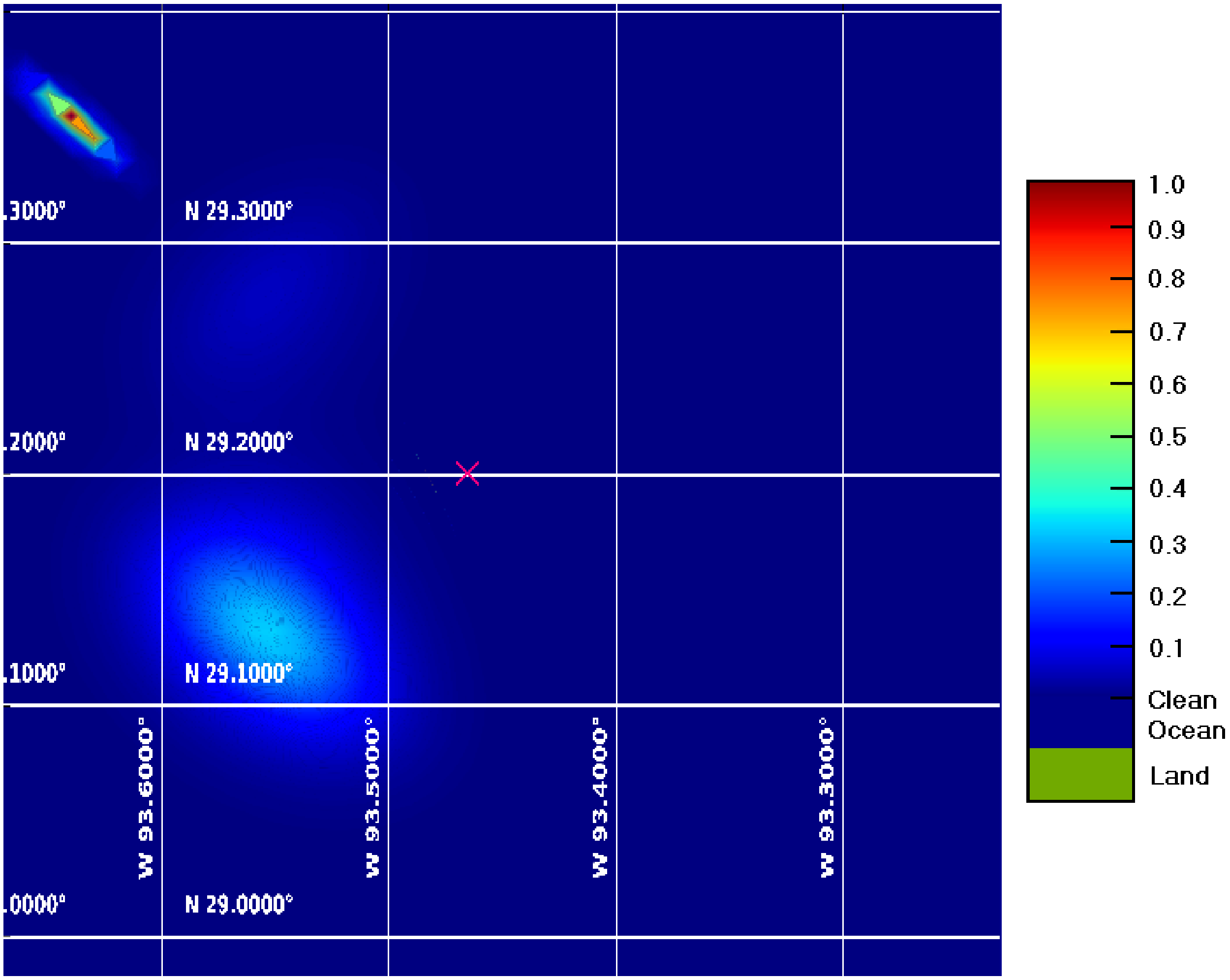

Figure 4.11 Relative probability of finding sunken oil 19.5 days after the spill.

Figure 4.9, 4.10 and 4.11 show the output resulting from the data on the DBL 152 spill made available to the research team for use in this project, at coordinates 29.205° N, 093.4683° W. Although red represents the highest relative unconditional probability of finding oil in each figure, the concentration at such hotspots decreases in time as the sunken oil patches advance in space and disperse. That is, the hue scale is not constant from one figure to another. As shown, the formation of two satellite patches in addition to the main patch was predicted by SOSim by inference based on the data of the single sampling campaign available to the project team and the assumed time of oil collection on the bay bottom. By way of comparison, NOAA Scientifics wrote “We envision the T/B DBL-152 oil breaking up into smaller pieces and dispersing horizontally as it moves downcoast” (Beegle-Krause *et al.*, 2006). This vision is not inconsistent with the figures developed using SOSim, in that the oil breaks into smaller patches and two of them spread while moving offshore and horizontally, with one headed towards land.

### 4.3.2 Verification Scenario 2: Synthetic Multi-Modal, Multiple Sampling Campaign Data on Relatively Flat-Bottom Bay within Coastal Environment

Table 4.3 indicates required and optional input and default and optional output for this verification case:

| Input | Output |
|---|---|
| Required input:<br>• Synthetic spill coordinates and time: ( 32.80° N, 079.465° W), the 1st of January of 2010.<br>• Subjective relative concentration data and sampling times: Figure 4.12, first sampling campaign at 4 AM on January the 7th,, 2010, made of 90 data points; and second sampling campaign at 4 AM on January the 11th, 2010, also with 90 data points<br>• Desired prediction dates and times: 4 AM January the 9th, (two days after the first sampling campaign and 8 days after the spill), 4 AM January the 12th, (one day after the second sampling campaign), and 4 AM, January the 14th, 13 days after the spill.<br>Optional input:<br>• User-defined modeling area: about 0.27° latitude x 0.27° longitude within the coastal area<br>• Interactive spatial scale and resolution: default (25 x 25 grid nodes) | Default output:<br>• Maps of relative concentration (unconditional probability) at desired times: Figure 4.14, 4.16 and 4.17.<br>Optional (post-processing) output:<br>• Revised maps based on subsequent data (new sampled area), Figure 4.15 and 4.17. |

Table 4.3. Input and output for Scenario 2

The purpose of this second synthetic scenario is to verify model capabilities in terms of registering and analyzing multiple boundary conditions in time and multiple sampling campaigns, as a sunken oil patch approaches a coast line. The statistical sampling procedure described in a previous chapter of this report was used to simulate data for the exercise. Figure 4.12 depict the simulated data and spill coordinates. Figures are rendered for the oceanic area sampled and affected by the initial spill; the general region showing the location of the spill is as in Figure 4.13. Each marker in Figure 4.12 represents one simulated sampling point, having a relative concentration in percent as indicated by the color key below the plot.

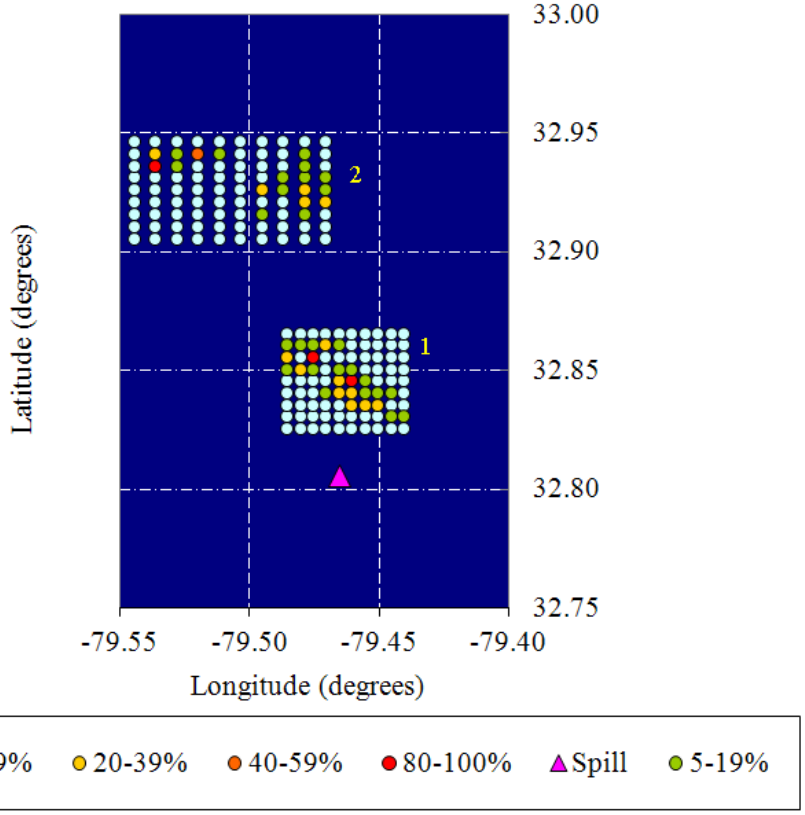

Figure 4.12. Synthetic data on relative sunken oil concentrations in percent, for samples assumed collected on two different days, (1) 6 days after the spill, and (2) 10 days after the spill.

The modeled spill is located at (32.8 °N, 079.465 °W), as shown in the figures. In Figure 4.12, both sampling campaigns 1 and 2 have been synthetically derived to represent two separate patches of oil collecting on the bottom, as indicated by the colors shown. The first sampling event covers an approximate area of 25 km$^2$ (9.8 mi$^2$) and the second an approximate area of 35 km$^2$ (13.67 mi$^2$).

2

1

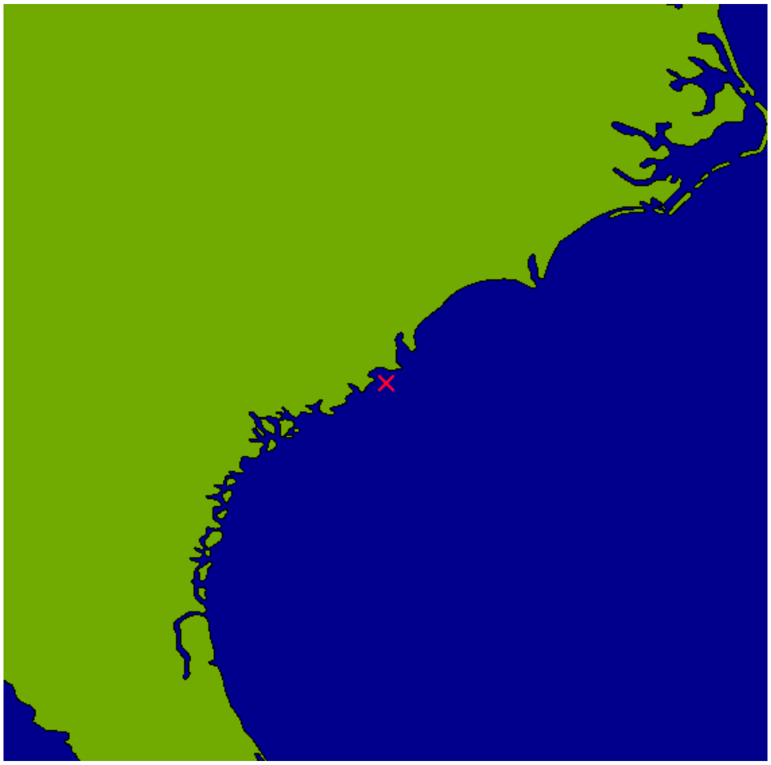

Figure 4.13. General location of the simulated spill scenario of Scenario 2

Figure 4.14 to 4.17 show maps of relative unconditional probabilities of finding sunken oil, interpreted roughly as relative sunken oil concentrations, on the bottom given the imposed boundary conditions, within the user-selected geographical area.

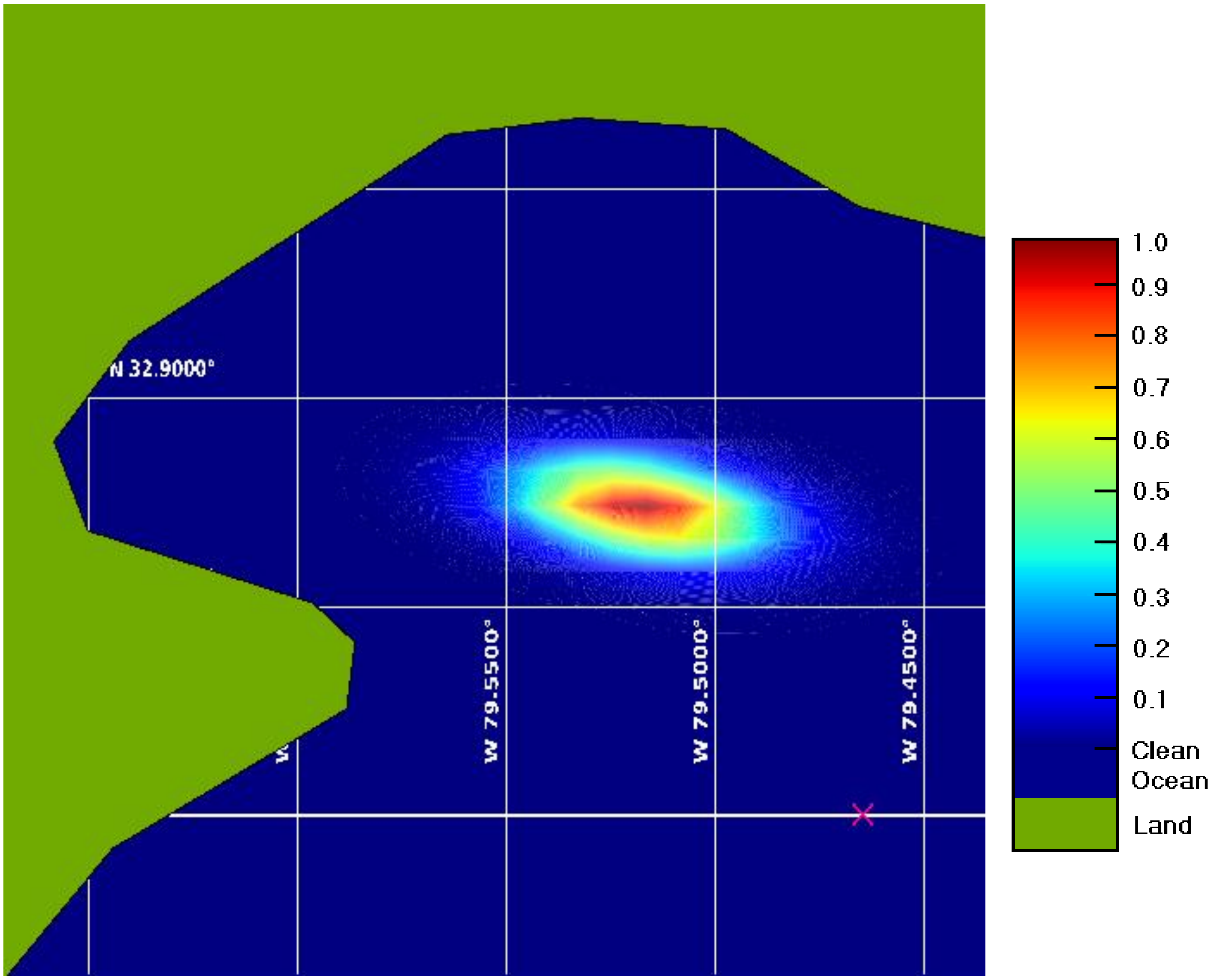

Figure 4.14. Relative probability of finding sunken oil 8 days after the spill (1 day after the first sampling campaign).

Although the first sampling campaign represents two overlapping patches, so close to each other that the model infers a single patch.

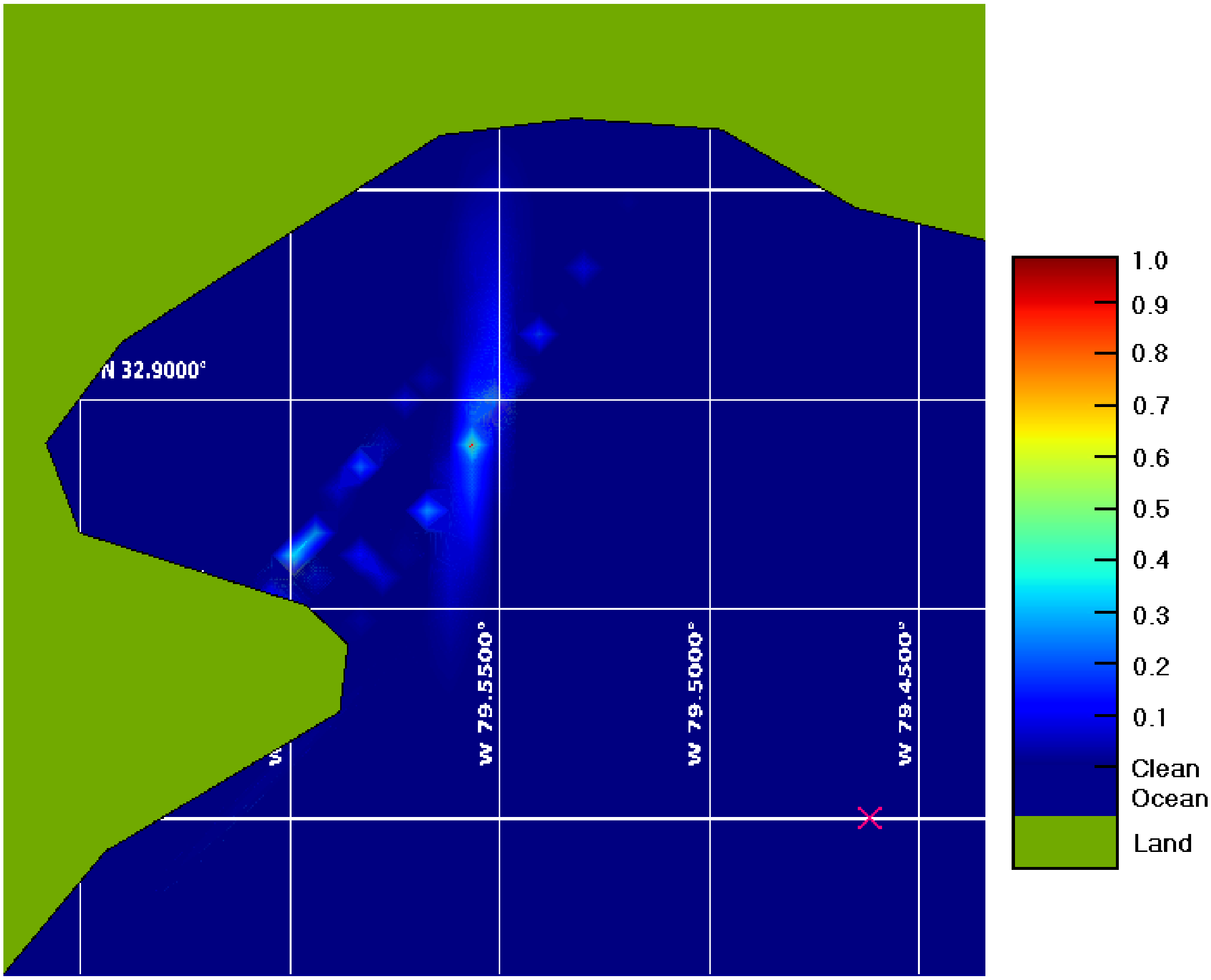

Figure 4.15. Relative probability of finding sunken oil 11 days after the spill (5 days after the first sampling campaign and 1 day after the second sampling campaign), updated based on the second data set.

Figure 4.15 represents an updated prediction considering the second sampling campaign. After 11 days the oil mass is dispersed and is not predicted to impact the shoreline significantly.

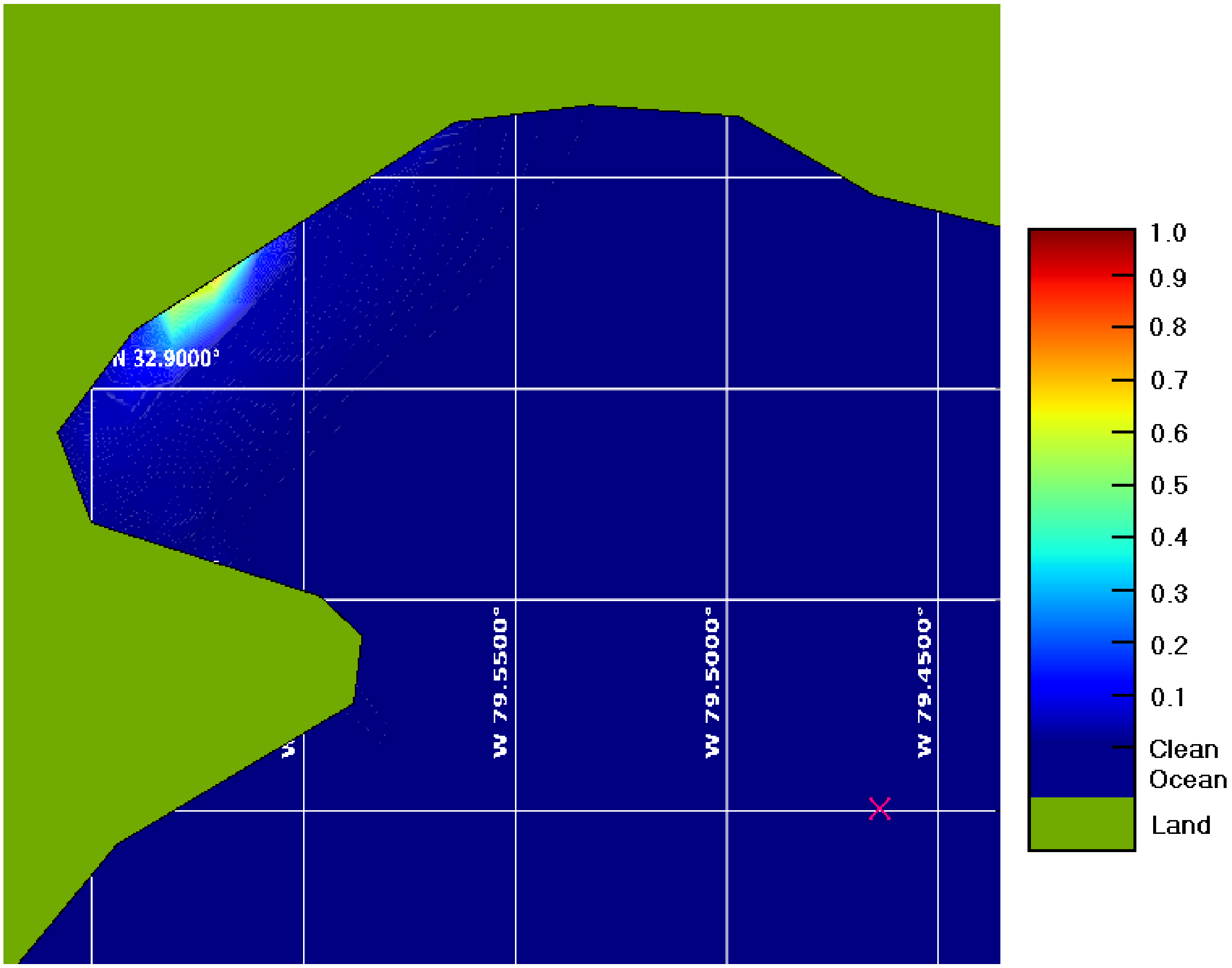

Figure 4.16. Relative probability of finding sunken oil 13 days after the spill (3 days after the second sampling campaign).

After 13 days the oil is predicted to impact shoreline, being reflected into a deeper section of the cove in the direction of oil movement indicated by the difference in oil mass locations assumed between the first and second sampling campaigns. In subsequent versions of the model, the effect of bathymetry, such as slope away from the shoreline, can be considered as prior information to refine these predictions. Predicting oil locations following resuspension of the oil by storm events would generally require data to be collected after the storm. Overall, results observed are considered conservative and representative for a relatively flat-bottomed bay environment, given current model capabilities.

The two verification scenarios presented, along with continual checks on relative normalization and other internal consistencies, are considered to confirm the code developed for Version 1.0 of SOSim. The proposed predictive Bayesian multi-modal Gaussian is operational for use with limited, randomly-sampled, available subjective and numeric data on sunken oil concentrations in relatively flat-bottomed bays. Model operation, however, is open to continued verification, and the approach is recommended for refinement.

## 5.0 Discussion and Importance to Oil Spill Response/Restoration

The SOSim model represents a new approach to modeling, coupling a Lagrangian modeling technique with predictive Bayesian capability for computing unconditional probabilities of mass as a function of space and time. Incorporated are new methods for computation of two-dimensional boundary conditions by images, and combinatorial techniques for computing unconditional multimodal probability distributions. The approach addresses the current need of NOAA to rapidly deploy modeling capability without readily accessible information on ocean bottom currents. Another aspect is the stand-alone application developed, including a user-friendly interactive graphical user interface that can be employed without the need for knowledge of Bayesian or other modeling techniques, to track sunken oil during emergency response missions.

The SOSim predictive Bayesian statistical model is expected to be useful for identifying sunken oil hotspots, addressing the need for tracking of sunken oil following a spill, and to target cleanup activities and to support cleanup termination decisions using a minimum of resources from responder teams: only limited and non-demanding field data after a spill has occurred are required. In particular, knowledge of bottom currents is not needed. Results are displayed in maps of geographic areas, produced based on user input supplied to an interactive graphical user interface. The model was developed with the intent of being used on desktop computers for maximum accessibility, and therefore the intrinsic computational limits and approaches incorporated into the model are consistent with this vision. However its performance can be enhanced considerably if this condition is relaxed.

The occurrence of the BP spill in 2010, just as this report was being written, underscores the importance of supporting emergency response and recovery efforts regarding sunken oil, such as with the computational tool developed in this project. The work addresses the need for cost-effective location and tracking of sunken oil masses in time, offering the possibility of saving “enormous dollar-per-barrel recovery costs” for sunken oil following a spill.

Limitations of the model are principally in terms of the types of information that can be exploited as model input, and model resolution. Several model refinements and enhancements are suggested, to make the model more useful, as follows.

1. First, default information employed for model development should be refined by, or with input from, experienced oil spill modelers and responders;
2. Second, a decision should be made as to whether in the longer term the model will be operated locally using desktop computing equipment, or centrally on a more powerful processing system, as this decision will affect subsequent decisions. Most subsequent recommendations in this section will require more processing power than typical desktop computers currently offer, as run times are currently on the order of 10 hours on desktop computers. If designed for use on a cluster system, the code should be parallelized as needed;
3. Sunken oil tends to move by gravity, and therefore the addition of capability to enter bathymetry as prior information is recommended;

4. Bottom current information is becoming available, e.g. for the Gulf of Mexico which supports high density oil vessel traffic and drilling operations, and capability for entering such information as prior information would be a high priority at the point when such data is considered readily accessible;
5. Other prior information may be related to such factors as oil type and geographical environment of the spill. For example, sediment is typically transported greater distances along the shelf than across the shelf (Beegle-Krause *et al.*, 2006), and this observation could be used in the development of Bayesian prior probability distributions for coefficients of advection and dispersion in directions perpendicular and parallel to shore;
6. Given adequate processing power, several aspects of model resolution should be enhanced, including resolution of the uncertain parameter space to be integrated over, resolution of the geographical area to be modeled, the number of vertices allowed to approximate the shoreline, and the number of different polyline boundaries to account for separated landforms such islands and straits;
7. Given adequate field data, specification of model time in hours rather than days, and a consequent increase in the number of times at which samples can be recorded, can be considered. For example, the ability to record and enter a unique sampling time for each sample could improve short-term performance; and
8. Additional processing power would enable the model to be implemented in three dimensions, for application to oil suspended in the water column.

# 6.0 Technology Transfer

Dissemination of the results of this project have occurred via the project website, presentation at the Clean Gulf Conference, 2009, and through press releases, media interviews, political forums, news briefs, and electronic communications in connection with the catastrophic drilling rig explosion event that is ongoing as this report is written. As such, audiences include engineers and scientists within the oil spill community, the public at large, and administrators, decision-makers, and operators with responsibilities related to oil spills.

### 6.1.1 Clean Gulf Conference

A presentation to specialized audiences at the Clean Gulf Conference of 2009 in the City of New Orleans, Louisiana was well received and generated significant interest. In particular, William Lehr, Senior Scientist, NOAA Emergency Response Division, has contacted the PI regarding possible further development and extensions.

### 6.1.2 University of Miami Panel Discussion on the Deepwater Horizon Oil Spill

The PI is scheduled to participate as one of three panelists at "Crisis in the Gulf: A Panel Discussion on the Deepwater Horizon Oil Spill," Sept. 14, 2010, Glasgow Hall, University of Miami School of Architecture. The panel discussion is being convened by the Butler Center for Volunteer Service and Leadership Development, 1306 Stanford Drive, Room 240, Whitten University Center, Coral Gables, Florida, and is open to selected students, faculty, and administration & community leaders.

### 6.1.3 Website

Project proposal, objectives, and progress reports have been available via the project website. It is further planned to post discussions, the SOSim v. 1.0rc1 and other required software as advised by the NOAA Liaison, for download at http://www.cae.miami.edu/sunken-oil-mass/projects.html. Information requests can also be answered via distribution of the computer application, Users Manual, and demo by CD ROM. Other related material will be transferred by means of the website in accordance with NOAA-CRRC grant requirements.

### 6.1.4 Media Coverage

As a result of the catastrophic Horizon deepwater oil spill in the Gulf of Mexico, the University of Miami issued a press release on the project, shown below:

**Public release date: 26-May-2010**
[ | E-mail | Share ]

Contact: Marie Guma-Diaz
m.gumadiaz@umiami.edu
305-284-1601
University of Miami

# UM researchers develop model for locating and forecasting sunken oil following spills

CORAL GABLES, FL (May 26, 2010)--A team of researchers at the University of Miami (UM) has developed a computer model for finding and projecting in time sunken oil masses on the bottom of bays, after an oil spill. The unique model can be used in oil spill planning, response, and recovery applications.

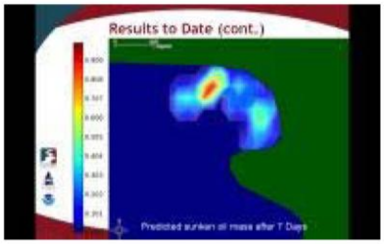

**IMAGE:** These are images showing relative concentrations of sunken oil on the bottom of a bay inlet, assessed for a simulated spill scenario. The new computational model was developed by a...

Click here for more information.

"Sunken oil is difficult to 'see' because sensing techniques show only a small space at a point in time. Moreover, the oil may re-suspend and sink, with changes in salinity, sediment load, and temperature, making fate and transport models difficult to deploy and adjust," says James Englehardt, UM professor of environmental engineering in the College of Engineering and team leader for the project. "For these reasons, we have developed a unique approach to the problem, bridging sampling plan techniques with pollutant transport modeling, to create models of sunken oil.

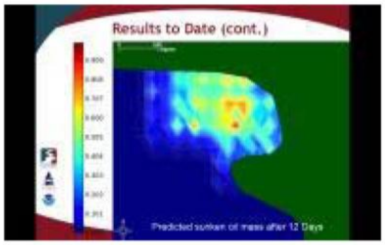

**IMAGE:** These are images showing relative concentrations of sunken oil on the bottom of a bay inlet, assessed for a simulated spill scenario. The new computational model was developed by a...

Click here for more information.

The model was developed for the Emergency Response Division of NOAA/NOS/OR&R (NOAA's Ocean Service Office of Response and Restoration), in Seattle, and the project was funded by the Coastal Response Research Center, University of New Hampshire.

The two-year project had three main objectives:

1. compile and summarize data on the occurrence of sunken oil, directed by the project team including end users and NOAA liaison;
2. develop a 2-D multimodal predictive Bayesian Gaussian model of sunken oil locations across a bay to accept spatial field data and hydrodynamic information and forecast sunken oil locations in time; and
3. verify the model versus sunken oil data, as possible, and simulated datasets.

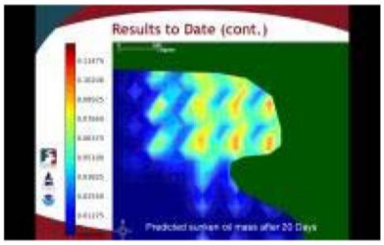

**IMAGE:** These are images showing relative concentrations of sunken oil on the bottom of a bay inlet, assessed for a simulated spill scenario. The new computational model was developed by a...

Click here for more information.

###

The University of Miami's mission is to educate and nurture students, to create knowledge, and to provide

The release shown above generated substantial media interest, including e-mails and telephone interviews conducted by the PI. Selected coverage included:

1. A televised interview for Channel NBC 6 News in Miami, for which the PI recorded a 45-minute interview, of which about 5 minutes aired at 6:00 pm on Thursday, May 27;
2. A 45 minute telephone interview with Justin Gillis of the New York Times, June 30, 2010;
3. A second television interview with Channel NBC 6 News in Miami, following a Roundtable Discussion with Florida Governor Charlie Crist to which the PI was invited (see next section). At the time of this report, a media clip including excerpts of the interview can be viewed at http://www.nbcmiami.com/news/local-beat/Governor-on-Oil-Dont-drill-near-our-shores-98458644.html.

Also as a result of the UM press release, the following new brief appeared in USA Today.

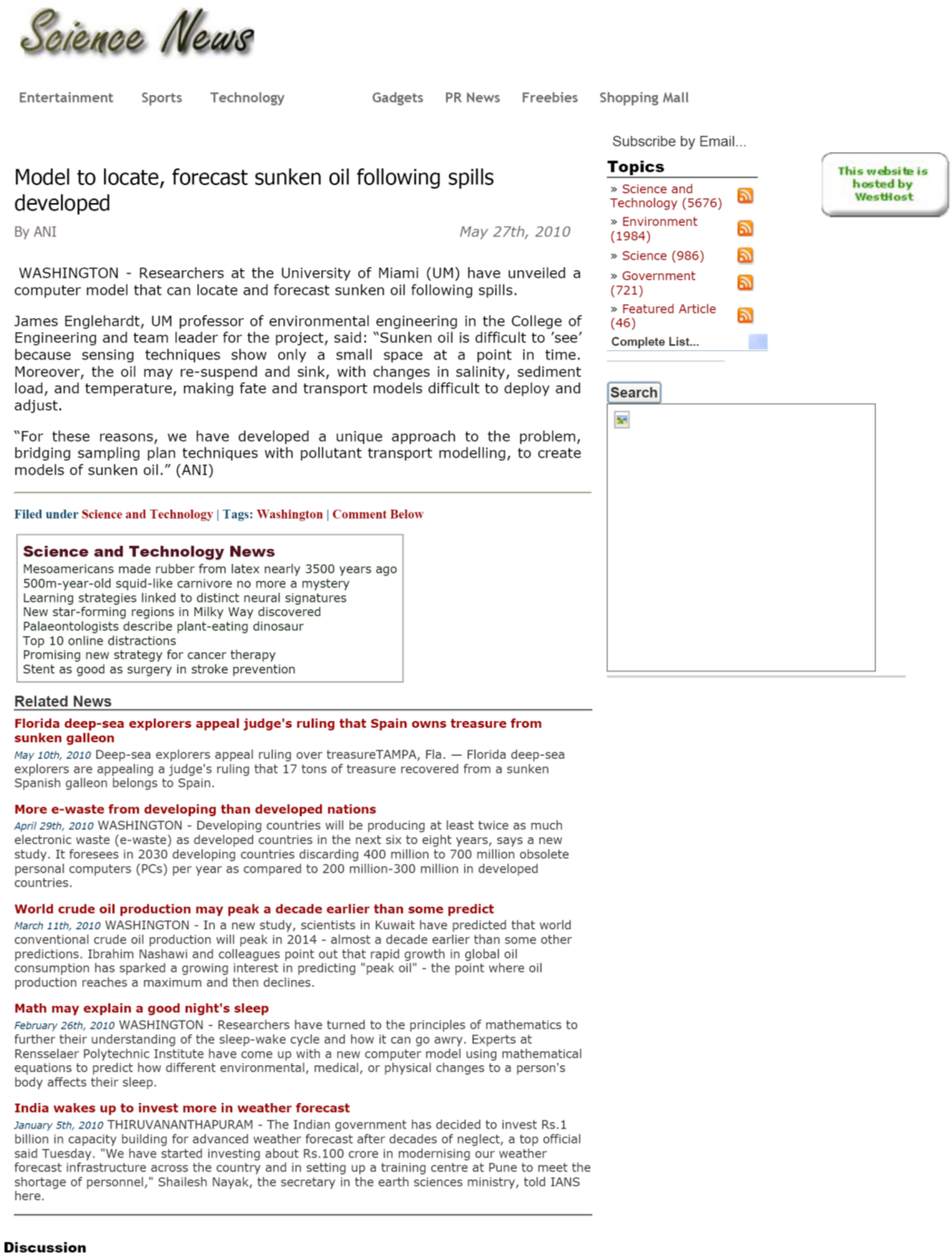

Science News

Entertainment Sports Technology Gadgets PR News Freebies Shopping Mall

# Model to locate, forecast sunken oil following spills developed

By ANI May 27th, 2010

WASHINGTON - Researchers at the University of Miami (UM) have unveiled a computer model that can locate and forecast sunken oil following spills.

James Englehardt, UM professor of environmental engineering in the College of Engineering and team leader for the project, said: "Sunken oil is difficult to 'see' because sensing techniques show only a small space at a point in time. Moreover, the oil may re-suspend and sink, with changes in salinity, sediment load, and temperature, making fate and transport models difficult to deploy and adjust.

"For these reasons, we have developed a unique approach to the problem, bridging sampling plan techniques with pollutant transport modelling, to create models of sunken oil." (ANI)

Filed under Science and Technology | Tags: Washington | Comment Below

**Science and Technology News**

Mesoamericans made rubber from latex nearly 3500 years ago
500m-year-old squid-like carnivore no more a mystery
Learning strategies linked to distinct neural signatures
New star-forming regions in Milky Way discovered
Palaeontologists describe plant-eating dinosaur
Top 10 online distractions
Promising new strategy for cancer therapy
Stent as good as surgery in stroke prevention

## Related News

**Florida deep-sea explorers appeal judge's ruling that Spain owns treasure from sunken galleon**

*May 10th, 2010* Deep-sea explorers appeal ruling over treasureTAMPA, Fla. — Florida deep-sea explorers are appealing a judge's ruling that 17 tons of treasure recovered from a sunken Spanish galleon belongs to Spain.

**More e-waste from developing than developed nations**

*April 29th, 2010* WASHINGTON - Developing countries will be producing at least twice as much electronic waste (e-waste) as developed countries in the next six to eight years, says a new study. It foresees in 2030 developing countries discarding 400 million to 700 million obsolete personal computers (PCs) per year as compared to 200 million-300 million in developed countries.

**World crude oil production may peak a decade earlier than some predict**

*March 11th, 2010* WASHINGTON - In a new study, scientists in Kuwait have predicted that world conventional crude oil production will peak in 2014 - almost a decade earlier than some other predictions. Ibrahim Nashawi and colleagues point out that rapid growth in global oil consumption has sparked a growing interest in predicting "peak oil" - the point where oil production reaches a maximum and then declines.

**Math may explain a good night's sleep**

*February 26th, 2010* WASHINGTON - Researchers have turned to the principles of mathematics to further their understanding of the sleep-wake cycle and how it can go awry. Experts at Rensselaer Polytechnic Institute have come up with a new computer model using mathematical equations to predict how different environmental, medical, or physical changes to a person's body affects their sleep.

**India wakes up to invest more in weather forecast**

*January 5th, 2010* THIRUVANANTHAPURAM - The Indian government has decided to invest Rs.1 billion in capacity building for advanced weather forecast after decades of neglect, a top official said Tuesday. "We have started investing about Rs.100 crore in modernising our weather forecast infrastructure across the country and in setting up a training centre at Pune to meet the shortage of personnel," Shailesh Nayak, the secretary in the earth sciences ministry, told IANS here.

**Discussion**

Subscribe by Email...

**Topics**

» Science and Technology (5676)
» Environment (1984)
» Science (986)
» Government (721)
» Featured Article (46)
Complete List...

Search

This website is hosted by WestHost

### 6.1.5 Roundtable Discussion with Florida Governor Charlie Crist

The PI was invited to advise Charlie Crist, Governor of the State of Florida, on state response to the Horizon deepwater spill crisis, and to participate in discussion of the need for a ban on oil drilling off the coast of Florida. In the photo below, Governor Crist is at the far end of the table, the PI is second from the right, and other Florida politicians and scientists are shown at the table and in attendance. At the time of this report, a media clip covering the Roundtable can be viewed at http://www.nbcmiami.com/news/local-beat/Governor-on-Oil-Dont-drill-near-our-shores-98458644.html.

### 6.1.6 Support for the 2010 Gulf of Mexico Spill

The PI answered a request from the State of Florida for advice concerning the estimated amount, fate, behavior and transport of sunken oil, and another request concerning how to sample for sunken oil, to collect data as input to the SOSim. The team offered to run SOSim for the State, if data was provided.

Follow-on proposals were submitted as follows:

1. “Adaptation and Use of the Predictive Bayesian SOSim Model to Locate and Track Submerged/Sunken Oil for Deepwater Horizon Spill Response,” proposal to Deepwater

Horizon Response BAA HSCG32-10-R-R00019, Deepwater Horizon Unified Command, Department of Homeland Security, United States Coast Guard Research and Development Center, $69,108, June 14, 2010; and

2. "Adaptation of SOSim to Location and Tracking of Submerged Oil from Continuous Releases and Immediate Use for Horizon Spill Response," proposal to BP/Florida Institute of Oceanography, Gulf Oil Spill Prevention, Response, and Recovery Grants Program, www.marine.usf.edu/fio/oilspillgrants, $200,000, July 7, 2010.

Ultimately the team was not able to obtain data, and support for follow-on proposals was not received. Therefore, it was not possible to run the model and distribute results.

### 6.1.7 Computer Application

As described in the sections on computational methodology, a set of Python modules were developed that find support in several other Python modules and a computer application with Python binary version. The SOSim set of modules along with all its dependencies were consolidated in a distributable, executable Windows 32 package named SOSim v.1.0rc1. This first release is expected to work with any Microsoft Windows 32-bit operating system without the need of previous Python installation.

### 6.1.8 Software Documentation for Training Purposes

Appended to this report is the SOSim Users Manual. As part of the documentation prepared for the software, the electronic version of the Users Manual contains an electronic demo that supplements the manuscript. The User Manual guides the user through the installation and operation of SOSim. Knowledge of statistics is not required. Input of information as required for modeling a spill, including accident coordinates, sampling data (basic Microsoft Excel® skills are required to assemble a sampling campaign file), and criteria to define desired prediction times. This documentation, including Users Manual and Demo, are also distributed with the binary file SOSim.exe.

## 7.0 Achievement and Dissemination

Planned and accomplished achievements and dissemination activities include:

*Peer Reviewed Publications*

- Echavarria Gregory, M. A., J. Englehardt. 2010. Development and Application of the Bayesian Sunken Oil Mass Simulator SOSim (in preparation). *Environmental Modeling and Software*, Elsevier, expected submission September 2010.
- Echavarria Gregory, M. A., J. Englehardt. 2010. Stochastic and Combinatorial Research Technique for the Simulation and Risk Assessment of Sunken Oil in the Ocean (in preparation). *Stochastic Environmental Research and Risk Assessment*, SpringerLink, expected submission October 2010.

*Other Publications*

- Echavarria Gregory, M. Angelica, 2010. *Development of a Predictive Bayesian Data-Derived Multi-Modal Gaussian Model for Location and Simulation of Sunken Oil Mass in Time*. Ph.D. Dissertation, University of Miami, Department of Civil, Architectural, and Environmental Engineering, August.

*Conference Presentations*

- Englehardt, J., A. Echavarria Gregory, and P. Avellaneda. 2009. Development of a Predictive Bayesian Data-Derived Multi-Modal Gaussian Maximum-Likelihood Model of Sunken Oil Mass. Invited presentation, *Clean Gulf*, Ernest N. Morial Convention Center-New Orleans, New Orleans, Louisiana, November 17-19.

*Students and Post-Doctoral Fellow Supported*

- M. Angelica Echavarria Gregory, MS., E.I., Ph.D. Candidate and Doctoral Research Assistant, 2007 – 2010. Degree awarded: Doctor of Philosophy. Dissertation title: Development of a Predictive Bayesian Data-Derived Multi-Modal Gaussian Model for Location and Simulation of Sunken Oil Mass in Time.

- Pedro Avellaneda, MS., PhD, Post-Doctoral Fellow, Risk Assessment Thrust Area Leader, 2008 – 2009. Currently Assistant Professor, National University of Colombia at Bogotá, Colombia.

# References

Aitchison, J. and I. Dunsmore. 1975. Statistical Prediction Analysis. Cambridge University Press, New York, Chapter 2, 1975.

Anex, R. and J. Englehardt. 2001. Application of a Predictive Bayesian Model to Environmental Accounting. Journal of Hazardous Materials, Elsevier, vol. 82, no. 2, pp. 99-112.

Barker, C. 2009. Personal electronic communication. Oceanographer, National Oceanographic and Atmospheric Administration, NOAA Ocean Service Office of Response and Restoration, October 20, 2009.

Bear, J. 1979 Hydraulics of Groundwater. McGraw-Hill, 1979.

Beegle-Krause, CJ, C. Barker, G. Watabayashi and W. Lehr. 2006. Long-Term Transport of the Oil from the T/B DBL-152: Lessons Learned for Oils Heavier than Seawater. Arctic and Marine Oil Pollution Conference 2006 Proceedings, Vancouver, B.C., Canada, June 6-8, 2006. Ottawa, Ontario: Environment Canada.

Bloetscher, F., J. Englehardt, D. Chin, J. Rose, G. Tchobanoglous, V. Amy, and S. Gokgoz. 2005. Comparative Assessment of Municipal Wastewater Disposal Methods in Southeast Florida. Water Environment Research, vol. 77, no. 5, pp.480-490.

Boehm, P.D., Barak, J.E., Fiest, D.L. and Elskus, A.A. 1982. A Chemical Investigation of Transport and Fate of Petroleum Hydrocarbons in Littoral and Benthic Environments: The Tsesis Oil Spill. Marine Environmental Research, v6, 1982, pp. 157-188. Massachusetts, USA.

Cedre. 2007. Understanding Black Tides. Centre of Documentation, Research and Experimentation on Accidental Water Pollution, Brest Cedex, France. Website accessed 2010. http://www.cedre.fr/en/contact.php.

Chin, D.A. 2006. Water-Quality Engineering in Natural Systems, Wiley, 2006.

CRRC. 2007. Coastal Response Research Center. FY 2007 Annual Request for Proposals. May 16, 2007

CRRC. 2007. Coastal Response Research Center. Submerged Oil – State of the Practice and Research Needs Workshop. Coastal Response Research Center, Durham, New Hampshire, December 12-13, 2006, Draft Report Issued May, 2007.

Dean, R.G., and R.A. Dalrymple. 1991. Water Wave Mechanics For Engineers and Scientists. World Scientific, Singapore, 1991.

DeGroot, Morris H. 1989. Probability and Statistics. 2nd. ed., Addison-Wesley Publishing Co., Reading, MA, Chapter 6, 1989.

Douligeris, C., E. Iakovou, J. Englehardt, H. Li, C. Ip, and C. Mooers. 1998. Development of a National Marine Oil Transportation System Model. Spill Science & Technology Bulletin, Elsevier Science Ltd., vol. 4, no. 2, pp. 113-121.

Einstein, Albert; R. Fürth, transl. by A. D. Cowper. 1926, reprinted in 1956. On the Movement of Small Particles Suspended in a Stationary Liquid Demanded by the Molecular-Kitetic Theory of Heat. Investigations on the theory of the Brownian motion. Dover Publications, 1956.

Englehardt, J. 2004. Predictive Bayesian Dose-Response Assessment for Appraising Absolute Health Risk from Available Information. Human and Ecological Risk Assessment, The Association for Environmental Health and Sciences, vol. 10, no. 1, pp. 69-74.

Englehardt, J. and J. Swartout. 2004. Predictive Population Dose-Response Assessment for Cryptosporidium Parvum: Infection Endpoint. Journal of Toxicology and Environmental Health Part A: Current Issues, vol. 67, no. 8-10, pp. 651-666.

Englehardt, J., H. An, H., L. Fleming, and J. Bean. 2003. Analytical Predictive Bayesian Assessment of Occupational Injury Risks: Municipal Solid Waste Collectors. Risk Analysis, Society for Risk Analysis, vol. 23, no. 5, pp. 919-927.

Englehardt, J., and C. Peng. 1996. A Bayesian Benefit-Risk Model Applied to the South Florida Building Code. Risk Analysis, Society for Risk Analysis, vol. 16, no. 1, pp. 81-92.

Englehardt, J. 1995. Predicting Incident Size from Limited Information. Journal of Environmental Engineering, American Society of Civil Engineers, vol. 121, no. 6, pp. 455-464.

General Counsel for Natural Resources/NOAA Office of Response and Restoration. 2009. Case: Tank Barge BDL 152, Federal Waters of the Gulf of Mexico. Site accessed 2010. http://www.darrp.noaa.gov/southeast/dbl152/index.html, revised by GCNR May 2009.

ITOPF. 2009. The International Tanker Owners Pollution Federation Limited. Website accessed 2010. http://www.itopf.com/, 2009.

Jaynes, E. 1957. Information Theory and Statistical Mechanics. Physical Review, 106, 620-630, 1957.

Kapur, J. 1989. Maximum Entropy Models in Science and Engineering. Wiley & Sons, New York, pp. 67-68, 1989.

NOAA. 2006. Submerged Oil Working Group. Technical Guidelines on Sunken Oil Assessment and Removal Techniques, Website last accessed 2010, http://www.crrc.unh.edu/submerged_oil/guidelines_sunken_oil_italy2.pdf

Obie, D. and J. Englehardt. 1996. A Bayesian Model to Predict Oil Spill Consequences of Management Plans in the Gulf of Mexico. Proc. Eco-Informa '96: Global Networks for

Environmental Information, Epcot Science and Technology, Lake Buena Vista, FL, 4-7 November.

PSF. 2001. Python Software Foundation. Website accessed 2010. http://www.python.org/

QGIS Organization. 2009. Website last accessed April 2010, http://www.qgis.org.

Qt Development Frameworks. 2009. Website last accessed April 2010, http://qt.nokia.com.

Research Planning Inc. 2001. Sunken Oil Pathways: Protocols for NRDA Surveys. Website accessed 2010, http://www.researchplanning.com/services/nrda/Sunken.oil.pathways.pdf.

Research Planning Inc. 1994. Natural Resource Damage Assessment Emergency Guidance Manual. Version 1.1, Columbia, SC, 1994, Damage Assessment Center, NOAA, Rockville, MD.

Shannon, C. E. 1948. A Mathematical Theory of Communication. The Bell System Technical J. 27, 379-423 and 623-656, July and October 1948.

Summerfield, M. 2007. Rapid GUI Programming with Python and Qt, the Definitive Guide to PyQt Programming. Prentice Hall, 2007.

Todd, D.K, L. Mays. 2005. Groundwater Hydrology. Third edition, Wiley, 2005.

United States Coast Guard, U.S. Department of Homeland Security. 2005. Press Release: Update on Rough Weather Hinders Barge Salvage Operations. November 29, 2005. http://www.piersystem.com/go/doc/425/89575/ , as of April 2010.

# Appendices

## Appendix A: Users Manual

# SOSim Users Manual

**Submitted to:**

**The Coastal Response Research Center**
**Gregg Hall**
**University of New Hampshire**
**35 Colovos Road**
**Durham, New Hampshire 03824**

**Submitted by:**
**M. Angelica Echavarria-Gregory, M.S.**

**Principal Investigator:**
**Dr. James D. Englehardt, Ph.D., P.E.**

**Department of Civil, Architectural and Environmental Engineering**
**University of Miami**
**1251 Memorial Drive**
**McArthur Engineering Building, Suite 321**
**Coral Gables, Florida, 33124-0630**

**Project Period: August 15, 2008 to August 14, 2010**

**Submission Date: September 8, 2010**

This project was funded by a grant from NOAA/UNH Coastal Response Research Center.
NOAA Grant Number(s): NA04NOS4190063. Project Number: 08-088

# Table of Contents

## List of Figures and Tables

# 1.0 Introduction

SOSim is a modeling tool developed to help locate sunken oil in relatively flat bays based on limited available field data collected shortly after a spill, when oil has begun appearing on the bottom. This User Manual will guide the operator through model installation to model operation and results management, to obtain maps of relative probabilities of finding sunken oil at user-specified times of prediction that are not conditional upon the values of uncertain parameters of the model.

## 1.1 What is SOSim?

SOSim is a predictive Bayesian multi-modal Gaussian model of relative probabilities of finding sunken oil at points on a bay bottom and in time, designed to accept primary information in the form of limited field data at one or more sampling times. The predictive relative probabilities produced are not conditional on the values of uncertain model parameters such as the water velocity and coefficients of dispersion on the bay bottom. These probabilities can be interpreted as *relative oil concentrations*, depicted to occur on the bottom in somewhat more disperse patches than are actually occurring due to uncertainty in the advective and dispersive forces acting on the oil at depth. Due to the lack of information on the total oil sinking as a function of time, the model cannot assess absolute concentrations, but rather relative concentrations showing oil “hotspots” and areas where oil may not be collecting.

SOSim has been programmed in Python in its entirety. The SOSim model, although using and relying for much of its functionality on several existing Python packages and modules, consists of three principal Python modules developed by the doctorate research assistant: the graphical user interface (GUI) module, the operating and processing interface (OPI) module , and the core module. The GUI module (ui_SOSim.py in the electronic deliverable) automatically layouts and keeps characteristics of widgets, labels, canvases and templates in the graphic user interface, holds raw user’s input and imports Windows palettes and display.  The OPI module (SOSimOPI.py in the electronic deliverable) is the executable file. It imports and links all other modules together, it captures the input information  that is entered by the user in the GUI module and operates interrelated buttons and activities of the GUI; it filters, organizes, and processes the input,; passes ready-to-use variables and attributes to the core code; accepts modeling results back from the core module; processes the results; and sends display signals to the GUI module’s canvas layout for it to depict relative sunken oil concentrations on a map  for further user interaction. It also controls modal behavior of the main windows, pop outs, menus and toolbars. The core module (SOSimCore.py in the electronic deliverable) uses variables and attributes passed by the OPI module to compute the predictive Bayesian relative concentrations, saves output files, and passes results back to the OPI module for display by the GUI or for further use. The GUI has the capability to communicate with the core module through the OPI module during a model run, after a predictive result has been presented, to allow the user to request the modeling of contiguous or other areas as needed.

The GUI contains three basic layouts other than the main toolbars and menus: (1) the pre-run layout or input section, where the user is prompted for input information concerning the spill, sampling campaign(s) and time(s), land boundary, desired modeling area, and prediction times, (2) the canvas layout, where results are displayed in interactive, georeferenced maps, and (3) the post-run layout or output section, which contains tools that allow the user to display the results at different times of prediction, run the model for contiguous areas, save results, print images, and perform other formatting tasks.

### 1.2 Why Python?

The Python programming language was chosen for development of the SOSim model based on the following criteria:

- The programming software is non-proprietary and open source,
- The programming environment supports relatively rapid prototyping and testing,
- The language is robust in terms of functioning in various operating environments with minimal damage, alteration or loss of functionality, and
- The source code is viewable at all times.

Python is a general-purpose, high-level programming language first released by Guido Van Rossum in 1991 in The Netherlands. Python is flexible, applicable to many programming domains and available on many platforms. The language has an open, community-based development model managed by the non-profit Python Software Foundation. Python’s design philosophy emphasizes programmer productivity and code readability (core syntax and semantics are minimalistic, employing white spaces and easy commands). Python supports multiple programming paradigms (primarily object oriented) and features a fully dynamic type system and automatic memory management, similar to Perl, Ruby, Scheme, and Tcl.

The Python programming language has an open, general public license (GPL) that allows source code modification, addition of original code as “imported” packages, and publication of derived work (as GPL). Packages that are created around the world are available to the Python community. Python has also been used as an extension language for many existing systems, including GIS, Web programming, numerical tools, and the R statistical package.

### 1.3 Objectives of the user manual: a guide to the SOSim GUI

The objective of this user manual is to guide the operator through installation and operation of SOSim. The GUI is the point of connection between the user and the processing modules, which perform all required processing of raw input from users and provide the core module with the appropriate information. Among the most important tasks of the GUI, aided by the OPI module, are:

- Collection of basic information on the spill in terms of time of occurrence, and coordinates (longitude and latitude);
- Display of the location of the spill on the map canvas within a 2-degree radius around the spill to allow selection of the desired modeling area;
- Storage and processing of input data from single or multiple sampling campaigns;
- Assignment of the resolution and scale (rectangular) of the results based on default values or a user-defined number of modeling nodes in each direction: north-south and west-east, within the desired or default modeling area;
- Setting of customized dates and times at which sunken oil mass prediction is desired,
- Processing, storage, and passage to the core module of user input;
- Acceptance of output from the core module and geo-referencing of it on the local map; presentation of relative probabilities of finding sunken oil, (0-1), on a relative, color-coded scale, with hotspots in red (1) fading to blue (0). Although probabilities of sunken oil decrease in time, the hue is re-rendered in every time calculation, such that the areas with the highest probability of finding sunken oil are shown in red at each modeled time, independently of relative probabilities shown for other times of prediction; and
- Processing of optional post-run operations include display of results at different prediction times and performance of partial recalculations to view results for contiguous modeling areas. Useful documentation functions including saving the results as images and printing are also included in the GUI.

### 1.4 Scope of Model Applicability

Version 1.0 of SOSim is designed for application to:

- Sunken oil;
- Relatively flat bay bottoms, dredged bays, reef flats and lagoons or pools protected by offshore rocks; bays with steeply sloped bottoms would require capability for the use of bathymetric data as prior information, a possible future enhancement;
- Resolution down to the scale of the tidal excursion (oil locations effectively averaged across this excursion);
- Prediction up to the time that the majority of the oil mass is predicted to reach the shoreline;
- Discrete accidental oil releases (as opposed to natural, progressive oil seepage); and
- Relatively uncomplicated concave and convex shoreline geometries; modeling in straits, inland water bodies, harbors, islet areas, and like geographies are not addressed due to computational limitations and the sometimes transient nature of small-scale features.

# 2.0 Installation

## 2.1 Hardware Requirements

SOSim Version 1.0rc1 has been developed for use within the Microsoft Windows 32 bit operating system environment, though porting to other platforms including the Mac OS could be considered for future versions. The software has also been shown in initial tests to run on Microsoft Windows 64 bit platforms, although development was not intended for this application. To achieve reasonable performance in terms of computational speed (hours), a 3.0 GHz processor or better is required. In cases in which the machine will be expected to perform tasks in addition to SOSim, an active duo or second processor is required.

SOSim can run on a computer with a page file (virtual memory) of minimum 2.3 GB. Nevertheless, it is recommended that the memory card is of a minimum of 3.0 GB. Memory requirements of SOSim are determined by the fact that Python can allocate memory only up to a total of 2.3 GB, including memory required for all machine functions prior to running the model, when implemented on the Windows 32 bit platform (this limitation is not expected if the model is developed in the future for the Windows 64 bit OS). The total memory used by all processes before starting to run SOSim is typically about 512 MB on machines not having many applications installed and many idle processes to run by default, except for Windows 7 and some editions of Windows Vista which may consume up to 1 GB when idle. Therefore, for the majority of spill cases to be solved with optimal resolution and including recalculations, it is estimated that a computer would require an available memory of about 1.7 GB (that is, a difference of about 1.7 GB between the 2.3 GB limit and the kernel memory taken up by idle processes). Indirect warning messages provided by the GUI will guide the user in setting the best possible resolution to achieve optimal performance in terms of memory.

## 1.1. Software Installation

Python and all related prerequisites of SOSim are included in the OSGeo4W console, a compilation of open-source packages developed by the Quantum GIS project. The OSGeo4W console is distributable and therefore is included with the SOSim package distribution. You need to have administration privileges in the machine that you will install in. Steps required for the installation of SOSim are as follows. Note that additional advanced or updated installation procedures may be needed by a developer for future continued development of the Simulator.

1. Open the distribution SOSim v. 1.0rc1. You will see two icons, one for SOSim itself and one for OSGeo4W. Copy and paste the SOSim icon (folder) that comes with the distribution directly to the *C:\Program Files* directory of your machine;
2. The OSGeo4W package is required and should be installed when installing SOSim using the executable file osgeo4w-setup.exe provided with the distribution. This executable has

an online installer, which means that your machine needs an internet connection at the time of the installation. Double-click on the icon and choose “Desktop express install” when prompted for installation preferences, and then keep the following default options checked. Once installed, you will find several shortcut icons on your desktop; only the desktop shortcut to OSGeo4W console is needed, all others can be deleted.

3. Once installed, go to *C:\OSGeo4W\apps\qgis\bin* and find the qgis_core.dll and qgis_gui.dll libraries. Copy and paste them to the directory *C:\OSGeo4W\apps\qgis\python\qgis*;
4. Add to your system or edit the environment variable below:

   PYTHONPATH: C:\OSGeo4W\apps\qgis\python

   Environment variables must be changed from an account with “administrator” access privileges, and for all users. To change an environment variable in a Windows 32 bit machine, right-click on the “My Computer” icon from the Start menu and select “Properties”. In the System Properties box, under “Advanced”, select “Environment Variables” at the bottom. System variables are in the lower part of the box and you only have access to them if you have administrator privileges on the machine. Screen the list to see if the environment variable that you need already exists; if it does, click on it and on “Edit”, then type a semicolon after the existing text and then type the given path, without spaces. If the environment variable does not exist, click on “New” and type the name in capital letters, then the given path.

Now the SOSim software is callable from the OSGeo4W console using the following steps 1 - 3:

1. Double-click on the OSGeo4W shortcut logo on your desktop,
2. Type in the window: *cd C:\Program Files\SOSim*, and
3. Type *SOSimOPI.pyw*. The SOSim GUI will pop up and will be ready to use.

If your Windows version cannot open the file and requests to select a program from a list, click cancel and close the OSGeo4W console, and then call SOSim using the following alternative steps 1 - 3:

1. Double-click on the OSGeo4W shortcut logo on your desktop,
2. Type in the window: *python*
3. Type *execfile(“C:/Program Files/SOSim/SOSimOPI.pyw”)*. The SOSim GUI will pop up and will be ready to use.

Repeat the last 3 steps at your convenience, as needed to execute SOSim.

## 3.0 Input

Required input is prompted in the area located to the left of the canvas (see Figure 3.1) . The results of the prediction depend on the input. In particular, movement of the oil will be predicted based on relative oil concentrations at the field sampling points at and around a spill site, the time and location of the spill and of the samples collected, and shoreline boundaries. Other essential model input determining output characteristics including run time and resolution includes basic geographic information about the spill, extent of the modeling area, desired spatial resolution of the graphical output, geographic conditions within the modeling area such as proximity to the shoreline, and the dates at which predictions are desired. The GUI's input area is organized according to functionality, as described in the following sections.

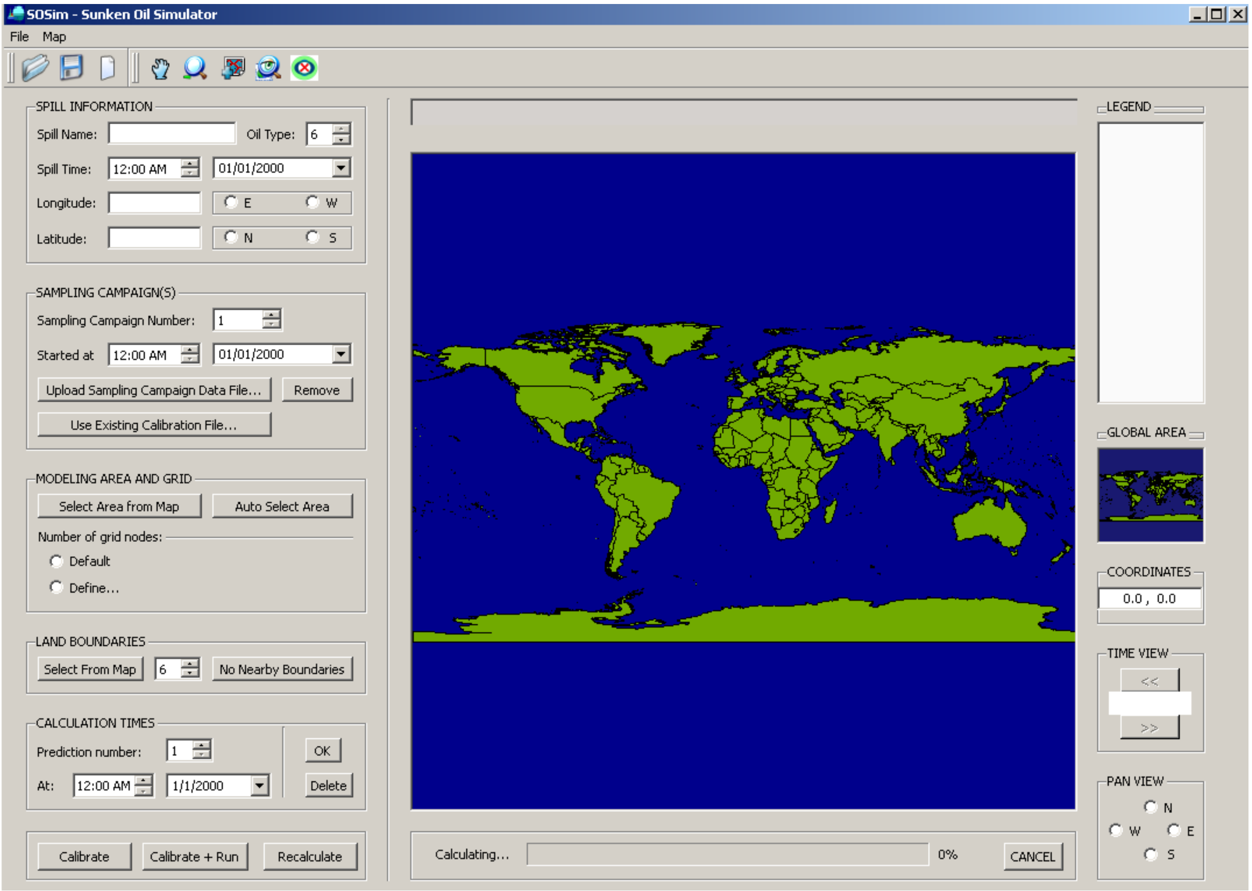

SOSim - Sunken Oil Simulator

SPILL INFORMATION

Spill Name:

Oil Type: 6

Spill Time: 12:00 AM 01/01/2000

Longitude: ○ E ○ W

Latitude: ○ N ○ S

SAMPLING CAMPAIGN(S)

Sampling Campaign Number: 1

Started at 12:00 AM 01/01/2000

MODELING AREA AND GRID

Number of grid nodes:

○ Default

○ Define...

LAND BOUNDARIES

6

CALCULATION TIMES

Prediction number: 1

At: 12:00 AM 1/1/2000

Calculating... 0%

COORDINATES

0.0 , 0.0

PAN VIEW

○ N

○ W ○ E

○ S

Figure 3.1. Main screen of the computer application, before starting a new project.

## 3.1 Spill Information

Information on the spill name, oil type, location, and time are first entered as shown in Figure 3.1

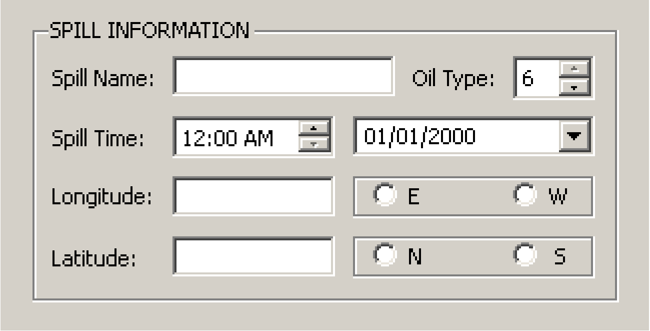

SPILL INFORMATION

Spill Name: 　 Oil Type: 6

Spill Time: 12:00 AM 　 01/01/2000

Longitude: 　 ○ E ○ W

Latitude: 　 ○ N ○ S

Figure 3.2. Spill Information input prompts in the GUI.

This spill information is used to set the geographic system of reference for the run. Required information includes the spill time and the coordinates at which the accident most likely occurred. A spill name is also prompted for use in saving and distinguishing output figures and files. The oil type refers to the classification of oils into six generally accepted classes by weight and other properties affecting their behavior in the environment (Research Planning Inc, 1994), as explained below under *Oil Type*.

The following conditions apply to the Spill Information input section:

- Only a point source spill occurring at a pair of coordinates, in degrees of longitude and latitude) can be modeled;
- *Spill Name* prompt: allows the user to set the title of the spill, e.g. "DBL-152". Characters /, \, *, <, >, ", | and ? are not accepted but blanks between words are recognized. If a change in typing is required, an informational message will pop up after all inputs to the Spill Information panel have been entered;
- *Oil Type*: set the spin box from 1 to 6 according to the type of spilled oil, as follows (Research Planning Inc, 1994). Type 1 oils are very light, perhaps ~31 °API gravity, including gasoline and very volatile hydrocarbons. Type 2 are moderately volatile and soluble, including jet fuels, diesel fuel, number 2 fuel oil, and light crude oils. Type 3 includes most crude oils, characterized by their persistence and diminished propensity to evaporate (about one third of the total mass evaporates within 24 hours). Type 4 oils may have ~10 °API gravity, little propensity to evaporate or dissolve, and high likelihood of sinking. Type 5 oils have essentially no evaporation potential, weather very slowly, and sink immediately, including heavy industrial fuel oils. Type 6 oils include heavy animal or plant oils.
- *Spill Time*: set the spin box to the time at which the most significant oil loss occurred. Notice that you can edit the hour and minutes using either the mouse cursor or the arrows of the spin box, or both.  Then, set the day, month and year of the spill using the smart

calendar that pops up when you click in the drop-down menu located to the right. The date line edit can also be changed manually using the mouse cursor and the keyboard.

- *Longitude*: this line prompts for a decimal quantity in degrees (WGS) corresponding to the longitude coordinate at which the spill occurred. All quantities must be greater than zero and must have decimal figures that can be zero. In front of the prompt the user shall select the radio button “E” (longitude east) or “S” (longitude south), which will assign a direction to the quantity you typed and will guide the canvas to the world’s geographic meridian closest to the longitude of the spill site.
- *Latitude*: this line prompts for a decimal quantity in degrees (WGS) corresponding to the latitude coordinate at which the spill occurred. All quantities must be greater than zero and must have decimal figures that can be zero. In front of the prompt, select the radio button “N” (latitude north) or “S” (latitude south), which will assign a direction to the quantity you typed, will guide the canvas to the world’s geographic parallel closest to the latitude of the spill site, and will mark the spill site with an X (Figure 3.3).

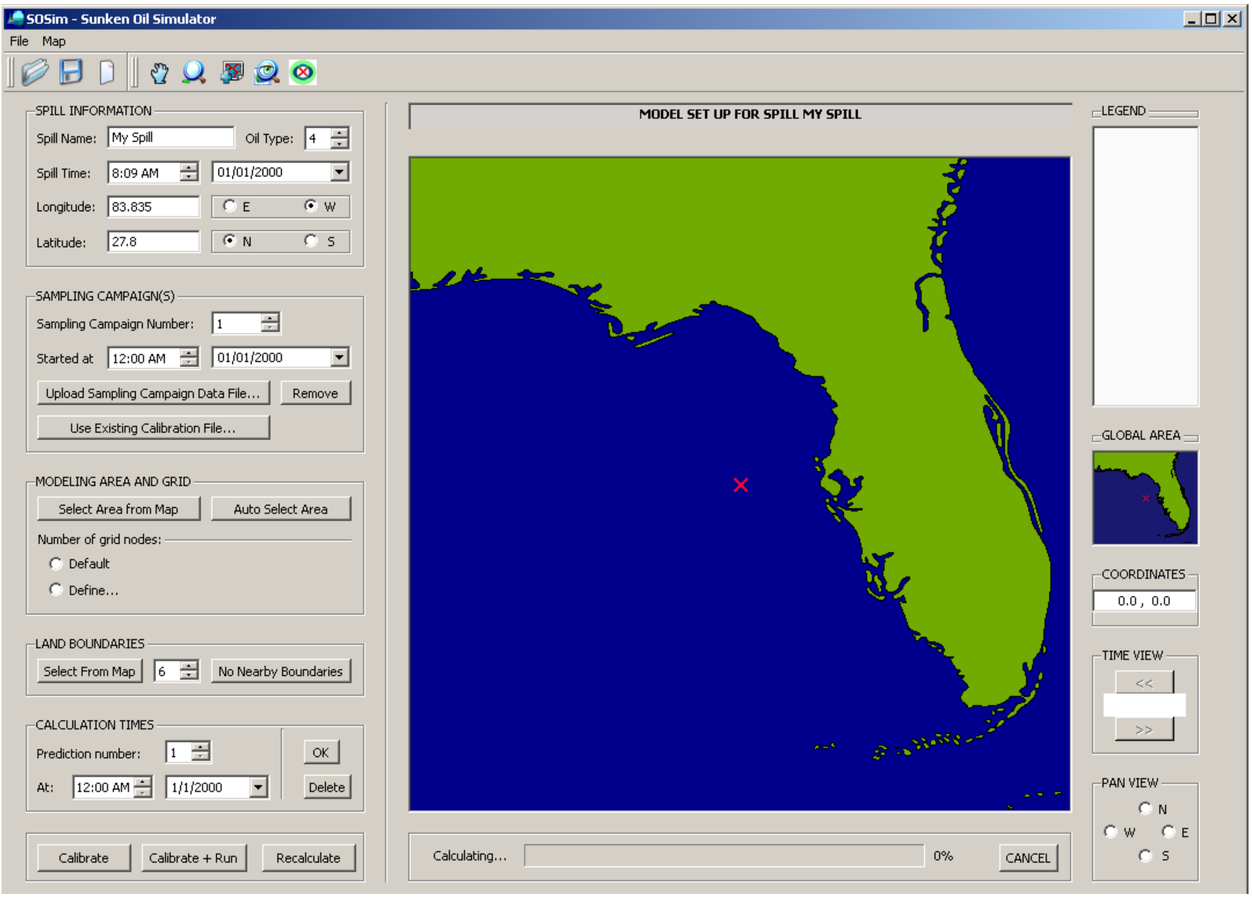

SOSim - Sunken Oil Simulator

SPILL INFORMATION
Spill Name: My Spill
Oil Type: 4
Spill Time: 8:09 AM 01/01/2000
Longitude: 83.835 ○ E ● W
Latitude: 27.8 ● N ○ S

SAMPLING CAMPAIGN(S)
Sampling Campaign Number: 1
Started at 12:00 AM 01/01/2000

MODELING AREA AND GRID
Number of grid nodes: ○ Default ○ Define...

LAND BOUNDARIES
6

CALCULATION TIMES
Prediction number: 1
At: 12:00 AM 1/1/2000

MODEL SET UP FOR SPILL MY SPILL

COORDINATES
0.0 , 0.0

Calculating... 0%

Figure 3.3. Marked spill site after selection of longitude, latitude values and directions.

- If you wish to modify the spill name at this point, you would have to proceed with the change and then repeat the last step *'Latitude'*.

## 3.2 Sampling Campaign(s)

Oil movement on the bottom is inferred by the model based principally on the relationship between the location and time of the spill, and the locations and relative concentrations at subsequent sampling times. For purposes of SOSim input, a sampling campaign is defined as a set of qualitative measurements of relative oil concentration on the bottom, taken at approximately the same time. Spill and sample coordinates are entered in WGS (World Geodesic System) units (decimal degrees of longitude and latitude). Time differences from sampling point to point of up to a few hours may not need to be considered, as the model was not designed to track possible cyclic excursions of the oil due to the tidal cycle. SOSim v. 1.0 accepts and has capability for processing up to 10 different sampling campaigns.

Each sampling campaign file must be created in a separate Microsoft Excel spreadsheet, closely following the instructions below:

- The spreadsheet must use only the first 4 columns: A, B, C and D
- A title (field name) for the column must be included in the first line of each column,
- In Column A, enter index numbers for the data points, beginning with the numeral "1" to be entered on line 2;
- In Column B, enter the longitude coordinate, in decimal degrees, at which the sample was collected, starting on line 2;
- In Column C, enter the latitude coordinate, in decimal degrees, at which the sample was collected, starting on line 2;
- In Column D, enter a positive or zero value for the measured relative oil concentration on a relative scale of range scale of 0 – 100 (that is, enter a percentage of oil without the percent sign), starting on line 2. If quantitative measurements are available, measurements can be entered with accuracy of up to several decimal places.

When complete, the Excel file must be saved as a *".txt (tab-delimited)"* file in the location of your preference. Figure 3.4 shows an example of the Excel file.

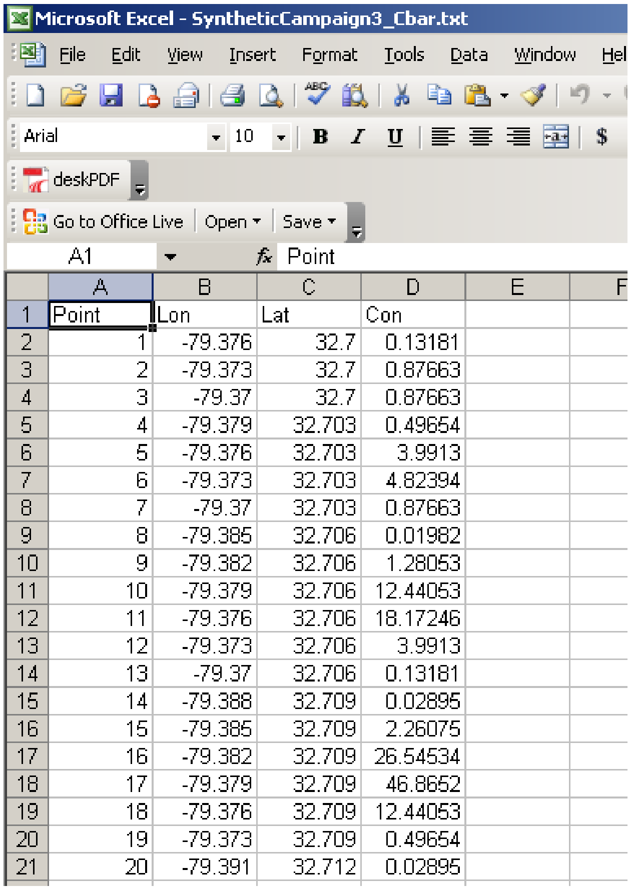
Microsoft Excel - SyntheticCampaign3_Cbar.txt
File Edit View Insert Format Tools Data Window Hel
Arial 10
deskPDF
Go to Office Live Open Save
A1
Point

|  | A | B | C | D | E | F |
|---|---|---|---|---|---|---|
| 1 | Point | Lon | Lat | Con |  |  |
| 2 | 1 | -79.376 | 32.7 | 0.13181 |  |  |
| 3 | 2 | -79.373 | 32.7 | 0.87663 |  |  |
| 4 | 3 | -79.37 | 32.7 | 0.87663 |  |  |
| 5 | 4 | -79.379 | 32.703 | 0.49654 |  |  |
| 6 | 5 | -79.376 | 32.703 | 3.9913 |  |  |
| 7 | 6 | -79.373 | 32.703 | 4.82394 |  |  |
| 8 | 7 | -79.37 | 32.703 | 0.87663 |  |  |
| 9 | 8 | -79.385 | 32.706 | 0.01982 |  |  |
| 10 | 9 | -79.382 | 32.706 | 1.28053 |  |  |
| 11 | 10 | -79.379 | 32.706 | 12.44053 |  |  |
| 12 | 11 | -79.376 | 32.706 | 18.17246 |  |  |
| 13 | 12 | -79.373 | 32.706 | 3.9913 |  |  |
| 14 | 13 | -79.37 | 32.706 | 0.13181 |  |  |
| 15 | 14 | -79.388 | 32.709 | 0.02895 |  |  |
| 16 | 15 | -79.385 | 32.709 | 2.26075 |  |  |
| 17 | 16 | -79.382 | 32.709 | 26.54534 |  |  |
| 18 | 17 | -79.379 | 32.709 | 46.8652 |  |  |
| 19 | 18 | -79.376 | 32.709 | 12.44053 |  |  |
| 20 | 19 | -79.373 | 32.709 | 0.49654 |  |  |
| 21 | 20 | -79.391 | 32.712 | 0.02895 |  |  |

Figure 3.4. Creation of a sampling campaign file. Recording spatial coordinates and observed relative concentration values (scale 0 to 100) for each sampling point in an Excel file.

To upload each sampling campaign file, make use of the prompts and buttons in the Sampling Campaign(s) panel of the user interface shown in Figure 3.5.

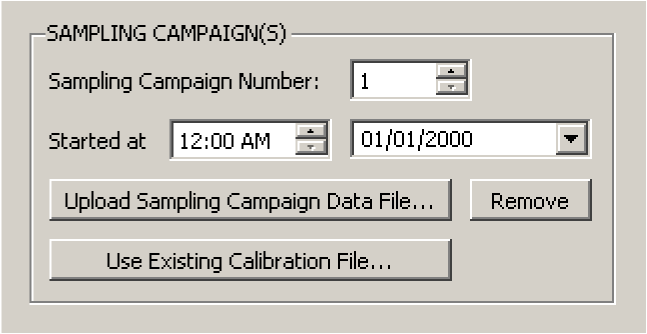
SAMPLING CAMPAIGN(S)
Upload Sampling Campaign Data File...
Remove
Use Existing Calibration File...

Sampling Campaign Number: 1

Started at 12:00 AM 01/01/2000

Figure 3.5. Sampling Campaign input prompts and buttons in the GUI.

The following descriptions and conditions apply:

- *Sampling Campaign Number*: adjust the number in the spin box to that of the sampling campaign that you want to upload and process. A campaign number greater than 10 is not accepted;
- *Start at: Time, Date:* set the spin box to the time representing the midpoint of the sampling campaign. Note that you can edit the hour and minutes by using either the mouse cursor or the arrows of the spin box, or both. Set the day, month, and year of the sampling campaign using the smart calendar that pops up when you click in the drop-down menu located to the right. Notice that the date line edit can also be changed manually with the mouse cursor. It is not necessary that the dates of previously uploaded campaigns have earlier sampling dates than the campaign currently being uploaded, but the dates of all sampling campaigns must be subsequent to the spill date entered and subsequent to the assessed retardation gap, during which oil may be still sinking depending on its type. A warning message will guide you in case of error. Sampling dates of different campaigns can even be the same (different response teams can take samples in different areas at the same time). Nevertheless, it is recommended that sampling be conducted at different times in order for the model to better account for changes in sunken oil movement due to e.g. tidal action, storm events, and sediment entrainment.
- *Upload Sampling Campaign Data File* button: this button opens an explorer dialog box that allows you to browse for your *".txt (tab-delimited)"* Excel file containing the sampling campaign information which you want to upload. It is recommended that every sampling campaign file have a different name and be identified with a number. If the sampling campaign entered happens to be during the assessed sinking retardation time, the sampling campaign will be invalidated, and a warning issued.
- *Remove Sampling Campaign* button: this button automatically removes from the record the data of the campaign that corresponds to the current number in the *Sampling Campaign Number* spin box. A confirmation message pops up to confirm the deletion, along with the number of the sampling campaign that was removed. However, deletion of the file does not change the numbers of any other uploaded campaigns, so that there will now be a campaign number with no assigned data.
- *Use Existing Calibration File* button: this button allows the modeler to use an existing calibration file, which must have been named and saved by the user after a previous calibration. By clicking on this button, a search dialog box will open and will prompt for the directory and file location. An informational message will confirm that the calibration file has been loaded when found.

An example uploaded sampling campaign data file is shown in Figure 3.6.

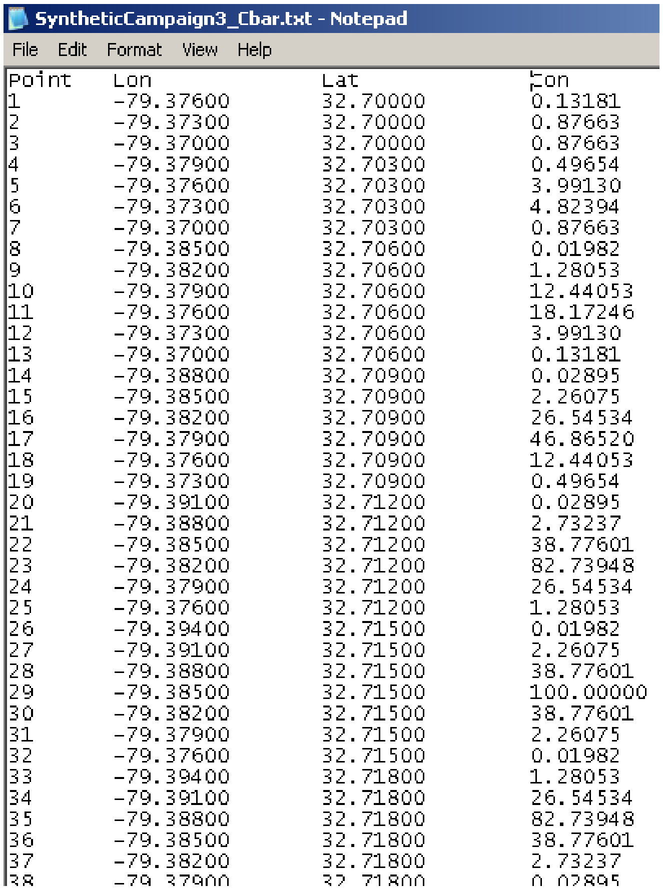
SyntheticCampaign3_Cbar.txt - Notepad
File Edit Format View Help

```
Point   Lon         Lat         Con
1       -79.37600   32.70000    0.13181
2       -79.37300   32.70000    0.87663
3       -79.37000   32.70000    0.87663
4       -79.37900   32.70300    0.49654
5       -79.37600   32.70300    3.99130
6       -79.37300   32.70300    4.82394
7       -79.37000   32.70300    0.87663
8       -79.38500   32.70600    0.01982
9       -79.38200   32.70600    1.28053
10      -79.37900   32.70600    12.44053
11      -79.37600   32.70600    18.17246
12      -79.37300   32.70600    3.99130
13      -79.37000   32.70600    0.13181
14      -79.38800   32.70900    0.02895
15      -79.38500   32.70900    2.26075
16      -79.38200   32.70900    26.54534
17      -79.37900   32.70900    46.86520
18      -79.37600   32.70900    12.44053
19      -79.37300   32.70900    0.49654
20      -79.39100   32.71200    0.02895
21      -79.38800   32.71200    2.73237
22      -79.38500   32.71200    38.77601
23      -79.38200   32.71200    82.73948
24      -79.37900   32.71200    26.54534
25      -79.37600   32.71200    1.28053
26      -79.39400   32.71500    0.01982
27      -79.39100   32.71500    2.26075
28      -79.38800   32.71500    38.77601
29      -79.38500   32.71500    100.00000
30      -79.38200   32.71500    38.77601
31      -79.37900   32.71500    2.26075
32      -79.37600   32.71500    0.01982
33      -79.39400   32.71800    1.28053
34      -79.39100   32.71800    26.54534
35      -79.38800   32.71800    82.73948
36      -79.38500   32.71800    38.77601
37      -79.38200   32.71800    2.73237
38      -79.37900   32.71800    0.02895
```

Figure 3.6. Example uploaded sampling campaign data file.

## 3.3 Modeling Area and Grid

The modeling area is the geographical area over which the user wishes to predict oil locations in time. Due to limitations in terms of computational time and the corresponding resolution of the statistical computations and output, assignment of modeling areas larger than 50 km wide by 50 km long (approximately 0.50 longitude by 0.5 latitude degrees) is not recommended. However, assignment of larger regions is allowed by SOSim, for example to allow the user to first check the overall movement or direction of a spill before modeling smaller areas. In that case, a warning message will pop up requesting permission from the user to assign such a large area, and warning of the disadvantage in doing so. An alternate approach for viewing results over a larger area, is conduct a run for the principal area first, then conduct partial re-runs of the program for contiguous regions using the post processing *"Pan-posteriori"* and *"Recalculate"* set of tools located to the right of the screen, once their use become available after processing the current run. However, in this case the results for each area modeled will have a new color scale, not continuous with the first (because the highest relative concentration predicted for each run will be colored dark red, for example, though these concentrations will not likely be equal), making interpretation more difficult.

The grid is a set of orthogonal points in the west-east and north-south directions defined on a Cartesian plane, representing the area to be modeled. Results of the prediction are calculated and plotted at every node in the grid. The more nodes requested in each direction, the better the spatial resolution of the mapped output and the longer the run time. These characteristics are entered in the panel “Modeling Area and Grid” shown in Figure 3.7:

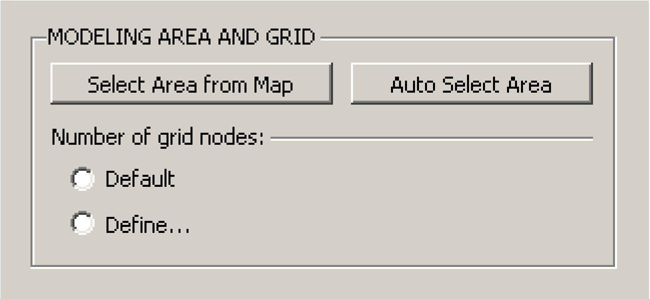

Figure 3.7. Modeling Area and Grid input prompts and buttons in the GUI.

Information is entered as follows:

- *Select Area from Map* button: this button is a map tool that enables a selection cursor. To select the modeling area, left click on the map point that corresponds to the north-east corner of the desired modeling area. Then drag the pointer, without releasing the left button, to the south-east corner of the area to be mapped. Release the mouse left button to set the area (Figure 3.8). It is not necessary to include the spill site (marked with an X) within the modeling area, though it may be helpful to model the vicinity around the spill site first;

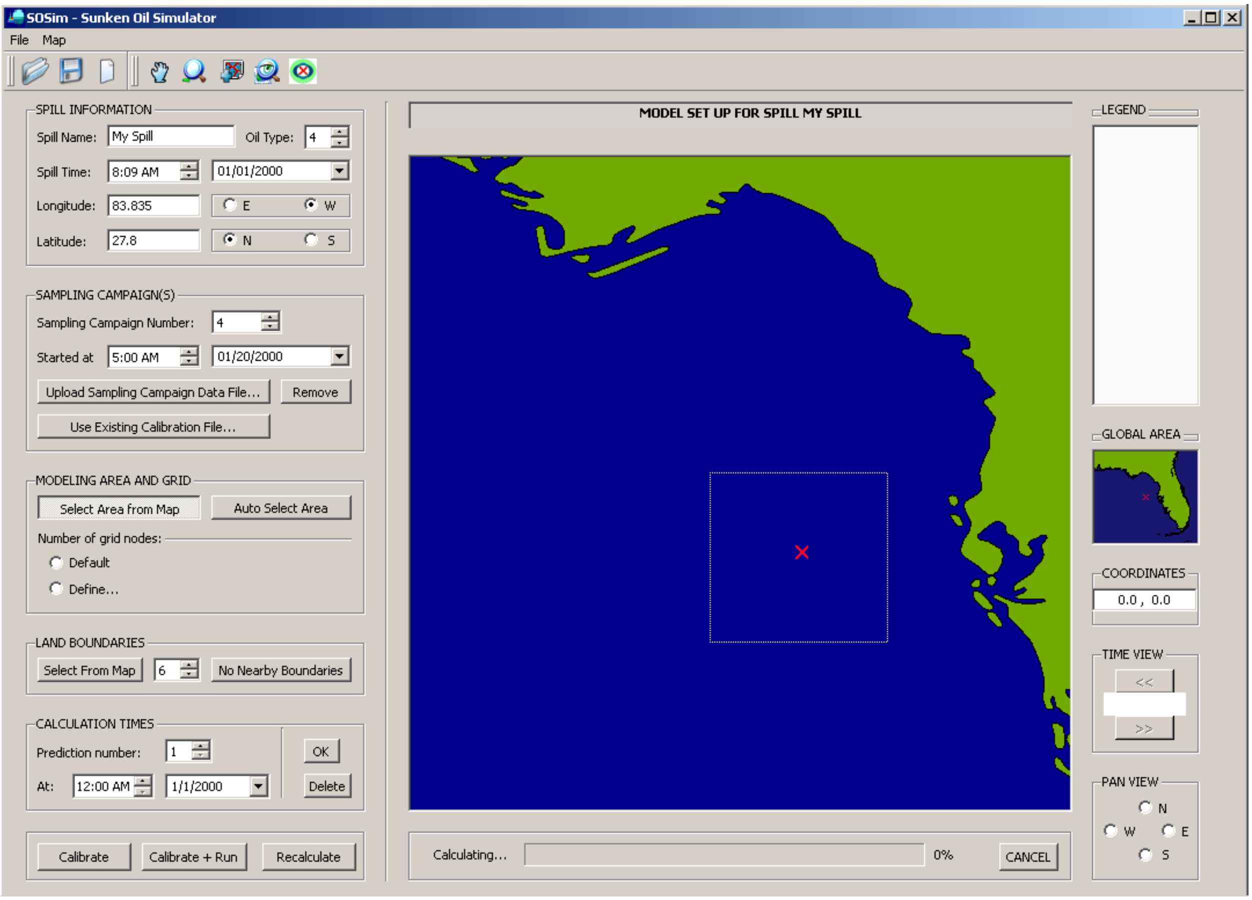

Spill Name: My Spill  Oil Type: 4

Spill Time: 8:09 AM  01/01/2000

Longitude: 83.835  ○ E ● W

Latitude: 27.8  ● N ○ S

Sampling Campaign Number: 4

Started at 5:00 AM  01/20/2000

Land boundaries: 6

Prediction number: 1

At: 12:00 AM  1/1/2000

Calculating... 0%

Coordinates: 0.0 , 0.0

Figure 3.8. Selecting the modeling area in the GUI.

- *Auto Select Area* button: this button automatically zooms in and selects a region of 0.25 degrees longitude by 0.25 degrees latitude around the spill site (approx. 25 by 25 km or approx. 15.6 by 15.6 miles). This feature can be used along with the post processing *"Pan-posteriori"* and *"Recalculate"* set of tools when the user plans to consecutively run SOSim for contiguous geographical regions of the same size so as to obtain a mosaic of a large area; and
- *Number of Grid Nodes*: as mentioned previously, resolution of the output is defined by the number of nodes desired in the west-east and north-south directions within the modeling area. Two options are available to the user. The first is the *Default* radio button, which assigns 25 nodes in each direction. Using this option, if the modeling area is been defined using the *Auto Select Area* button, then a node is placed every 0.01 degrees (approximately every kilometer). The second is the *Define* radio button, which makes available one prompt line in each direction, for the user to assign equal or different numbers of east-west and north-south nodes.

### 3.4 Land Boundaries

Shoreline boundaries are accounted for by SOSim if the user indicates that land is present in the area to be modeled. Two options are available to the user, as indicated in Figure 3.9:

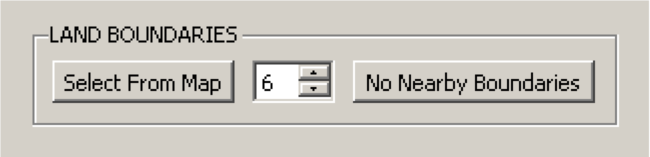

Figure 3.9. Land Boundaries input buttons and spin box in the GUI.

Limitations on the boundary conditions accepted by SOSim v. 1.0 include (a) only one mass of land can be defined in each modeling area (e.g. a single polyline within a single modeling area), (b) irregularly-shaped geographic features close to shore, such as islets and mangroves, should be considered part of a single land mass, and (c) the maximum number of vertices is set at 10. This latter restriction is not inherent to internal model computations, but was fixed so as to limit run times on desktop computers to the order of one day. Input is entered as follows:

- Boundaries spin box: by default, this box is set to 6, but can spin from 2 to 10. The number set in this box is the number of vertices that the user wishes to select on the map so as to mimic the boundary conditions by the use of a polyline. If the number is not changed before clicking on the *Select from Map* button, the number of vertices defaults to 6.
- *Select from Map* button: clicking on this button enables two functionalities. First is a message box that instructs the user to "Please select *X* points on the land border shown on the canvas." where *X* is the number in the spin box, 6 by default. Straight shorelines can be approximated by two points, slightly curved shorelines may be approximated with three points, and so on, offering the potential to greatly reduce run time. Second, the map tool with which the user defines these points is enabled. To select each point, click the left mouse button at a point on the shoreline depicted in the GUI canvas, release it in the same position, and then proceed to the next point. A thin yellow line will follow and connect these points to create a 2 to 10-vertex polyline approximating the actual boundary. Note that if a very large modeling area is selected that includes land, but all shorelines are far from the spill and dispersing oil, the predicted results will be negligibly different from the results that could be obtained much more quickly by selecting the *"No Nearby Boundaries"* option; and

- *No Nearby Boundaries* button: this button communicates to the model the lack of need for computing reflection of sunken oil from shoreline boundaries within the modeling area, for example when the geographic area to be modeled includes only open sea.

### 3.5 Prediction Times

The selection of prediction times is the last segment of required input. In order to enter these times, all previous input sections must be completed. An error message pops up if input information is missing. Projection times are the dates and hours the user wishes to view predicted sunken oil relative concentrations. The user can request up to five times of prediction per model run. However, computational run time will be longer for each projection time requested, and it is recommended that one time at a time is modeled with the aim to plan and make timely decisions about subsequent run needs. Times are input to the panel shown in Figure 3.10.

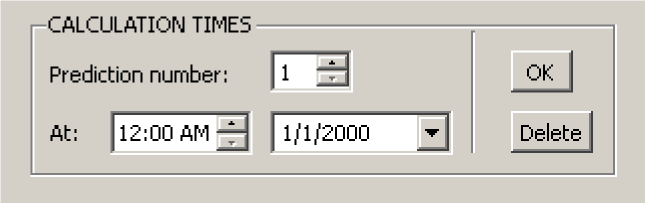

Figure 3.10. Prediction Times input buttons in the GUI.

SOSim v. 1.0 calculations are based on the assumption that sunken oil impacting the shoreline will be reflected back into the water. This assumption allows modeling of accumulation at the shoreline. However, the assumption may not be realistic at times after which the majority of the oil mass is predicted to reach the nearshore environment. At these later times, predictions may indicate a “bouncing” of the patch off of the shoreline. To attempt to avoid this potentially unrealistic result, a warning message will pop up if the requested prediction time is estimated by the model *a priori* to be after the time of predicted landfall. The user should be aware that such predictions in the nearshore environment may potentially occur, even in some cases if no *a priori* warning is issued. In general, predictions of substantial sunken oil occurrence at the shoreline should be interpreted with care.

Input is entered as follows:

- *Prediction number* spin box: Assign a whole number index to each desired time of prediction. If the index number is not changed in the spin box when adding a new date and hour, a warning message will appear;
- *At* hour spin box and time line prompt: Complete these fields with, respectively: (a) the hour, including minutes if desired, and (b) the date, from the smart calendar pop-up, at which predictions are desired. The user must confirm final entry by clicking the *OK* button;
- *OK* button: Add the current hour and time to a list of prediction times, and assign it to the index position indicated by the *“Prediction number”* spin box. The GUI will then estimate whether the time entered is likely to be within the time required for the oil mass to reach the shoreline, if the oil is apparently moving towards the shore. If the time entered is determined to be potentially after the time of landfall, a warning message will pop up. Any prediction time prior to the most current sampling campaign cannot be modeled as the likelihood is affected by all sampling campaigns. A message will appear requesting that only sampling campaigns prior to the requested prediction time be on file.

- *Delete* button: If desired, you can use this button to cancel the addition of the prediction time that corresponds to the current value in the *"Prediction number"* spin box. If a prediction time is deleted by mistake, the hour and date can be added using a different, new index or *"Prediction number"*.

## 3.6 Default Input

Default input includes the internally-specified ranges of the uncertain model parameters. These default values can be modified by an experienced oceanographer or other operator, to refine the accuracy of the simulated predictions. Modified ranges may be based on dynamic field conditions or on site-specific information on a particular spill environment. Default input may be modified each time SOSim is launched, as needed.

To modify the default input, go to the *Options* menu of SOSim and click on *Modify Default Settings*. A tabbed widget will guide you through the three settings that can be modified, including the default initial parameter ranges, the default number of grid nodes, and the default resolution. Change the settings as required, noting that some values are restricted by the software given mathematical and physical constraints. Figure 3.11 displays a preview of the *Parameters Range* tab.

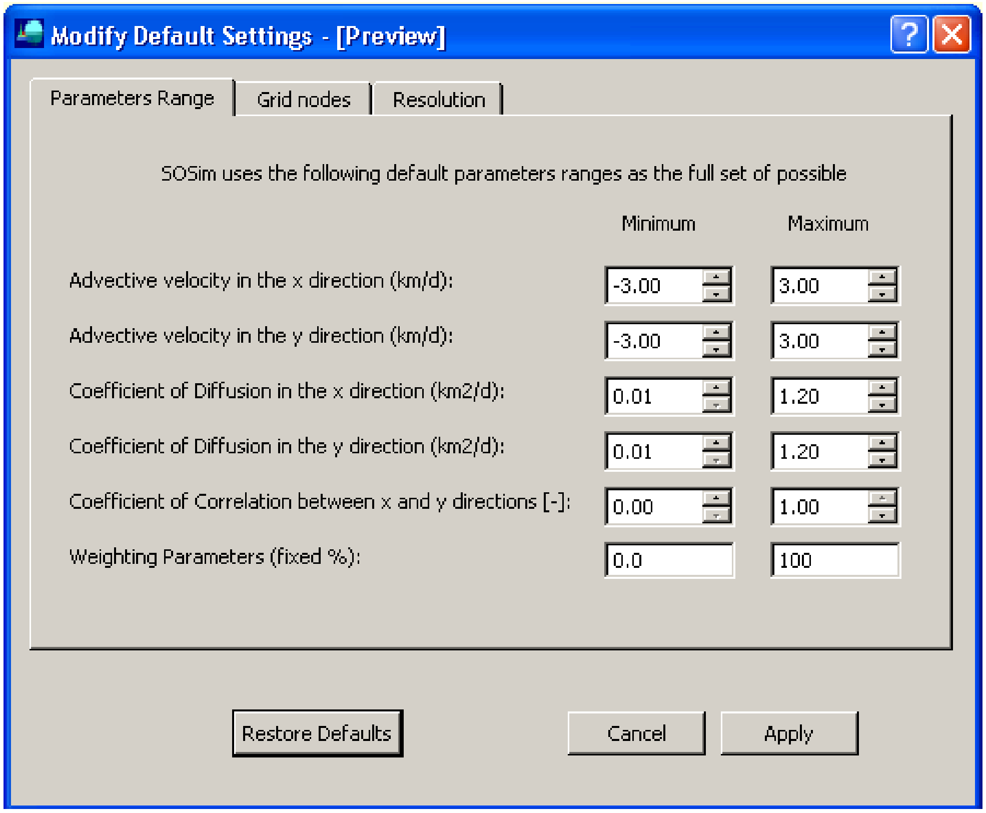

SOSim uses the following default parameters ranges as the full set of possible

| | Minimum | Maximum |
|---|---|---|
| Advective velocity in the x direction (km/d): | -3.00 | 3.00 |
| Advective velocity in the y direction (km/d): | -3.00 | 3.00 |
| Coefficient of Diffusion in the x direction (km2/d): | 0.01 | 1.20 |
| Coefficient of Diffusion in the y direction (km2/d): | 0.01 | 1.20 |
| Coefficient of Correlation between x and y directions [-]: | 0.00 | 1.00 |
| Weighting Parameters (fixed %): | 0.0 | 100 |

Figure 3.11. Modify default input settings dialog box.

## 4.0 Processing

This section describes operation of the model.

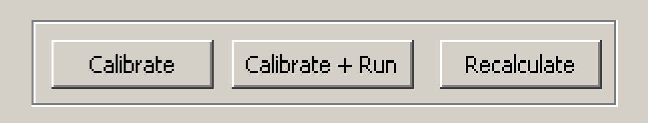

Figure 4.1. Processing buttons

### 4.1 The Calibrate, Calibrate + Run, and Recalculate Buttons

*Calibrate* button: this button is used if it is intended only to calibrate the model by using only the sampling campaign(s) uploaded files, the spill information, and the characteristics of the geographic area. No prediction times need be selected to run a calibration. When finished, the calibration files can be saved by the user for future use.

*Calibrate + Run* button: this button is used to instruct SOSim to first calibrate the model using the sampling campaign files and then immediately begin computations for prediction. This button is intended to obtain the results of a complete scenario by investing time in only one initial configuration. Overnight calibration-and-runs sessions are possible using this button. No changes to the input are allowed at this point until the core module has completed the Bayesian processing stage.

*Recalculate* button: this button has several uses. First, the button may be used to generate results for the same spill scenario at a different time prediction, without data entry and recalibration. Second, the button may be used to obtain a new prediction following a change in resolution, boundaries, or geographical area (post processing and optional output), again without additional data entry or recalibration. Third, the button can be used to generate results using an existing calibration file that has been imported using the *"Use Existing Campaign"* button, in the Sampling Campaign(s) section.

### 4.2 Run Time and Progress Bar

Run time increases as function of (a) the number of output nodes, or geographical resolution, selected by the user, (b) the existence of boundary conditions within the selected modeling area, and (c) the number of vertices in the polyline representing the shoreline, if present. A longer time of calculation (about 5 times longer) should be allowed when modeling spills within a coastal area. The progress bar indicates the total number of operations completed.

# 5.0 Output

Output is produced as a map representation of predicted relative oil concentrations within the modeling area. There are two classes of output: the default and the optional output.

## 5.1 Default Output

The map at the first requested time of prediction is automatically displayed in the GUI canvas immediately after the processing stage is completed. In addition, a portable raster map (PNG format) of this result is saved to the desktop, along with a corresponding world file required for automatic georeferencing in any geographic information system. If more than one time of prediction was initially requested, map results corresponding to all prediction times will be available for the user to display on the canvas and save to disk, as the user requests with the "*next*" and "*previous*" buttons located to the right of the display.

Output maps are color-coded such that dark red areas are predicted to have high relative sunken oil concentrations (near 100), and dark blue areas are predicted to have low relative concentrations (near zero). Predicted relative concentrations are effectively averaged across smaller scale patchiness of the sunken oil, and across cyclic movement due to tidal excursions. Also, total sunken oil masses are not known as a function of time. In fact, although relative concentrations may decrease with time due to oil dispersion, total sunken oil mass may simultaneously be changing due to sinking and re-suspension. Therefore, colors are not related from one time of prediction to another (that is, the same colors in different maps do not indicate the same relative concentration values). Rather, a scale of dark red to dark blue is presented at each time, indicating relative spatial probabilities of finding sunken oil at each time independently. The same interpretation applies whether individual prediction times are requested as part of the same run or in separate runs. It should be noted that the internal calculations of SOSim assume a constant total sunken oil mass in time, so as to maintain internal consistency and quality control checks on the integration computations. However, this assumption does not affect model output.

## 5.2 Optional Output

Optional output includes (1) map results for areas that are either contiguous to the current modeling area, zoomed-in within the current modeling area, or zoomed-out to include a larger area; and ( 2) maps updated with new or revised sampling campaign data. Optional output is obtained as follows.

To model areas contiguous to a current output map:

- Under the section "*Pan View*", select the direction in which the desired contiguous region is located with respect to the current output map in the display. For example, if the desired new modeling area is the continuation of a coastal region that extends to the north, select the button "N" under the "*Pan View*" section.

  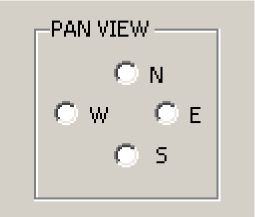

  Figure 5.1. Pan View button set

  The canvas will move towards an area of the same map scale and size in the selected direction;

- A pop-up message will request the user to complete the boundary conditions for the new area, along with the desired resolution (number of nodes in the east-west and south-north directions) for this contiguous case. Of course, any change in resolution may result in changes to the grid of the output map. If the new area is being modeled with the intention of creating a mosaic of multiple runs, a constant resolution is recommended;
- Prediction times can be changed, but be aware that in order to see the continuation of the original output, the same times of prediction are required; and
- Press the "*Recalculate*" button in the "*Pan View*" panel. Pressing this button instead of the "*Run*" button will instruct SOSim to use previous input information regarding the sampling campaigns and the spill, and will require much shorter runtime than would be required to rerun the case from scratch using the "*Run*" button.

To model zoomed-in areas of a current output map, or larger zoomed-out areas:

- From the panel "*Modeling Area*" press the "*Select Modeling Area*" button. Use the tool as before, making sure to select the resolution (number of nodes in each direction) and new boundary conditions desired before starting the run. The "Zoom in" tool under the "*Map*" toolbar also works to select a modeling area, if the user subsequently confirms the nodes and boundaries;
- Change times of prediction, if desired; and
- Press the "*Recalculate*" button under the "*Pan View*" section. Pressing this button instead of the "*Run*" button will instruct SOSim to use previous input information regarding the sampling campaigns and the spill, and will require much shorter runtime than would be required to rerun the case from scratch using the "*Run*" button.

To update the current output map based on new or revised sampling campaign data:

- If a sampling campaign is no longer needed or requires revision, remove it using the "*Remove Sampling Campaign*" button, making sure to select the correct campaign number from the drop-down menu;
- Upload the new sampling campaign data as usual; and
- If the modeling area, boundaries, and prediction times are not to be changed, then press the "*Run*" button. The "*Recalculate*" button is not useful in this case because the model run must be computed from scratch using the new field data, conserving only the desired prediction date(s), areas, boundaries and initial spill information.

## 6.0 Post Processing

Post processing activities include uploading previous raster output for viewing in a GIS (geographic information system), saving output, saving calibration files for further use, and printing images. The post processing tools are located in the "*Map*" toolbar of the GUI. SOSim Version 1.0 provides only for saving the output of a current project, but not for saving the contents of the prompts to be opened as a project later.

## 7.0 Portability of Results

To allow the posting of SOSim output data to the World Wide Web for rapid, long-distance, widely-accessible transfer of information, output image data is produced and saved in Portable Network Graphics (PNG extension) format. PNG is an extensible file format for the lossless, portable, well-compressed storage of raster images. As a complement of any output map created by SOSim, a corresponding world or georeferencing file (with PGW extension) is created and saved. The PGW file must accompany its parent PNG raster file in order for any output map to be ported to any GIS (geographic information system) that supports common PNG raster images, including but not limited to ArcGIS, QGIS, GRASS, and SOSim itself. PNG figures can be imported, inserted, printed, and used like any other common image file.

## 8.0 Software Portability

SOSim version 1.0 comes in an executable package for the Microsoft Windows 32 bit platform, allowing easy portability among computers having this common operating system. Portability to other OS platforms may be considered for future versions.

## 9.0 References

Englehardt, James D., M. Angelica Echavarria Gregory, and Pedro Avellaneda. 2010. “Development of a Predictive Bayesian Data-Derived Multi-Modal Gaussian Maximum Likelihood Model of Sunken Oil Mass.” Final Report to NOAA/UNH Coastal Response Research Center, NOAA Grant Number NA04NOS4190063, Project Number 08-088, September 8, 2010.

Research Planning Inc. 1994. *Natural Resource Damage Assessment Emergency Guidance Manual. Version 1.1*, Columbia, SC. Damage Assessment Center, NOAA, Rockville, MD.